

406-UM TerpRanger
Light Helicopter Upgrade Program



Alfred Gessow Rotorcraft Center
Department of Aerospace Engineering
University of Maryland
College Park, MD 20742

University of Maryland



Alfred Gessow Rotorcraft Center
Department of Aerospace Engineering
University of Maryland
College Park, MD 20742.

406-UM TerpRanger Light Helicopter Upgrade Program

In response to the 2002 Annual AHS International
Student Design Competition – Graduate Category
July 2, 2002

Jason Pereira – Team Leader

Dr. Inderjit Chopra – Faculty Advisor

Felipe Bohorquez

Tracy DuVall

Mustapha Chehab

Jacob Park

Ronald Couch

Beerinder Singh



This design proposal is dedicated to the memory of Professor Alfred Gessow.



Acknowledgments

The TerpRanger design team wishes to acknowledge the following people and thank them for their advice and assistance:

Dr. Vengalattore T. Nagaraj – Visiting Professor, Dept. of Aerospace Engineering, University of Maryland, College Park

Marat Tishchenko – Visiting Professor, Dept. of Aerospace Engineering, University of Maryland, College Park, and former Chief Designer, Mil Design Bureau

Dr. J. Gordon Leishman – Professor, Dept. of Aerospace Engineering, University of Maryland, College Park

Matthew Tarascio, Anubhav Datta, Kiran Singh, Paul Samuel, Jayanarayanan Sitaraman, Jinwei Shen, Beatrice Roget, Marc Gervais, Aubrey Goodman – Graduate Students, Dept. of Aerospace Engineering, University of Maryland, College Park

Andreas P. F. Bernhard – Dynamicist, Sikorsky Aircraft Corporation

Taeoh Lee – Engineer, Bell Helicopter Textron

Chris Van Buiten – Manager, New Product Definition, Sikorsky Aircraft Corporation

Mark Rager – Director of Maintenance, Capitol Rising / Glenwood Aviation LLC

Tom Gorman – Chief Inspector, Capitol Rising / Glenwood Aviation LLC

David Peterson – Marketing Manager, Bell Helicopter Textron Inc.

Marion Zinn – Bell Helicopter Textron Inc.

Eric Tossavanien – Resident Sales Manager, MD Helicopters, Inc.

Victor DiSanto – Naval Air Systems

Steven Smith, Inflatable Restraint Systems Product Manager, Simula Safety Systems Inc.

Douglas Daigle – Tridair Helicopters

Kyle Gass and Jack Black- Tribute

Richard Aboulafia – Analyst , Teal Group Corporation



Table of Contents

Acknowledgments	iv
List of Figures	x
List of Tables	xii
Proposal Requirements Matrix	xiv
Executive Summary	1
Tables of Physical Data	5
Performance Summary	5
1 - Introduction	6
2 - Helicopter Selection	7
2.1 - Selection Methodology	8
2.2 - Concept of Upgradability	8
2.3 - Selection Matrix	8
2.3.1- Weighting Factors	9
2.4 - Vehicle Selection	9
2.5 - Selection Criteria	9
2.5.1- Primary Criteria	9
2.5.2 - Secondary Categories	10
2.5.3 - Tertiary Categories	11
2.6 - Qualitative Performance Summary	12
2.7 - Completed Selection Index	14
2.8 - Candidate Vehicle Selection	14
2.9 - Candidate Vehicle Selection	14
2.9.1 - Number of Aircraft (Revisited)	16
2.10 - Final Vehicle Selection	16
3 - Description of the TerpRanger Upgrade Program	16
4 - Upgrade Configuration Trade Study	21
4.1 - Methodology	21
4.1.1 - Analysis	21
4.1.2 - Determination of Upgrade Candidates	21
4.2 - Implementation	22
4.3 - Limitations	22



4.4 - Validation of Analysis Code	22
4.5 - Independent Design Parameters	23
4.5.1- Preliminary Estimation of the Equivalent Flat Plate Area	24
4.5.2 - Preliminary Estimation of Blade Loading	24
4.5.3 - Preliminary Estimation of Tip Speed	24
4.6 - Engine Performance	24
4.7 - Weight Analysis	24
4.8 - Cost Analysis	25
4.9 - Trade Study Results	24
4.9.1-Finalist Candidate Upgrades	26
4.9.2 - Final Selection of the Upgrade Configuration	26
4.10 - Summary of Final Configuration	27
5 - Main Rotor and Hub Design	27
5.1 - Baseline Rotor	28
5.2 - Aerodynamic Design of the Blades	28
5.2.1 - Airfoil Sections	29
5.2.2 - Twist and Taper	29
5.2.3 - Blade tips	30
5.3 - Blade Structural Design	30
5.3.1 - Blade Structural Details	31
5.3.2 - Lightning Protection and Electromagnetic Shielding	31
5.4 - Hub Design	32
5.4.1 - Hub Details	32
5.5 - Autorotation Characteristics	33
5.6 - Rotor Dynamics	33
5.6.1 - Dynamic Analysis	33
5.6.2 - Aeroelastic Stability Analysis	35
5.6.3 - Ground Resonance	36
6 - Anti-Torque System and Empennage Design	37
6.1 - Anti-Torque Configuration Selection	37
6.1.1 - Weight Comparison of Anti-Torque Configurations	38
6.1.2 - Power Comparison	38
6.2 - Rotor/Hub Assembly	38
6.3 - Design Parameters	39



6.3.1 - Tail Rotor Diameter	39
6.3.2 - Tail Rotor Chord.	39
6.4 - Empennage Design	39
6.5 - Power Requirement	40
7 - Powerplant and Propulsion System Design.	41
7.1 - Engine Selection	41
7.2 - Engine Performance	41
7.3 - Engine Losses	42
7.4 - Structural Integration	42
7.5 - Transmission Design	43
7.5.1 - Design Strategy	43
7.5.2 - Transmission Configuration	44
7.5.3 -Transmission Optimization Process	45
7.5.4 - Weight Estimation	45
7.5.5 - Parameter Optimization	46
7.5.6 - Oil System	47
7.5.7 - Auxiliary Gearbox	49
7.5.8 - Tail Rotor Gear Box	49
8 - Airframe Design and Cabin Layout	52
8.1 - Structural Strengthening	52
8.2 - Airbag System	52
9 - Vibration and Noise Suppression	54
9.1 - Sources of Vibration	54
9.2 - Vibration Suppression Strategies	55
9.3 - Previous Vibration Suppression Methods	55
9.4 - Main Rotor Vibration Suppression	55
9.4.1 - LIVE Isolator	56
9.4.2 - Antiresonance Force Isolators	56
9.4.3 - Active Vibration Reduction System (AVRS)	56
9.4.4 - AVRS Implementation	57
9.5 - Active Tracking Tabs	58
9.5.1 - SMA Actuated Tracking Tab	58
9.5.3 - Locking Mechanism	59
9.5.4 - Control Strategy	59



9.5.5 - Tracking Tab Characteristics	59
9.6 - Noise Reduction	60
9.7 - Pricing	61
9.8 - TerpRanger 406 Standard Vibration Suppression Package	61
9.9 - Alternate Vibration Suppression Strategy	61
10 - Sub-systems	62
10.1 - The Fuel System	62
10.2 - The Engine Oil System	63
10.3 - Hydraulic System.	63
10.4 - Electrical System	64
10.5 - Flight Control System	64
10.6 - Cockpit and Avionics Upgrade Options	64
10.6.1 - Option 1: FADEC Control and Display Only	65
10.6.2 - Option 2: Modern digital avionics and flight instrument displays including an advanced GPS system	65
10.6.3 - Option 3: Modernized Avionics including Meggitt MAGIC MFDs and Passive Collision Avoidance Systems.	65
10.6.4 - Option 4: Modernized Avionics including Meggitt MAGIC MFDs and Active Collision Avoidance Systems	65
10.6.5 - Summary	66
10.7 - Health and Usage Monitoring Systems (HUMS)	68
11 - Stability and Control Analysis	68
11.1 - Stability and Control Derivatives	69
11.1.1 - Longitudinal Modes	69
11.1.2 - Lateral Modes	69
11.2-Handling Qualities	71
12 - Weights and Balance	71
12.1 - Weight Estimation	71
12.2 - Center of Gravity Estimation	73
13 - Performance Analysis	74
13.1 - Drag Estimation	75
13.1.1 - Parasite Drag	75
13.1.2 - Drag-Reduction Measures	76
13.1.3 - Vertical Drag	78



13.2 - Hover Performance	78
13.3 - Forward Flight Performance	79
14 - Manufacturing	83
14.1 - Lean Manufacturing	84
14.2 - Manufacturing Details	85
14.2.1 - Main Rotor	85
14.2.2 - Main Rotor Hub	85
14.2.3 - Tail Rotor	86
14.2.4 - Transmission	86
15 - Cost Analysis	86
15.1 - Cost Reduction Features	86
15.2 - Acquisition Cost	87
15.3 - Operating Costs	87
15.3.1 - Fuel Cost Driver DOC Calculation	88
15.3.2 - Maintenance Cost Driver DOC Calculation	88
15.3.3 - Tishchenko Method	89
15.4 - Ownership DOC	89
15.5 - Cost Comparison	90
15.6 - Analysis Limitations	91
16 - Summary of Upgrade Options and Multimission Capability	91
16.1 - Interchangeable Upgrade Options	92
16.1.1 - Avionics Upgrades	92
16.1.2 - Vibration Suppression	92
16.1.3 - Aircraft Options Cost Summary	92
16.2 - Multimission Capability	93
16.2.1 - Passenger/VIP Transport	93
16.2.2 - Search and Rescue (SAR)	93
16.2.3 - Military Operations	93
17 - Conclusion	94
Appendix: MIL-STD-1374 Weight Statement	95
References	99



List of Figures

4.1 - Flow Chart of Selection Process	22
4.2 - Design Algorithm Flow Chart	23
4.3 - Selection of Finalist Upgrade Configurations	26
4.4 - Finalist Upgrade Configuration Costs	26
5.1 - Comparison of Actual and Computed Power Curves for the Baseline Helicopter (Sea level, ISA)	29
5.2 - Power Curve for the TerpRanger	29
5.3 - Rotor Blade Planform	30
5.4 - Blade Cross-section	31
5.5 - Blade Stiffness and Mass Distribution	35
5.6 - Rotor Fan Plot	36
5.7 - Pitch-Flap Flutter/Divergence Stability Boundaries	36
5.8 - Flap/Lag/Pitch Stability	36
5.9 - Ground Resonance Analysis	37
5.10 - Air Resonance Analysis	37
6.1 - Tail Rotor Power vs. Forward Speed	40
7.1 - Engine Power Available vs. Altitude	42
7.2 - Transmission Configuration	44
7.3 - Hertz Stress Level vs Year of Design	47
7.4 - Auxiliary Gearbox Configuration	49
8.1 - Cockpit Airbag System for the OH-58D Kiowa Warrior	53
9.1 - AVRS Components	57
9.2 - Schematic of Active Tracking Tab	59
9.3 - Active Strut Concept [Gemb99]	60
10.1 - Avionics Upgrade Option 1: FADEC control/display	66
10.2 - Avionics Upgrade Option 2	66
10.3 - Avionics Upgrade Option 3	67
10.4 - Avionics Upgrade Option 4	67
10.5 - Antenna locations for Option 2 (Top, Left), Option 3 (Top, Right), and Option 4 (Bottom)	67
11.1 - TerpRanger Longitudinal Poles	71
11.2 - TerpRanger Lateral Poles	71



12.1 - TerpRanger Longitudinal CG Travel	74
13.1 - Maximum Rate of Climb vs. Altitude	79
13.2 - Weight vs. Hover Ceiling	79
13.3 - Fuselage drag variation with angle of attack	79
13.4 - Specific Range Variation With Forward Speed	80
13.5 - Power Required, Sea Level, ISA. Design Gross Weight	80
13.6 - Power Required Variation With Forward Speed	81
13.7 - Fuel Flow Variation With Forward Speed	81
13.8 - Specific Fuel Consumption Variation With Forward Speed.	82
13.9 - Power Req'd. for 140 kts and Max. Continuous Power Available	82
Variation With Altitude	82
13.10 - Cruise Speed and Max. Endurance Speed Variation With Altitude.	82
13.11 - Specific Range Variation With Altitude	82
13.12 - Minimum Fuel Flow Variation With Altitude	83
13.13 - Payload-Range Diagram	83
13.14 - Payload-Endurance Diagram	83
13.15 - Maximum Rate of Climb Variation With Altitude and Service Ceiling	83



List of Tables

2.1 - Initial Selection Pool	8
2.2 - (a) Weighting Factors	9
2.2 - (b) 3 Point Ranking System	9
2.3 - Selection Criteria Rubric	12
2.4 (a) - Criteria Data Summary: Primary Categories	13
2.4 (b) - Criteria Data Summary: Secondary Categories	13
2.4 (c) - Criteria Data Summary: Tertiary Categories	14
2.5 - Selection Index	15
4.1 - Calculations for 1 Independent Design Parameter Combination	25
4.2 - Finalist Upgrade Configuration Pool	27
5.1 - Comparison of New Main Rotor with Baseline Design	28
5.2 - Material Properties.	31
5.3 - Autorotation Characteristics Comparison	33
5.4 - Main Rotor Design Parameters	35
6.1 - Final Design Configurations	40
7.1 - Comparison of Engine Characteristics [Ahsd01]	41
7.2 - Transmission ratings in hp [Harr86]	43
7.3 -TerpRanger Weight Estimation Factors	46
7.4 - TerpRanger Estimated Transmission Weight Breakdown	46
7.5 - TerpRanger Transmission, 420 shp TO Power, 390 shp Max. Continuous Power	48
7.6 - Auxiliary Gearbox Design Features.	50
7.7 - Tail Rotor Design Features.	50
9.1 - TerpRanger 406 Main Rotor Vibration Suppression Options Summary	55
9.2 - Pricing Summary	61
10.1 - Technical Summary of Avionics Upgrades	66
11.1 - Stability derivatives	70
12.1 - JetRanger Component Weight Breakdown.	72
12.2 - TerpRanger Component Weight Breakdown	73
12.3 - JetRanger Longitudinal C.G. Location	74
12.4 - TerpRanger C.G. Locations	74



13.1 - Performance Summary	75
13.2 - Drag Build-Up	76
13.3 - Hovering Ceiling for Different Atmospheric Conditions	78
15.1 - Baseline Helicopter Acquisition Cost Breakdown	88
15.2 - DOC/fh Calculations and Comparison	89
15.3 - Operating Cost Breakdown	90
15.4 - Cost and Performance Comparison	91
16.1 - Upgrade Options Cost Summary	93



Proposal Requirements Matrix

Candidate Helicopter:		Bell 206A/B JetRanger:
Aging light helicopter	✓	1960's design, 3200 lbs GTOW
Commercial or military	✓	Commercial with military derivatives
4-6 place (including crew)	✓	5-place
Turbine	✓	Turbine
Typically capable of 110-130 kts	✓	115 kts cruise, 122 kts V _{NE}
Minimum 450 in service	✓	6000 in service

Design Objectives / Requirements:

Performance		
Cruise Speed	140 kts	✓ 145 kts
Absolute Range	400 naut. mi.	✓ 433 n.mi.
Payload	Increase	✓ 1550 lbs → 1800 lbs
Seating Capacity	Increase is a bonus	✗ 5-place → 5 place
Regulatory Compliance	FAR Parts 23 & 27, and other appropriate standards	✓
Safety	Improve	✓
Navigational Aids	Improve	✓
Reliability	Improve	✓
Versatility (Multi-mission capability)	Retain	✓
Affordability / Cost		
Manufacturing Cost	Minimize man-hours for fabrication and re-manufacture	✓
Acquisition Cost	Fraction of cost of acquiring a newly manufactured commercial helicopter	✓
Operating Cost	Reduce	✓

Subsystems to be Upgraded:

Main Rotor	✓	p. 27
Tail Rotor	✓	p. 37
Body / Fuselage	✓	p. 52
Landing Gear	✓	p. 75
Powerplant Structure	✓	p. 52
Propulsion / Powerplant	✓	p. 41
Drive System / Transmission	✓	p. 43
Flight Controls	✓	p. 64
Instruments	✓	p. 64
Hydraulic System	✓	p. 63
Electrical System	✓	p. 64
Avionics	✓	p. 64
Furnishings & Equipment	✓	p. 52
Final Assembly	✓	p. 83

Proposal Data Package:

Executive Summary	✓	p. 1
Table of Physical Data	✓	p. 5
MIL-STD-1374 Weight Statement	✓	p. 95
Recurring Cost Breakdown	✓	p. 89
Performance Charts		
HOGE altitude vs. gross weight	✓	p. 79
Payload vs. range	✓	p. 83
Altitude vs. maximum continuous speed	✓	p. 82
Drawings		
General arrangement fold-out	✓	p. 19
Inboard profile fold-out	✓	p. 20
Drive system schematic	✓	p. 51
Description of Design Process	✓	pp. 6 - 94



Executive Summary

Introduction

The 406-UM TerpRanger is an upgrade program for the Bell Model 206 JetRanger, designed in response to the 2002 AHS International Request For Proposals (RFP) for a Light Helicopter Upgrade Program. The RFP recognized the existence of an abundant resource of aging light helicopters, retired or soon to be retired, that presents an opportunity for upgrade and re-manufacture for the purpose of increased performance, safety, and reliability, while at a fraction of the cost of acquisition of a newly manufactured commercial helicopter. The purpose of this student design competition, co-sponsored by Bell Helicopter Textron, was to identify a candidate helicopter and develop a commercially viable upgrade program for it. The design has been developed for an existing helicopter; consequently, it is envisaged that this upgrade program is to be implemented within the next five years. The TerpRanger upgrade therefore incorporates cutting-edge technology solutions that are expected to mature within this time period.

Mission Requirements

The target performance goals specified by the RFP are a cruise speed of 140 knots, an absolute dry-tank range of 400 nautical miles and an increase in payload capability. In addition, the upgraded helicopter must incorporate improvements in safety and reliability, retain its wide-ranging multi-role missions capability, and have a low acquisition and operating cost. As most light helicopters are typically capable of 110-130 knots, the 140 knot cruise speed is the most stringent of the requirements. The TerpRanger design has, therefore, been optimized for high-speed flight while maintaining low cost of operation and extensive multi-mission capability.

Selection of Candidate Helicopter

To select a helicopter for the upgrade program, a pool of potentially suitable candidates was examined. Each helicopter was ranked on the basis of an *index of upgradability*, which is a measure of the upgrade potential of a particular helicopter. The index is based on factors such as the age of a particular helicopter model, the materials used in its manufacture, the design of its main rotor, and the number of aircraft of that model in service. From this analysis, the JetRanger emerged as the helicopter with the most potential for a successful upgrade program.

Design Methodology

The TerpRanger upgrade design was conducted in conjunction with the Spring 2002 Helicopter Design course at the University of Maryland. The course is aimed at introducing students to the different aspects of a real-world helicopter design and manufacturing process, and providing them with a thorough understanding of the issues



involved. To this end, no commercial helicopter design or analysis tools were used. The University of Maryland Advanced Rotor Code (UMARC) was modified to carry out the detailed rotor design, including aeroelastic stability analysis and estimation of hub loads. The helicopter graphics were developed using I-DEAS CAD software.

Design Approach

With a high cruising speed being the principal performance goal for the design, the TerpRanger design focuses on minimizing the power required in cruise while simultaneously increasing the power margins of the propulsion system. The increases in speed and range must be accompanied by reductions in vibration levels; hence, special consideration has been given to this issue. Because the primary purpose of this upgrade program is to provide a high-performance helicopter at a price lower than that of a newly manufactured aircraft, low acquisition and operating costs are a fundamental consideration in the design process.

The TerpRanger: Improved Performance

The TerpRanger can cruise at 144 knots (SL/ISA), carrying a 1125 lb payload for a distance of 424 nautical miles. This represents with a 24% increase in cruise speed, a 20% increase in payload capability and a 15% improvement in range over the baseline JetRanger, for only a 2% increase in direct operating costs. Such a performance enhancement will allow, for example, non-stop travel from Washington, D.C., to Boston in less than 3 hours.

The key component of the upgrade program is a new *four-bladed, composite, hingeless main rotor system with modern airfoil sections and an advanced-geometry blade tip*. The new rotor postpones retreating-blade stall and advancing-blade drag-divergence to higher advance ratios by tailoring the airfoil distribution along the span, which in turn reduces the vibration levels and power requirements at the desired cruise speed. Fuselage drag is reduced by 15% through: tilting the main rotor shaft forward by 6° to reduce the fuselage angle of attack in cruise, shortening the main rotor shaft, and providing fairings for the high-drag components of the airframe – the main rotor hub and the skid landing gear.

The TerpRanger incorporates a *state-of-the-art engine*, the scaleable specifications for which are given in the RFP. The engine is based on the DoD/NASA/Industry Integrated High Performance Turbine Engine Technology (IHPTET) initiative and has a higher power-to-weight ratio and lower specific fuel consumption than other existing engines. The TerpRanger also features a *redesigned drivetrain*, in which modern design methods are used to increase the stress levels on the gearbox components, and hence reduce weight. New materials and manufacturing methods are used to improve their strength and reliability.

**The TerpRanger: Improved Passenger Comfort**

The TerpRanger upgrade guarantees a smooth, high-speed ride for its occupants. The four-bladed main rotor produces lower hub loads and associated vibration levels at high speeds. Complementing this is a choice of three different *vibration-reduction devices*: passive Liquid Inertia Vibration Eliminators or Anti-resonance Force Isolators that attenuate the primary 4/rev vibrations by 60-70%, or an Active Vibration Reduction System (AVRS) that adaptively reduces vibrations of all frequencies by over 50%. With the incorporation of AVRS, it may be possible to achieve a “jet smooth ride” in the TerpRanger. Cabin noise levels are also reduced by a piezoelectric actuated, active strut system bonded to the surface of the transmission support pylons.

The TerpRanger: Improved Public Acceptance

High noise levels are a major concern for broadening public acceptance of helicopters. The TerpRanger design addresses this issue by lowering the tip speed of its rotors and using an advanced-geometry blade tip on its main rotor, resulting in *lower noise levels*.

The TerpRanger: Improved Reliability

The TerpRanger’s dynamic components have been designed to lengthen service lives and minimize *maintenance requirements*. Both the main and tail rotors have components made of composite materials that only need to be replaced on-condition. The main rotor incorporates *active tracking tabs* that allow the pilot to track the blades while in flight, thereby doing away with the need to spend valuable time tracking the blades manually by conventional methods on the ground. The new engine is of modern design and requires far less servicing than the Rolls-Royce / Allison 250-series turboshaft that it replaces. A fully integrated HUMS and diagnostics system for both the rotors and drivetrain will be available as an optional system. Improved reliability translates into less maintenance downtime and lower operating expenses.

The TerpRanger: Improved Safety

Safety is an important feature of the design of the TerpRanger. A new layout for the pilot’s instrument panel with *Multi-Function Displays*, a *Global Positioning System* and other modern navigational aids help reduce pilot workload and improve situational awareness. The improved reliability of the dynamic components of the helicopter reduces the possibility of their failure during flight. In the unlikely event of an accident, the occupants are protected by the *excellent autorotational characteristics* of the helicopter, a *crashworthy fuel tank*, a new *cockpit airbag system* and *energy-absorbing stroking seats* for the pilot and front-seat passenger. Lightning protection for the composite main rotor is provided by the titanium leading-edge erosion strip that runs down the entire length of the blade, providing a conductive path to the hub and the airframe.



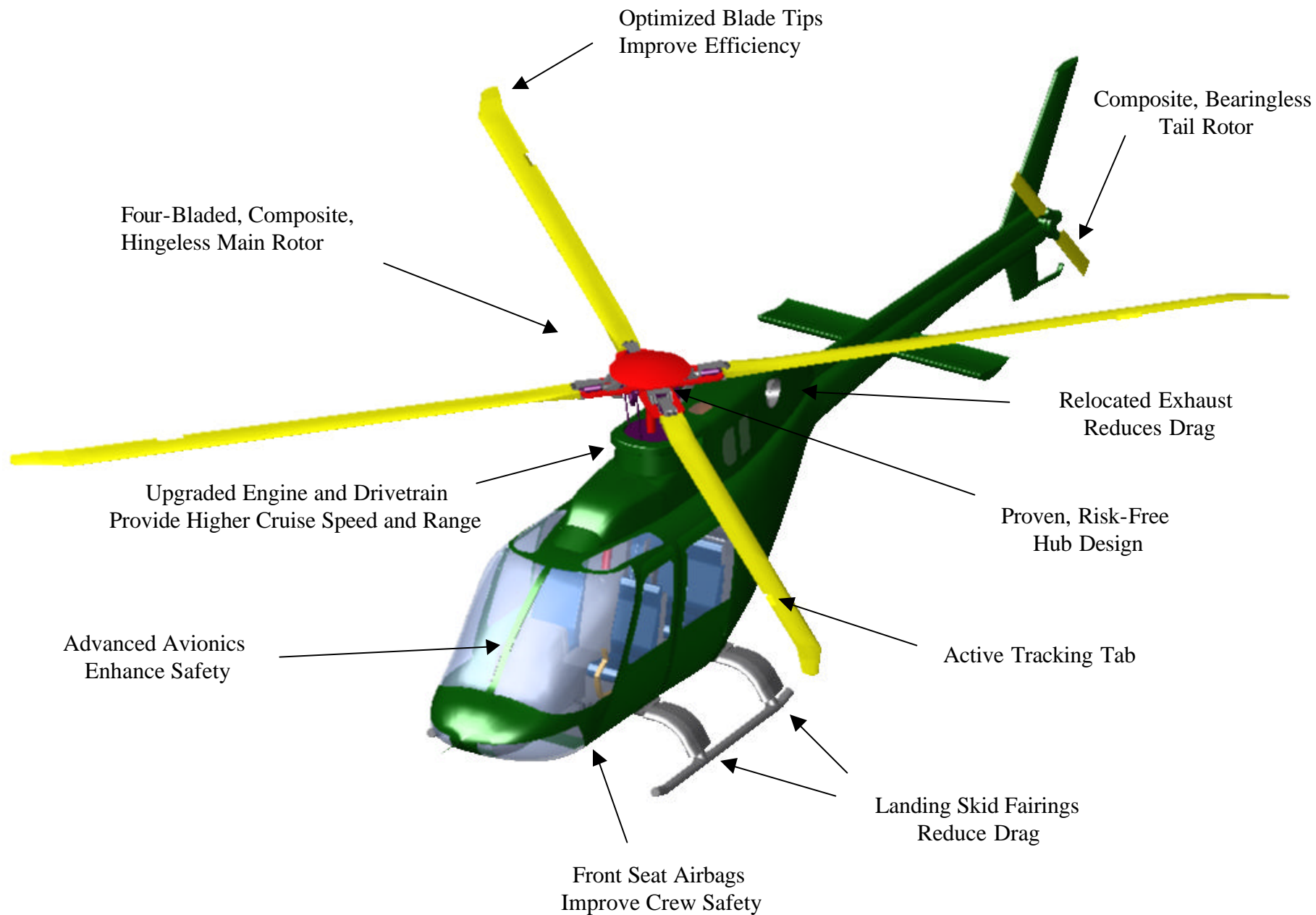
The TerpRanger: Improved Affordability

Operators of Bell helicopters greatly appreciate the simplicity of design that is their hallmark, and the TerpRanger design embodies this philosophy. *Design simplicity* translates into *ease and low cost of manufacture*, and consequently minimizes the purchase price of the aircraft. At \$1.16 million, the TerpRanger upgrade offers high performance, reliability, and safety at a price that compares favorably with that of other helicopters in its class: the MD 500E, the Schweizer 333, and the Eurocopter EC-120 Colibri. Furthermore, because of the lower maintenance requirements and improved fuel efficiency of its new engine, the TerpRanger also has *low operating costs* (\$410/FH), which is comparable to those of its competitors.

The TerpRanger: Improved Versatility

The Bell JetRanger is a *multi-role helicopter*, adaptable to a wide variety of missions. The TerpRanger design improves this versatility still further: its higher cruise speed and increased range and payload make it suitable for missions that are commonly performed by larger, more expensive aircraft, such as the Bell 430, and its low cost of ownership make it attractive to potential helicopter operators.

The JetRanger has been one of the world's most popular light helicopters for the past 25 years. The TerpRanger Upgrade Program will ensure that it retains this exalted status for many more years to come.



TerpRanger Highlights

Performance Summary and Physical Data

Sea-level Performance

	<i>JetRanger</i>		<i>TerpRanger</i>	
	<i>ISA</i>	<i>ISA + 20</i>	<i>ISA</i>	<i>ISA + 20</i>
Cruise speed (kts)	116	N/A	144	146
V _{NE} (kts)	122	N/A	158	161
Speed for best range (kts)	113	117	148	152
Speed for best endurance (kts)	48	N/A	62	64
Range (full fuel & payload), maximum (n. mi.)	368	368	424	450
Endurance (full payload), maximum (hrs)	4.6	N/A	4.05	4.21
HUGE ceiling (ft)	5,300	3,000	10,000	8,250
HIGE ceiling (ft)	13,000	10,200	13,900	11,850
Service ceiling (ft)	13,500	12,800	19,860	18,020
VROC, maximum (ft/min)	N/A	N/A	740	705
Climb Rate, maximum (ft/min)	1,280	N/A	1,715	1,590

Vehicle Dimensions

	<i>JetRanger</i>	<i>TerpRanger</i>
Fuselage length (ft)	31.2	31.2
Length overall, rotors turning (ft)	38.8	38.3
Height (hub) (ft)	9.5	8.6
Skid height (ft)	1	1
Fuselage width (ft)	4.33	4.33
Horizontal stabilizer span (ft)	6.4	6.4
Width of skids (ft)	6.4	6.4

Weights

	<i>JetRanger</i>	<i>TerpRanger</i>
Design gross weight (lb)	3200	3524
Empty weight (lb)	1647	1705
Useful load (lb) (Payload + Fuel) [*]	1382	1585
Maximum usable fuel (lb / US gal)	619 / 91	686 / 101
Payload with full fuel (lb)	763	899

^{*} Excluding the weight of the pilot

Main Rotor Specifications

	<i>JetRanger</i>	<i>TerpRanger</i>
Diameter (ft)	33.3	32.43
Number of blades	2	4
Chord (ft)		
Root	1.1	0.67
Tip	1.1	0.42
Twist (°)	-10	-13
Tip speed (ft/s)	687.59	672.4
Rotational speed (rpm)	394	396
Shaft tilt (°)	5	6
Tip sweep (°)	0	20
Tip anhedral	0	5
Root cut-out (%)	20	20
Airfoil sections	NACA 0012 mod.	OA-212, VR-12, VR-15

Tail Rotor Specifications

	<i>JetRanger</i>	<i>TerpRanger</i>
Diameter (ft)	5.42	5.4
Number of blades	2	2
Chord (ft)		
Root	0.5	0.46
Tip	0.5	0.46
Twist (°)	0	0
Tip speed (ft/s)	723.6	672.4
Rotational speed (rpm)	2550	2378
Airfoil sections	NACA 0012	NACA 0012

Power Ratings

	<i>JetRanger</i>	<i>TerpRanger</i>
Engine TO rating (shp)	420	500
Engine MCP rating (shp)	370	400
Transmission TO rating (shp)	317	420
Transmission MCP rating (shp)	270	390



Section 1 - Introduction

Recent years have witnessed a growing trend to refurbish and upgrade existing helicopter designs to new standards of performance, as opposed to developing completely new designs. The inherently high developmental cost of a new aircraft design has risen still higher because of lower tolerances for failure and more stringent certification requirements. With open international markets, competition exists from a greater number of manufacturers who offer helicopters in the same categories. In such a competitive arena, the upgrade of an existing, tried-and-tested design for a small additional cost appears to be an appealing strategy. An upgrade offers the customers the opportunity to modernize their helicopters at a fraction of the cost of acquiring a brand-new aircraft.

Additionally, there is the consideration that new designs take anywhere from ten to fifteen years before they are ready to be placed on the market. The upgrading of the vast pool of existing helicopters can therefore also be seen as an economically viable option for immediately meeting the needs of the customer, until new designs become available.

Helicopter upgrade programs are common in the armed forces. In the United States, the Marine Corps' H-1 Yankee/Zulu upgrade program for the UH-1 "Huey" utility helicopter, the AH-1 Cobra attack helicopter, the Army's CH-47F Improved Cargo Helicopter, and UH-60M/X BlackHawk modernization programs are just a few examples. The civilian sector has not seen such extensive re-manufacturing programs, perhaps because civil operators do not have the funds to pursue expensive ventures, and because their requirements do not change as dramatically and as rapidly as those of the military. Civil upgrades are usually limited to one or more of the following types:

- Improvements in engine power and efficiency, by installing a newer engine.
- Improvements in avionics and communication / navigation equipment.
- Improvements in main rotor design, thereby providing more thrust for less power.
- Improvements in reliability of the dynamic components, thereby reducing maintenance requirements and operating expenses.

Military upgrades augment these with re-designed cockpit layouts, increased-capacity transmissions, energy-absorbing crashworthy crew seats, strengthened airframes, vibration-suppression devices and mission-specific upgrades, resulting in substantially improved mission performance.

The Request For Proposals issued by AHS International and Bell Helicopter Textron calls for an upgrade of an existing light helicopter, with improvements in speed, range, payload, safety and reliability, while maintaining low recurring and non-recurring expenses. Of the performance enhancements, the 140-knot cruise speed



requirement is the most stringent, and necessitates an upgrade that is more extensive than that usually undertaken for a civil helicopter.

Designing an upgrade for a helicopter presents several unique challenges to the designers, which are normally not encountered in the design of a completely new aircraft. This is because the designer has to work within the constraints presented by the design of the existing helicopter and still be able to meet the customer's requirements. The modifications cannot be too extensive, because the "upgrade" then becomes equivalent to the design of a new helicopter, with the attendant increases in development, testing and certification costs. Therefore, the upgrade does not include such drastic modifications as changing the primary structure of the fuselage. For example, this could be an extension of the cabin with a fuselage plug to create more seating capacity. The designer also has to resist the temptation to not simply mimic the design of the other, more advanced members of the helicopter's family that are currently in production. It would serve no purpose to design the upgrade to be exactly like one of them.

The target customer-base to which the upgrade is being marketed must also be considered in designing the upgrade. Bell Helicopters has a long tradition of producing helicopters that are reliable, efficient, and have low operating costs. The JetRanger is Bell's entry-level helicopter, providing good performance and outstanding multi-mission capability at a cost lower than that of all other light turbine-engine aircraft on the market. It is for these reasons that the JetRanger has been produced in such vast quantities and is popular with operators all over the world. The 406-UM TerpRanger, the University of Maryland's design for the Bell Model 206 JetRanger, remains consistent with Bell's philosophy of fulfilling the customers' needs while maintaining simplicity of design and cost-effectiveness.

Section 2 - Helicopter Selection

This section details the vehicle selection for the proposed upgrade program. Upgrade candidates were evaluated based upon a range of criteria developed to quantitatively determine a helicopter's potential for upgrading. Furthermore, each helicopter was assessed based on how much improvement was necessary for it to achieve the required performance specifications outlined in the RFP.



2.1 - Selection Methodology

A large number of civilian helicopters were considered for an upgrade. Based upon the information provided in the RFP, a list of the possible upgrade candidates was assembled. Table 2.1 lists the initial selection pool of candidates. Only vehicles manufactured domestically or in Western Europe were considered because of the availability of large quantities of information on these vehicles. Furthermore, only first-order calculations were performed in this portion of the selection process. The initial selection pool is composed of only 4 to 6 passenger, turbine helicopters. To narrow down the list among the 14 candidates, a quantitative selection table was developed. A selection matrix based on information readily available in references such as Jane’s All the World’s Aircraft [Tayl00] and the Helivalues price guide [Heli01] was devised. A series of 11 criteria are defined to measure the upgradability of the aircraft.

Manufacturer	Model
Bell	206B JetRanger 2
Bell	206B JetRanger 3
McDonnell Douglas	500 C
McDonnell Douglas	500 D
McDonnell Douglas	500 E
Eurocopter	AS 350 B Astar
Eurocopter	AS 350 BA
Eurocopter	AS 350 B1
Eurocopter	AS 350 B2
Eurocopter	AS 350 D
Eurocopter	AS 355 F-2 Twinstar
Eurocopter	AS 355 F/F-1 Twinstar
Eurocopter	SA 315 Lama
Eurocopter	BO 105 CB/CBS

Table 2.1 - Initial Selection Pool

2.2 - Concept of Upgradability

In the selection process, it is first necessary to discuss, from a technical point of view, which helicopter is in most need of an upgrade. We define “Upgradability” as a quantitative measure of a helicopter’s potential to meet the RFP performance specifications, and need for modernization, for example, an older helicopter would have more upgradability potential than a newer, more modern helicopter.

2.3 - Selection Matrix

A quantitative selection matrix was developed to down-select the candidates from 14 to 2. Refer to Table 2.5 for the completed selection table. Economic and production feasibility issues are addressed indirectly and are not emphasized in this selection process. After two candidates have been selected, a more detailed analysis was carried out to make the final selection.



2.3.1 - Weighting Factors

Weighting factors for each selection criteria were established to determine the relative impact of the criteria on the upgradability index of the vehicle. Each criterion was placed in one of three categories: primary, secondary, and tertiary. Primary criteria were assigned the highest weighting because they have the most impact on defining the upgradability of the vehicle. Secondary criteria have a fair influence and tertiary have a limited or indirect impact on the vehicle's upgradability. Table 2.2(a) summarizes the weighting factors for each category.

For each criterion, a vehicle was assigned a number from one to three based on how well it fitted the criterion parameters. The scale for the ranking system is similar to the scale for the weighting factors. Table 2.2 (b) presents these factors.

Table 2.2 - (a) Weighting Factors

Category	Description	Weighting Factor
Primary	Major Impact	3
Secondary	Moderate Impact	2
Tertiary	Minor Impact	1

Table 2.2 - (b) 3 Point Ranking System

Ranking	Description
3	Most Desirable Quality
2	Moderately Desirable Quality
1	Least Desirable Quality

2.4 - Vehicle Selection

A selection matrix was assembled by assigning a rank to each criterion for each vehicle. Then, the rankings were multiplied by the weighting

factors respective to each criterion, and a composite score was calculated for each vehicle from the sum of the weighted rankings. The top two composite scores indicate the best candidates for upgrade. The selection matrix (refer to Table 2.5) shows the results of this assessment. Each vehicle was assessed relative to the "best" and "worst" vehicle for each criterion and was given a rating of good, fair or poor as a measure of this assessment.

2.5 - Selection Criteria

Sections 2.5.1 to 2.5.3 summarize the selection criteria and briefly state the rationalization of each criterion. A rubric containing the rating system for each criterion is also included. In the following analysis, the terms "payload" and "useful load" are used interchangeably.

2.5.1 - Primary Criteria

Number of Aircraft: This criterion was included to provide insight into the potential market for an upgrade. If a large number of aircraft exists, then the potential customer base for an upgrade is large, and the profitability of the upgrade program will generally be higher. This category judges the upgradability of the vehicle by placing more emphasis on vehicles with large numbers of existing aircraft.



Power, Speed, Weight: This criterion is defined as the maximum continuous power rating of the transmission divided by the product of the cruise speed and take-off weight. A good helicopter will have a small value for this criterion. For the purpose of this project, a vehicle with a low number is desirable. The transmission is a major component and the expense of changing the system may not be justified for an upgrade because of the effort involved. For this upgrade program, it was desirable to implement changes in the main rotor because this defines the overall capabilities of the vehicle. Thus, the most upgradeable helicopter has a low number in this category.

Maintenance Cost per Payload: This criterion provides insight into the magnitude of resources allocated per pound of payload. In general, the financial burden of a high maintenance cost may be offset if the vehicle in question is capable of carrying more payload. Similarly, a small decrease in payload capacity may be justified if the maintenance costs are sufficiently reduced. For the purpose of selection, a vehicle with a high maintenance cost normalized by payload is judged to be the candidate in most need of an upgrade.

2.5.2 - Secondary Categories

Number of Blades: Increasing the number of blades of an existing helicopter helps to reduce vibration and improves performance provided that there is an increase in rotor solidity. This factor was included to assess the possible improvement options of a helicopter's rotor. A helicopter with fewer blades is most desirable because of its potential for improvement with additional blades.

Blade Material: This category provides additional insight into the upgradability of the main rotor. Metal bladed rotors provide a greater upgrade potential than composite rotors. Advances in material science allow for composite blades to have superior fatigue characteristics and lighter weight than their metal counterparts.

Weight Efficiency: This is defined as the difference between the take-off and empty weight normalized by the take-off weight. While it is desirable to increase the payload capacity of a helicopter in this upgrade program, care should be taken to keep increases of the empty weight to a minimum. This is an attribute that will be improved in an existing vehicle, and therefore a weight inefficient model is regarded as an attractive candidate for upgrade.

Fuel Consumption Quotient: This criterion is defined as the fuel consumption per hour divided by the product of cruise speed and payload. This parameter indicates how much fuel is required to move one unit of payload over one unit of range. Because fuel consumption is a major component of the operating cost, a vehicle with



low fuel consumption is desired. The RFP stipulates a high range requirement; therefore a helicopter with a high value for this parameter needs to be improved and is a desirable candidate for upgrade.

Power Quotient: The quotient of the transmission rating and the installed power provides insight into the type of mission for which a vehicle is currently optimized. Helicopters with a quotient near 1.0 are best suited for missions involving higher operational altitudes at higher forward flight speeds. In contrast, a helicopter with a low quotient is best suited for missions involving extended periods of hover. In most cases, the weight of the engine is proportional to the installed power, therefore, a helicopter designed for hover intensive missions would require the weight to be kept to a minimum. The RFP stipulates a relatively high cruise condition and therefore, the helicopters with the most potential for an upgrade are those optimized for hover and subsequently receive the highest rankings.

Price & Payload Quotient: This criterion is an economic quality that compares the acquisition price normalized to useful load for the upgrade candidates. A low quotient indicates that the customer is paying less per pound of payload. Because the purchase cost and payload are related to the weight of the vehicle, in the context of an upgrade program these parameters are effectively fixed and are not necessarily under the direct control of the designer. Therefore, it is uncertain as to whether or not this category will be directly affected by an upgrade program and subsequently difficult to reduce as desired in a direct manner. To keep the quotient to a minimum, it is best to choose an already economical vehicle so that any increases as a result of this upgrade will be offset by the fact that the quotient is already low.

2.5.3 - Tertiary Categories

Cruise Speed: Although cruise speed is already incorporated into several of the criteria discussed above, it is necessary to compare each vehicle by its cruise speed independently to estimate the level of improvement required to match the RFP performance requirements. The most challenging potential upgrade will be one that requires the largest speed enhancement; therefore, a higher ranking was assigned to the slowest vehicles. This indicates that slow helicopters have more upgradability than the faster ones.

Fleet Age: This criterion rates a helicopter based on its average service age. The service age is defined as the average age of all the vehicles of a particular model from the first to the last year it was produced. Helicopters with service ages between 10 and 20 years are the target group for upgrade, and therefore receive the highest rating. Helicopters younger than 10 years are not yet old enough to require an upgrade, but will require one eventually so they receive the middle rating. A vehicle older than 20 years is beginning to become too old, and therefore, the effectiveness of an upgrade is limited. Excessive wear on the airframe associated with age, will



limit how long the vehicle’s service life may be prolonged, and cannot be reversed by an upgrade. Helicopters in this age class do not have enough life left to make an upgrade economically feasible and, therefore, receive the lowest rating. The rubric in Table 2.3 displays a complete breakdown of the selection criteria.

2.6 - Qualitative Performance summary

Tables 2.4 (a) through (c) summarize the data obtained for the set of selection criteria.

Table 2.3 - Selection Criteria Rubric

Primary Criteria		Fuel Consumption Quotient	
# of Aircraft		Power Quotient	
Over 2000	3	Below 6.0E-5 gal/(kt*lb)	3
Over 1000	2	Between 6.0E-5 & 1.0E-4 gal/(kt*lb)	2
Below 1000	1	Above 1.0E-4 gal/(kt*lb)	1
Power, Speed, Weight		Price & Payload Quotient	
Below 8.0E-4 hp/(kt*lb)	3	Below 300 \$/lb	3
Below 1.0E-3 hp/(kt*lb)	2	Between 300 and 500 \$/lb	2
1.0E-3 hp/(kt*lb) or above	1	Above 500 \$/lb	1
Maintenance Cost/Payload		Tertiary Criteria	
Above 10 cents per lb	3	Cruise Speed	
Between 8 and 10 cents per lb	2	Below 120 kts	3
Below 8 cents per lb	1	Between 126 and 120 kts	2
Secondary Criteria		Average Vehicle Age	
# of Blades		Above 126 kts	1
2 bladed rotor	3	Weight Efficiency	
3 bladed rotor	2	Below 46%	3
4 or more rotor blades	1	Between 46% and 50%	2
Blade Material		Above 50%	1
Metal rotor blades	3		
Composite rotor blades	1		



Table 2.4 – (a) Criteria Data Summary: Primary Categories

Model	Number of Aircraft (#)	Power, Speed, Weight (hp/(kt*lb))	Maint. Cost/Payload (\$/lb)
Bell 206B-2	2210	0.00073	0.093
Bell 206B-3	2318	0.00073	0.091
MD 500 C	660	N/A	0.070
MD 500 D	1195	0.00090	0.083
MD 500 E	547	0.00090	0.085
BO 105 CB/CBS	576	0.00112	0.097
SA 315 Lama	472	0.00123	0.159
AS 350 B AStar	1535	0.00102	0.086
AS 350 BA	557	0.00093	N/A
AS 350 B1	328	0.00102	0.069
AS 350 B2	937	0.00098	0.067
AS 350 D	551	0.00114	0.102
AS 355 F-2	305	0.00105	0.086
AS 355 F/F-1	365	0.00108	0.091

Table 2.4 (b) - Criteria Data Summary: Secondary Categories

Model	Number of Blades (#)	Blade Material (Metal or Composite)	Weight Efficiency (ratio)	Fuel Consumption (gal/(kt*lb))	Power Quotient (ratio)	Purchase Cost per Payload (\$/lb)
Bell 206B-2	2	Metal	0.501	0.0000569	0.793	115.48
Bell 206B-3	2	Metal	0.468	0.0000550	0.755	510.68
MD 500 C	4+	Metal	0.567	0.0000595	0.695	110.73
MD 500 D	4+	Metal	0.529	0.0000586	0.893	204.92
MD 500 E	4+	Metal	0.506	0.0000608	0.893	553.00
BO 105 CBS	4+	Composite	0.480	0.0000720	0.821	667.80
SA 315 Lama	3	Metal	0.476	0.0001040	0.656	355.47
AS 350 B AStar	3	Composite	0.430	0.0000616	0.828	395.24
AS 350 BA	3	Composite	0.449	0.0000552	0.828	454.33
AS 350 B1	3	Composite	0.480	0.0000537	0.863	326.74
AS 350 B2	3	Composite	0.484	0.0000525	0.806	465.61
AS 350 D	3	Composite	0.434	0.0000607	0.863	213.06
AS 355 F-2	3	Composite	0.467	0.0000678	0.817	619.27
AS 355 F/F-1	3	Composite	0.452	0.0000687	0.817	365.96



Table 2.4 (c) – Criteria Data Summary: Tertiary Categories

Model	Cruise Speed (knots)	Fleet Age (yr)
Bell 206B-2	116	30
Bell 206B-3	115	13
MD 500 C	124	30
MD 500 D	130	23
MD 500 E	130	10
BO 105 CB/CBS	112	16
SA 315 Lama	103	22
AS 350 B AStar	121	18
AS 350 BA	123	7
AS 350 B1	119	14
AS 350 B2	122	7
AS 350 D	108	21
AS 355 F-2	110	10
AS 355 F/F-1	113	18

2.7 - Completed selection index

Table 2.5 depicts the complete selection matrix.

2.8 - Candidate Vehicle Selection

Based on the results of the selection index, it was determined that the Bell 206B JetRanger and the MD 500D are the best candidates for upgrade and have the most upgrade potential. Because of the inherent similarities between the JetRanger II and III, it was decided that for this upgrade program they would be considered to be the same vehicle, and that any upgrade for the JetRanger II could also be applied to the JetRanger III.

2.9 Candidate Vehicle Selection

As previously stated, the selection index is an acceptable method for evaluating different vehicles based upon their specifications, but it does not consider other factors such as economic and production considerations. The final selection between the MD 500D and the JetRanger was decided based on these latter considerations.



Table 2.5 - Selection Index

CRITERIA	Weighting Factor	Bell 206 B JetRanger II	Bell 206B-3 JetRanger III	MD 500 C	MD 500 D	MD 500 E	BO 105 CB/CBS	SA 315 Lama	AS 350 B AStar	AS 350 BA	AS 350 B1	AS 350 B2	AS 350 D	AS 355 F-2 Twinstar	AS 355 F/F-1 Twinstar
Purchase Cost/Payload	2	6	2	6	6	2	2	4	4	4	4	4	6	2	4
Maintenance Cost/Payload	3	6	6	3	6	6	6	9	6	0	3	3	6	6	6
Fleet Age	1	1	3	1	1	3	3	1	3	2	3	2	1	3	3
Speed	1	3	3	2	1	1	3	3	2	2	2	2	3	3	3
Trans. Pow./Inst Pow.	2	4	4	6	4	2	2	6	2	2	2	4	2	4	4
# of Blades	2	6	6	2	2	2	2	4	4	4	4	4	4	4	4
Composition of Blades	2	6	6	6	6	6	2	6	2	2	2	2	2	2	2
# of Aircraft	3	9	9	3	6	3	3	3	9	3	3	6	3	3	3
Fuel Consumption Quotient	2	6	6	4	6	4	4	2	4	6	6	6	4	4	4
Weight Efficiency Factor	2	4	4	2	2	2	4	4	6	6	4	4	6	4	6
Transmission /(Speed* Weight)	3	9	9	6	6	6	3	3	3	6	3	6	3	3	3
Purchase Cost/Payload	2	6	2	6	6	2	2	4	4	4	4	4	6	2	4
Composite Score		60	58	41	46	37	34	45	45	37	36	43	40	38	42



2.9.1 - Number of Aircraft (Revisited)

Despite the fact that this category is of primary importance, the selection index above understates the importance of this category because it is not directly related to the technical aspects of a helicopter. Its importance is beyond the scope of this first order analysis. Furthermore, this category is a measure of the potential customer base for an upgrade program, and therefore, it is essential for a manufacturer to pay more attention to this before investing in an upgrade venture. Clearly, the Bell JetRanger has an advantage over others in its class because of the relatively large number of vehicles produced. Therefore, the JetRanger is more attractive than the MD 500D because of the fact that there are potentially more vehicles to upgrade.

2.10 - Final Vehicle Selection

After careful consideration, it was determined that the Bell 206B-3 is the most attractive candidate for an upgrade program. The selection index clearly establishes the vehicle's need for upgrade, and its near ubiquitous availability make it a sound choice for an upgrade venture. Modernization of the Bell 206B-3 to meet the performance requirements specified in the RFP will make it highly competitive with other, newer vehicles such as the Eurocopter EC-120.

Section 3 - Description of The TerpRanger Upgrade Program

The TerpRanger upgrade provides the operator with a 24% increase in cruise speed, a 20% increase in payload capability and an 15% improvement in range, with only a 2% increase in direct operating costs. This re-manufacturing program is more extensive than upgrades that are currently offered for civil helicopters, in terms of the performance enhancements and the modifications to the baseline helicopter. A summary of the upgraded features of the TerpRanger 406 program is given below. Page numbers of the relevant sections of the report are given in parentheses for easy reference to more detailed descriptions.

Main Rotor (page 27)

The two-bladed, metal, teetering rotor is replaced with a four-bladed, composite, hingeless main rotor that incorporates varying airfoil sections along the radius, -13 degrees of linear twist, advanced-geometry blade tips with sweep, taper and anhedral, and active trailing-edge tracking tabs.

Tail Rotor (page 37)

The two-bladed metal tail rotor is replaced with a composite, bearingless rotor of a similar configuration. The vertical fin offloads the tail rotor in forward flight. Stability and handling qualities analysis indicated that no further modifications were necessary for the helicopter empennage.

***Transmission and Gearboxes*** (page 43)

The drive train, including main and tail rotor gearboxes are replaced with components that are similar in configuration, but which are designed to transmit higher torques and require less maintenance. This is achieved by utilizing new materials and modern gear design methods and by using better lubricants for the gearboxes.

Health and Usage Monitoring System (page 68)

The TerpRanger upgrade includes the option of installing a Health and Usage Monitoring System (HUMS) for the main rotor and the drivetrain, which greatly enhances their reliability and maintainability, and reduces the operating costs of the helicopter.

Vibration-Reduction Devices (page 54)

The upgrade program offers the customer the opportunity to choose between three options for reducing fuselage vibration levels: (i) Liquid Inertia Vibration Eliminator (LIVE) isolators incorporated into the main rotor gearbox mounts, (ii) Anti-resonance Force Isolators (AFI) incorporated into the gearbox mounts, and (iii) an Active Vibration Reduction System (AVRS) which actively adapts to different vibration environments, and hence is not restricted to the attenuation of only one vibratory frequency.

Instrument Panel and Avionics (page 64)

The TerpRanger upgrade offers the customer a choice of four avionics / instrument package suites. Each suite enhances safety and improves situational awareness.

Hydraulic System (page 63)

To prevent pilot fatigue, the hydraulic servo boost actuators for the cyclic and collective controls are upgraded for the TerpRanger helicopter.

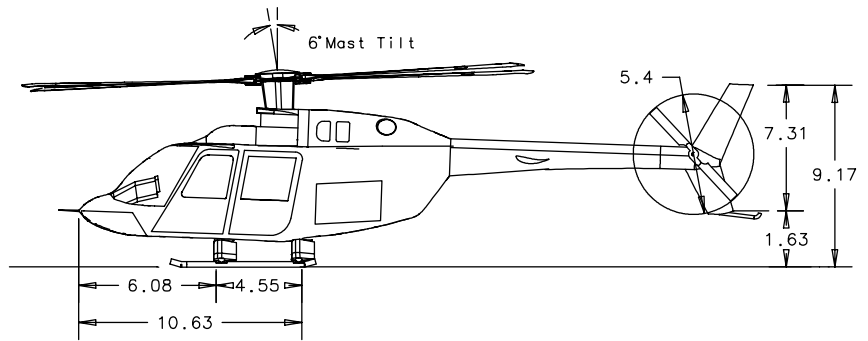
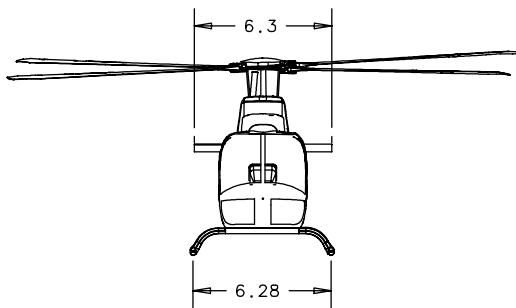
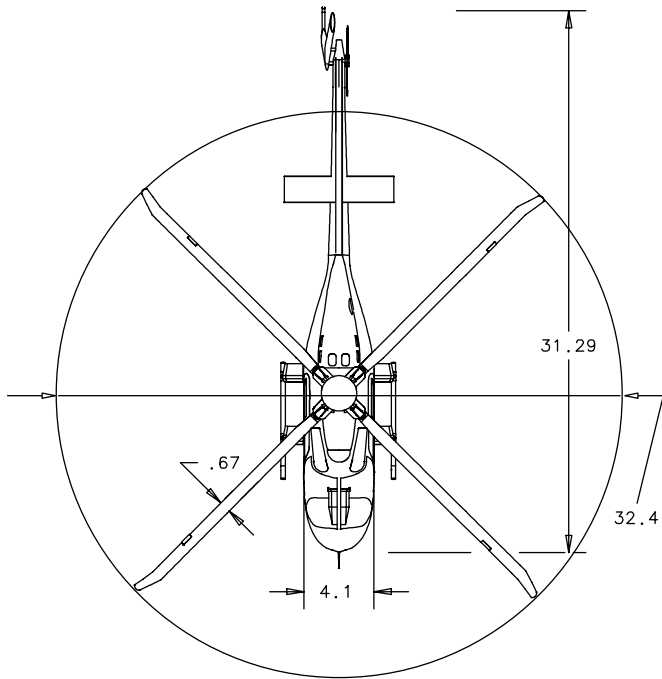
Fuel System (page 62)

To meet the 400-nm range requirement specified in the RFP, the TerpRanger requires a fuel capacity of approximately 101 U.S. gallons. The JetRanger has a fuel tank located below and behind the passenger seat bench with a usable fuel capacity of 91 gallons. In the TerpRanger, this is augmented by an auxiliary 10-gallon fuel tank that is fitted into the forward portion of the baggage compartment. A similar 20-gallon auxiliary fuel tank has already received FAA certification for incorporation into the Bell Model 407 helicopter.



Airframe and Cabin Layout (page 52)

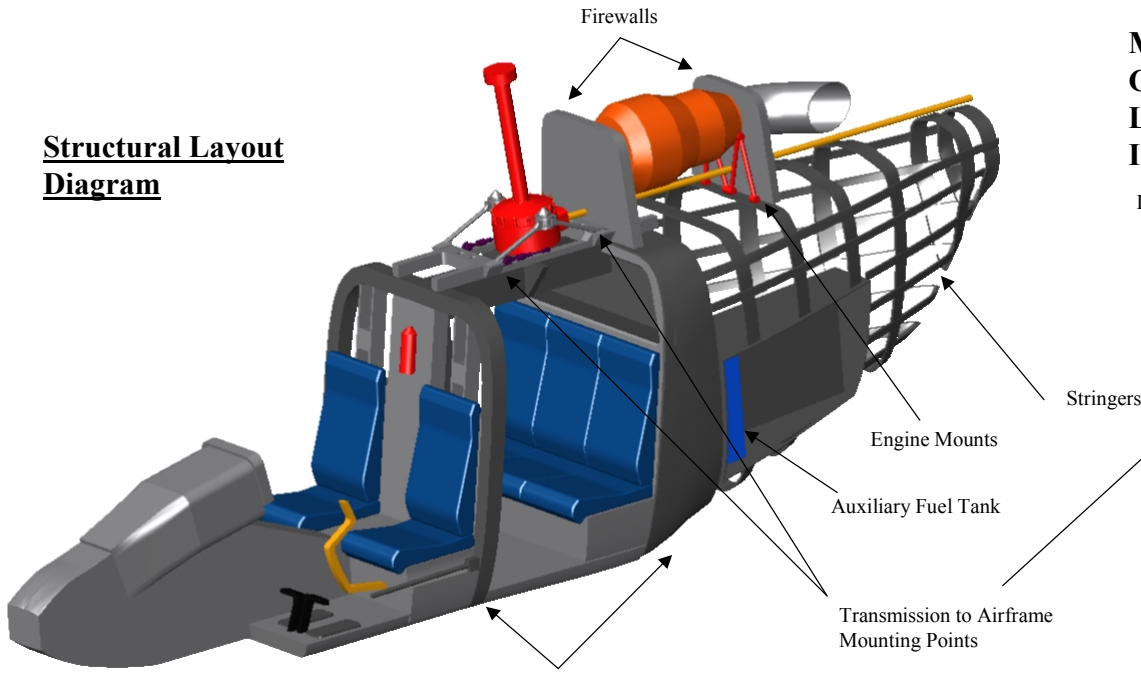
So as to safely withstand the higher loads due to the increase in gross weight of the helicopter, minor modifications are made to the airframe structure to increase their stiffness and strength. To reduce the drag of the fuselage, fairings are provided for the skid landing gear, the main rotor hub and for the opening in the cowling through which the main rotor shaft emerges. Airbags are provided for both of the front seats.



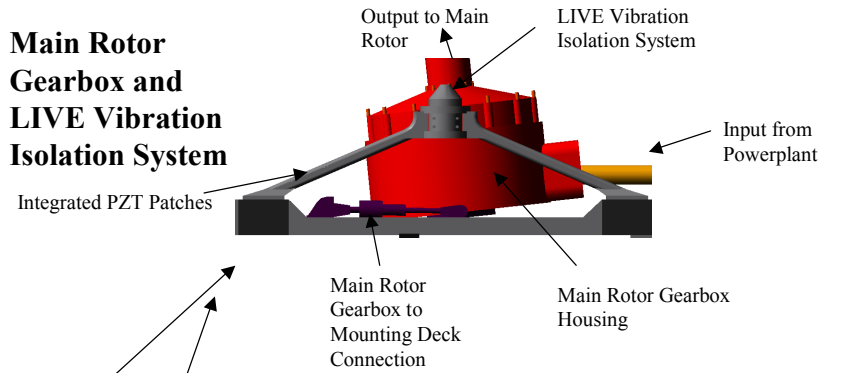
All dimensions in feet

Foldout 3.1 – Three-View Drawing

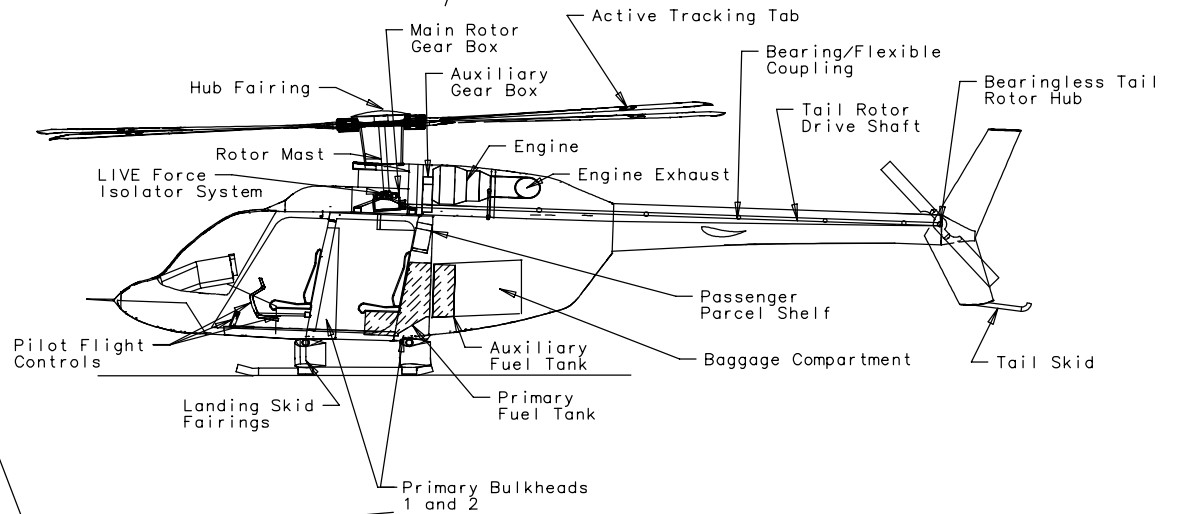
Structural Layout Diagram



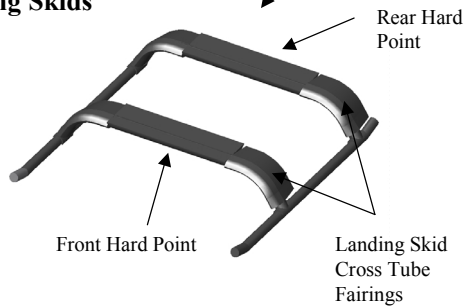
Main Rotor Gearbox and LIVE Vibration Isolation System



Foldout 3.2 – Interior and Structural Features



Landing Skids



Inboard Profile Drawing



Section 4 - Upgrade Configuration Trade Study

The methodology that is used to evaluate the various configurations of the selected helicopter is outlined in this section.

4.1 - Methodology

The goal of the trade study is to quantitatively compare a wide range of upgrade configuration types so that an optimum upgrade can be selected. The upgrade configuration must not only meet the performance requirements stipulated in the RFP but it also must provide a cost effective solution.

4.1.1 - Analysis

A series of candidate upgrade configurations are formulated in this trade study. The analysis is based on an original design code developed for rotorcraft sizing, and is customized for an upgrade program that conforms to the performance specifications listed in the RFP.

The fixed parameters of this study were range, payload, and cruise speed. Once specified, all of the helicopter configurations were calculated to meet or exceed these requirements. Additionally, independent design parameters included in this study were blade loading, main rotor tip speed, and parasite drag area. Several combinations of these parameters were included in the analysis to provide insight into the influence of factors such as stall margin and blade noise, for the potential helicopter upgrades.

The primary output of the trade study was the take-off weight of the upgraded helicopter configuration. The pricing equations specified in the RFP are dependent upon the weight of vehicle components, therefore, the trade study was organized to first calculate the weights of each system independently and then provide a preliminary estimate of the total take-off weight of the vehicle.

Varying the independent design parameters generated a series of candidate configurations. After a complete set of configurations was determined, an optimum configuration was chosen based on factors such as acquisition cost, implementation complexity, and total take-off weight.

4.1.2 - Determination of Upgrade Candidates

The selection pool of potential upgrades was composed of conceptual helicopter designs from each data set. For each set of independent parameters, sixteen candidate helicopters were generated. Table 4.1 below shows the candidate upgrade configurations for one set of independent design parameters. Only two to three



configurations advance to the selection pool as finalists. Through an exhaustive parameter design study, a final upgrade configuration was selected. A simplified flow chart of the selection process appears in Figure 4.1.

4.2 - Implementation

The algorithm implemented in this trade study was developed in-house, and was customized to meet the performance requirements expressed in the RFP. The method is similar to the one used by the Mil Design Bureau. [Tish02]. The methodology of this algorithm is summarized in the flow chart in Figure 4.2. The design code is flexible and simultaneously generates multiple rotor configurations. Rotor configurations with 2 to 5 blades with varying aspect ratios were evaluated. (Refer to Table 4.1 for details.)

4.3 - Limitations

Because this study is based on first order analysis, the required take-off and cruise power are slightly under-predicted. Despite this limitation, the design analysis calculated an acceptable estimate of the required power for each candidate configuration.

4.4 - Validation of Analysis Code

The analysis is validated by predicting the parameters of the original, unmodified version of the 206 JetRanger III and comparing them to the actual specifications [Bell02]. Once the algorithm is tuned to calculate the take-off weight of the unmodified vehicle, the independent design parameters may be estimated.

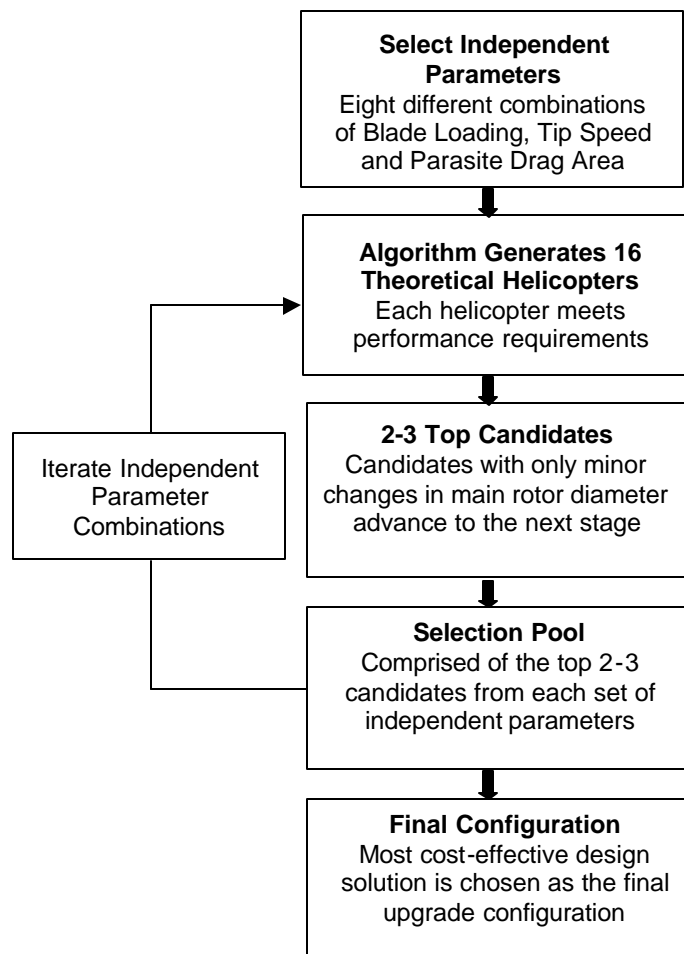


Figure 4.1 - Flow Chart of Selection Process

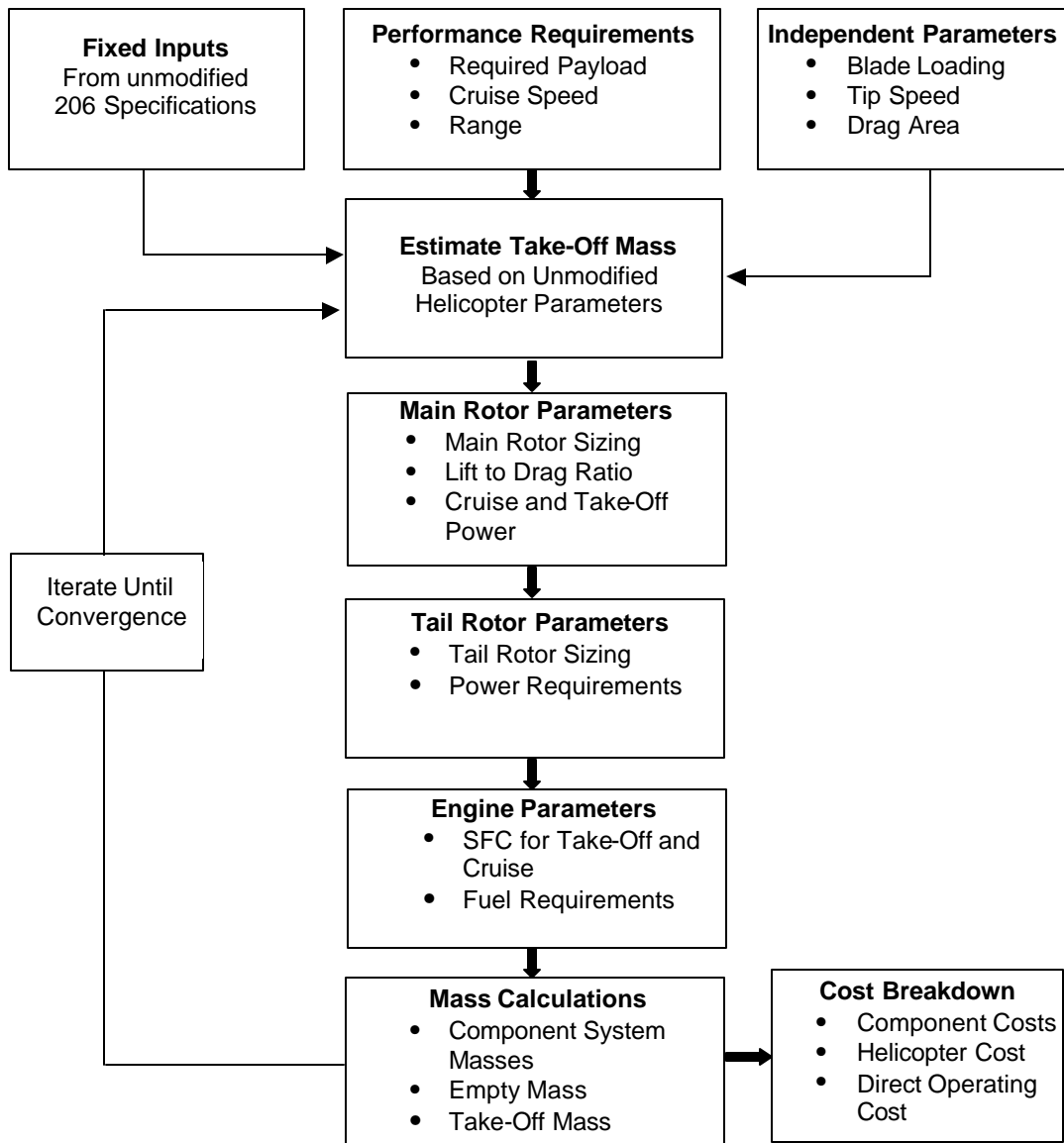


Figure 4.2 - Design Algorithm Flow Chart

4.5 - Independent Design Parameters

A set of candidate configurations were generated for each combination of independent design parameters. The selection pool of upgrade configuration candidates were comprised of the two or three finalists from all of the candidate sets. The upgrade configuration was then chosen from the selection pool. The three independent design parameters considered in this analysis are: blade loading, parasite drag area, and tip speed. Each parameter consists of two possible values that are explained below.



4.5.1 - Preliminary Estimation of the Equivalent Flat Plate Area

The equivalent flat plate drag area was estimated from the power curve of the unmodified 206 JetRanger. Details of this procedure are included in Section 5. The estimated drag area is 6.5 ft^2 for the unmodified 206B-3. Based on historical data, it is reasonable to assume a reduction of the equivalent drag area by 15% to 5.5 ft^2 for the TerpRanger upgrade [Wils90]. In addition, the influence of a more conservative value of 6.0 ft^2 is also considered in this study. A more detailed analysis of the drag area estimation is given in Section 13 of this proposal.

4.5.2 - Preliminary Estimation of Blade Loading

The blade loading coefficient, C_T/σ , was selected with respect to the baseline value of 0.08. To accommodate an increase in payload required for the upgrade, a higher blade loading is chosen. A value of 0.08 is desirable, however, the blade stall margin may be too small. Furthermore, the high blade loading of 0.08 may not allow for potential growth in the gross weight. For the purpose of comparison, a more conservative blade-loading coefficient of 0.075 is also considered.

4.5.3 - Preliminary Estimation of Tip Speed

Two tip speeds were considered in this trade study: 686 ft/sec and 673 ft/sec. The original tip speed of the unmodified 206B is 686 ft/sec, and this value is again considered for the upgraded versions. To minimize external noise levels, a lower tip speed of 673 ft/sec was also evaluated.

4.6 - Engine Performance

The engine performance was estimated using the powerplant data given in the RFP. These characteristics are scaleable and corrected for losses resulting from factors such as altitude, temperature, and installation. A complete performance analysis of the engine is shown in Section 7 of the proposal.

4.7 - Weight Analysis

The procedure for determining the empty and take-off weights of the helicopter is as follows. The upgrade candidates are divided into various subsystems and components, i.e. the main rotor, main gearbox, engine etc. The trade study algorithm calculates component weights by assigning mass coefficients to each system [Tish02]. The take-off weight of the helicopter is defined as the sum of the empty weight and the weights of the passengers, crew, cargo, and fuel. A detailed analysis of the component system weights and the determination of their associated mass coefficients are presented in Section 12. For the conceptual helicopters generated from each set of independent design parameters, the take-off weight is estimated.



4.8 - Cost Analysis

The acquisition price of the vehicle was calculated after the weights of the component systems were determined. Prices for each system are determined according to the cost formulas listed in the RFP. The base manufacturing price is the sum of the component system prices. The direct operating cost (DOC) of each helicopter configuration is also estimated in the trade study. The DOC is based on the manufacturing cost, the salary of the ground crew and pilot, the service life of the vehicle and the cost of fuel. A detailed calculation of the DOC for the vehicle is given in Section 15.

4.9 - Trade Study Results

As mentioned previously, all combinations of the independent design parameters were analyzed, and sets of conceptual helicopters are generated for each combination. Table 4.1 displays the candidate upgrade configurations generated from one set of parameters. Each column of Table 4.1 represents a different helicopter configuration that is capable of meeting the performance requirements stipulated in the RFP.

Table 4.1 - Calculations for 1 Independent Design Parameter Combination

Number of blades	2	2	2	2	3	3	3	3
Aspect Ratio	23.42	19.42	15.42	11.42	23.42	19.42	15.42	11.42
Empty Weight, lb	1852	1877	2147	2047	1727	1746	1807	1921
Empty W. Corrected, lb	1866	1891	2165	2062	1740	1759	1821	1935
Payload, lb	1521	1521	1521	1521	1521	1521	1521	1521
TO Weight, lb	3600	3633	3938	3844	3479	3509	3590	3739
Weight Efficiency	0.48	0.48	0.45	0.46	0.50	0.50	0.49	0.48

Number of blades	4	4	4	4	5	5	5	5
Aspect Ratio	23.42	19.42	15.42	11.42	23.42	19.42	15.42	11.42
Empty Mass, lb	1657	1683	1744	1876	1616	1650	1719	1858
Empty W. Corrected, lb	1669	1696	1757	1890	1628	1663	1732	1872
Payload, lb	1521	1521	1521	1521	1521	1521	1521	1521
TO Weight, lb	3418	3459	3544	3722	3388	3441	3540	3734
Weight Efficiency	0.51	0.51	0.50	0.49	0.52	0.52	0.51	0.50



4.9.1-Finalist Candidate Upgrades

A candidate configuration was chosen to advance to the selection pool only if its rotor diameter was within 1.7 ft of the original helicopter design. Because this is an upgrade program, a limit must be placed on how much baseline variation is allowed. Since the sizing of the main rotor defines the capabilities of the helicopter, major changes in its diameter cascade throughout the entire vehicle, resulting in a completely new aircraft rather than an upgraded version. As a result, only candidates with minor changes in rotor diameter were allowed to advance to the selection pool as finalists. Figure 4.3 displays a set of rotors calculated from one set of independent parameters.

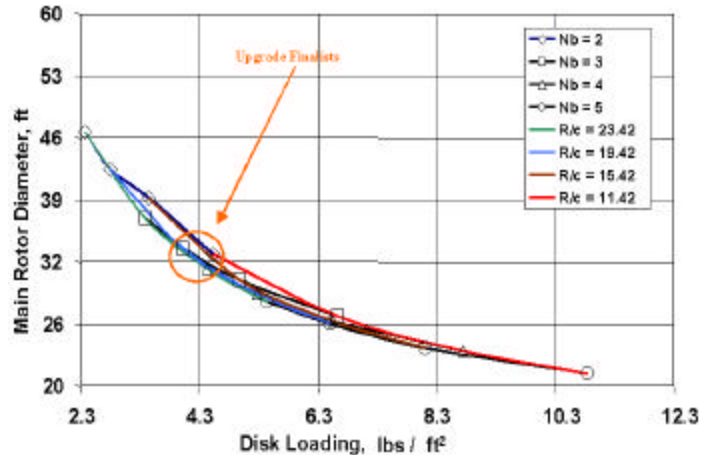


Figure 4.3 - Selection of Finalist Upgrade Configurations

4.9.2 - Final Selection of the Upgrade Configuration

The final arbiter for the selection process was the purchase price of the configuration. Ultimately, the least expensive configuration that meets the performance specifications was selected. For each independent parameter set, the cost of the helicopter was also determined. Figure 4.4 illustrates the acquisition prices for the set of independent parameters used to generate the helicopters given previously in Figure 4.3.

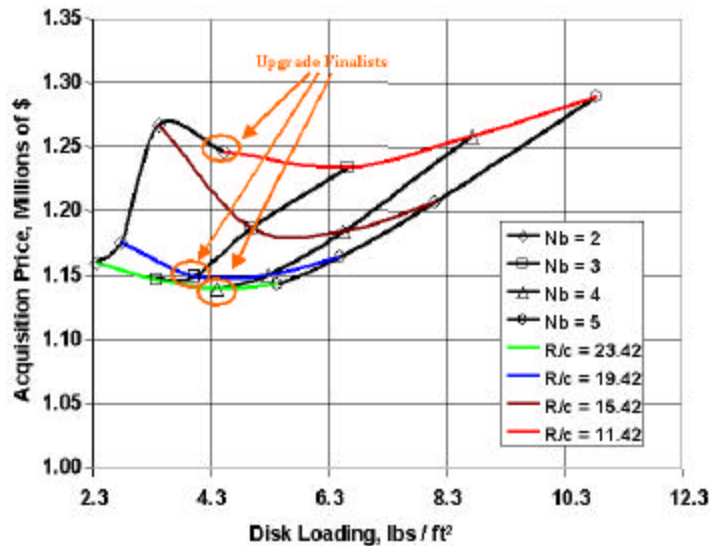


Figure 4.4 - Finalist Upgrade Configuration Costs
Nb = Number of Blades, R = Main Rotor Radius, c = chord

The acquisition price and independent parameters of each finalist upgrade are listed in Table 4.2. Configuration number 15 was selected as the final, optimized upgrade configuration.



Table 4.2 - Finalist Upgrade Configuration Pool

Configuration #	Ct/s (ratio)	Tip Speed (ft/sec)	Drag Area (ft ²)	Price Total (million \$)
1	0.08	673	5.5	1.23
2	0.08	673	5.5	1.14
3	0.08	673	5.5	1.13
5	0.08	673	6.0	1.27
6	0.08	673	6.0	1.17
7	0.08	673	6.0	1.16
8	0.075	686	5.5	1.25
9	0.075	686	5.5	1.16
10	0.075	686	5.5	1.15
11	0.075	686	6.0	1.29
12	0.075	686	6.0	1.19
13	0.075	686	6.0	1.18
14	0.075	673	5.5	1.25
15	0.075	673	5.5	1.15
16	0.075	673	5.5	1.14
17	0.075	673	6.0	1.29
18	0.075	673	6.0	1.19
19	0.075	673	6.0	1.17
20	0.08	673	5.5	1.23
21	0.08	673	5.5	1.15
22	0.08	673	6.0	1.27
23	0.08	673	6.0	1.18

4.10 - Summary of Final Configuration

Configuration 16 offers an affordable upgrade option that may be realistically developed. The blade loading coefficient of 0.075 is conservative, but assures that the rotor has an adequate stall margin that will be useful in meeting the 140 knot cruise requirement. Main rotor noise is minimized by choosing a reduced tip speed of 673 ft/sec which makes the upgrade more attractive to civilian operators that fly in developed areas. Although a reduction of the equivalent flat plate drag area to 5.5 ft² is optimistic, it is a reasonable goal for the upgrade program to achieve. Configurations 2 and 3 were also considered but ultimately rejected because of the higher blade loading, and subsequently, the lower stall margin. Details regarding the calculation of the drag area for the TerpRanger upgrade are given in Section 13. Finally, this 4-bladed main rotor configuration is one of the least expensive conceptual configurations considered in this study. (Refer to Table 4.2.)

Section 5 - Main Rotor Blade and Hub Design

The main rotor system is a key component in realizing the objectives stipulated in the RFP. As previously discussed, a preliminary sizing of the main rotor was carried out to determine the optimum number of blades,



rotor diameter, blade aspect ratio and solidity to achieve the required cruise speed, while also maintaining a low cost of the aircraft. The aerodynamic design of the rotor blades and the resulting rotor performance are discussed in detail in this section.

5.1 - Baseline Rotor

Power curves for the baseline helicopter (JetRanger) were matched with published data in the JetRanger product data book [Bell99]. This was done to validate the analysis tools that were developed in-house and also to match the equivalent flat plate drag area of the JetRanger.

The analysis tools are based on the assumption of constant inflow through the rotor disk. A rigid blade trim analysis was carried out at each advance ratio, and the shaft power required was determined from the rotor torque. A table lookup procedure was used for the airfoil properties. The analysis is capable of handling different airfoils along the blade span, arbitrary taper and arbitrary twist. Properties of the baseline rotor system are shown in Table 5.1, along with the properties of the new rotor. In Figure 5.1, the computed and actual power curves are compared for gross weights of 2000 lb and 3200 lb. Based on this analysis, the fuselage flat plate area for the baseline design was determined to be 6.5 ft².

Table 5.1 - Comparison of New Main Rotor with Baseline Design

Parameter	Baseline Design	TerpRanger
Max. gross wt. (lb)	3200	3524
No. of blades	2	4
Diameter (ft)	33.33	32.43
Tip speed (ft/s)	210	205
Solidity	0.0414	0.0525
Fuselage flat plate area (ft ²)	6.5	5.5
Blade Loading, C _T /s	0.078	0.075
Twist	-10° (linear)	-13° (linear)

5.2 - Aerodynamic Design of the Blades

The baseline JetRanger blades have a symmetric airfoil section with a modified leading edge, and a rectangular planform with -10 degrees of linear twist [Pegg69]. Since the Mach number and Reynolds number vary widely over the blade span, a single airfoil section along the blade generally does not provide optimum aerodynamic efficiency. With the availability of composite materials for blade construction, it is convenient to use different airfoil sections along the blade span to increase the efficiency of the rotor system and keep costs to a minimum. Twist and taper are also used to improve the performance of the rotor. Figure 5.2 displays the power curve for the TerpRanger, with the new four-bladed rotor.



5.2.1 - Airfoil Sections

The major factors influencing airfoil selection were: lift-to-drag ratio, maximum lift coefficient, drag divergence Mach number, zero lift, and pitching moment. For optimizing performance, three airfoil sections were used along the blade span. Due to its high maximum lift coefficient, the Boeing/Vertol VR-12 airfoil was used as the main lifting airfoil over 60-90% of the blade radius. However, the VR-12 airfoil produces high pitching moments. To offset these pitching moments, the ONERA OA-212

airfoil was used inboard of 60% radius, because it has a reflexed camber to produce nose down pitching moments. Finally, the Boeing/Vertol VR-15 airfoil, which has a low thickness-to-chord ratio and hence a higher drag divergence Mach number, was chosen for the tip region.

5.2.2 - Twist and Taper

Tapering the blade improves performance by unloading the tips to achieve a more uniform inflow distribution over the blade. The outermost 8.5% of the blade planform is tapered. Blade twist can be used to improve hover performance, delay retreating blade stall and reduce vibrations in forward flight. However, the maximum amount of blade twist is limited by criteria for safe autorotation. The blades were designed to have a linear twist of -13 degrees, which is the amount of twist on the Bell-407 rotor blades. Although a larger twist provides better hover performance, it would degrade the autorotational performance of the rotor.

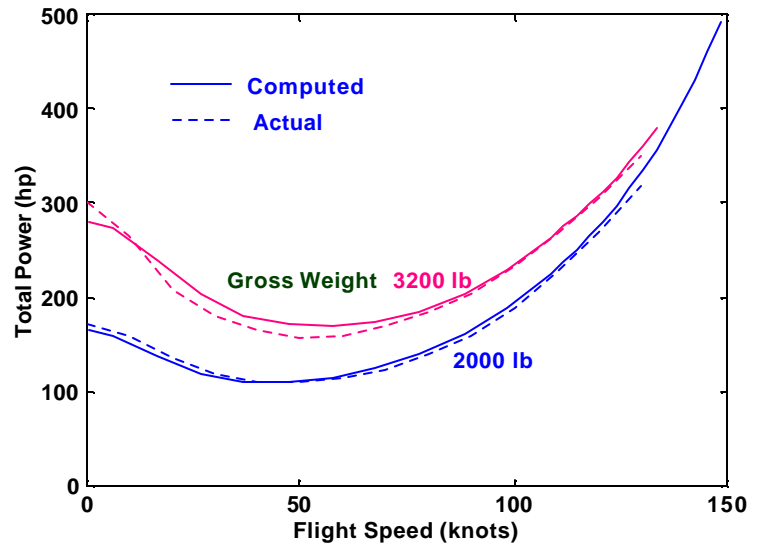


Figure 5.1 - Comparison of Actual and Computed Power Curves for the Baseline Helicopter (SL/ISA)

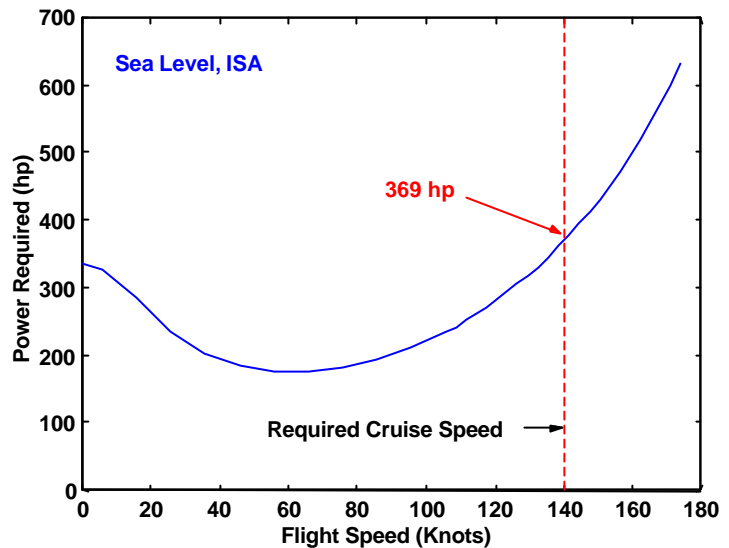


Figure 5.2 - Power Curve for the TerpRanger, GTOW = 3524 lbs



5.2.3 - Blade tips

The blade tips of the advancing blades encounter the highest dynamic pressure and Mach numbers. This is why special care needs to be taken in the design of an advanced tip shape. Three key parameters (sweep, taper, and anhedral) can be introduced to obtain improvements in rotor performance.

Sweep is used to reduce the Mach number normal to the leading edge of the blades, delaying to higher advance ratios the onset of the adverse effect of compressibility. In the TerpRanger, the maximum advance ratio and tip Mach number are 0.35 and 0.82 respectively. The drag divergence Mach number of the airfoil used at the tip (VR-15) is around 0.82. As shown in Figure 5.3, the blade tip is swept-back 20° starting at the outer 8.5% of the blade, which corresponds to the end of the transition region between the VR-12 and the VR-15 airfoils.

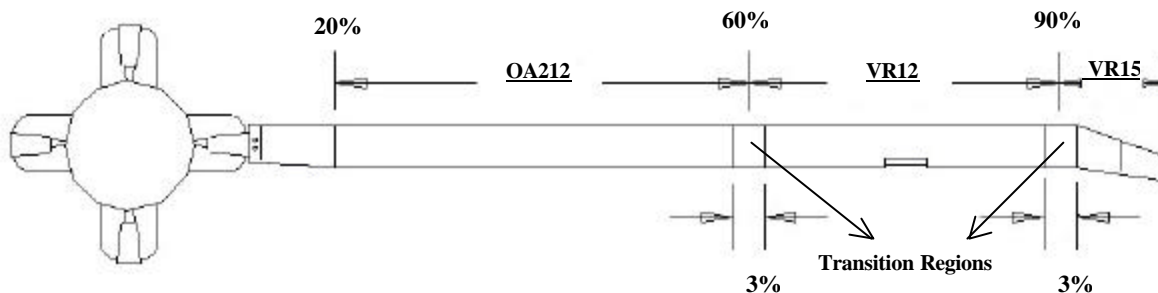


Figure 5.3 – Rotor Blade Planform

The introduction of anhedral and taper in the blade tips can significantly increase the Figure-of-merit of the rotor. Experimental studies ([Deso88]) on swept-tapered blade tips with anhedral, show that the power required to drive the rotor is reduced by up to 7% in hover and up to 10% in forward flight, when compared to the power required for rectangular blade tips. However, this large enhancement is obtained at blade loading coefficients of 0.07, and at an advance ratio of 0.4. For the thrust coefficients and maximum advance ratio of the TerpRanger, a reduction in power of 3% in hover and 4% in forward flight was achieved. A taper ratio of 1.6:1 over the outer 8.5% of the blade section, and an anhedral of 5° in the outer 4.25% of the blade were selected. Experiments also show that the use of a similar tip configuration reduces the noise produced by the rotor [Deso88].

5.3 - Blade Structural Design

The blades must be designed to withstand not only the centrifugal force, but also the flapping, lead-lag and torsion moments. Furthermore, the blades must also have adequate mass so as to give satisfactory autorotational inertia.



5.3.1 - Blade Structural Details

The blade consists of a D-shaped spar and an outer skin made up of two layers of glass/epoxy (+45°/-45°) composite. The spar is made up of a torsion wrap consisting of six (+45°/-45°) layers of graphite/epoxy enclosing fourteen uniaxial layers of glass/epoxy composite. Nomex honeycomb has been used for the core since it provides a good bond with the skin, and also because it has low moisture absorption. Tungsten ballast weights are placed at discrete locations along the blade span to move the blade center of mass to the quarter chord position. A de-icing blanket is bonded over the skin to heat the leading edge, and a titanium erosion strip protects the leading edge from particle damage. A cutaway of the blade cross-section is shown in Figure 5.4.

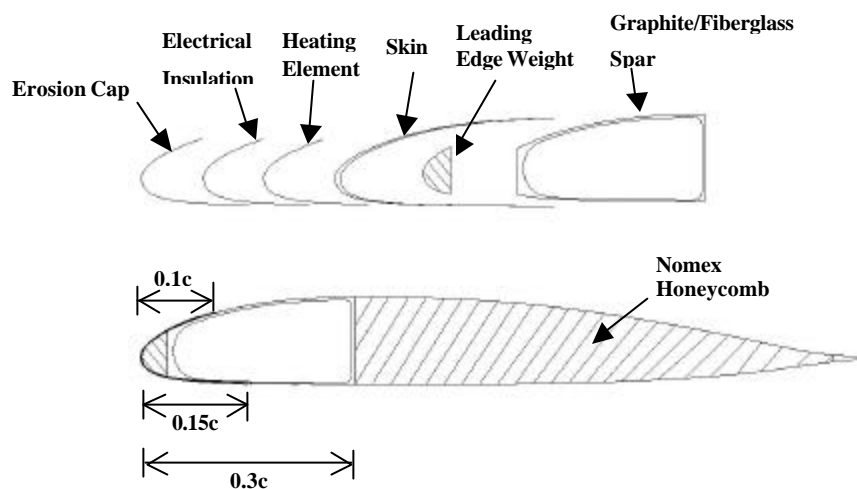


Figure 5.4 – Blade Cross-section

Table 5.2 lists the material properties of the different materials used.

Table 5.2 - Material Properties

Material	Density (lb/in ³)	Young's Modulus (ksi)	Shear Modulus (ksi)	Nominal ply thickness (in)
Glass/Epoxy	0.072	6.3×10^3	0.66×10^3	0.0069
+45° Graphite Epoxy	0.055	8.03×10^3	6.31×10^3	0.009
Nomex Honeycomb	0.00116	0.0105×10^3	0.0042×10^3	-
Tungsten	0.669	40×10^3	19.2×10^3	-

5.3.2 - Lightning Protection and Electromagnetic Shielding

Helicopter rotor blades are usually designed to withstand a 200 kA lightning strike and still permit flight of limited capability so that the aircraft can safely return to base [Alex86]. To prevent heat damage of critical composite components, it is preferred that the path of current flow be along the exterior of the blade. Also, the actuator assembly for the active tracking tab (see section 9.5) is vulnerable to any large flow of current. Parts of



the blade which contain large internal masses of metal are covered by exterior doublers made of conductive material. These doublers conduct the current to the titanium abrasion strip, which drains it along the blade to the root end attachment. To protect the actuator from stray electromagnetic fields, its housing is wrapped in nickel/iron alloy foil, which is effective for low frequency magnetic shielding.

5.4 - Hub Design

The main rotor hub must transfer blade loads from the rotating frame to the fixed frame, transfer the drive system torque to the rotor, and transmit collective and cyclic pitch changes from the fixed frame to the rotor blades. These functions must be performed while maintaining a low weight, low drag in forward flight, mechanical simplicity and low parts count, long fatigue life, freedom from dynamic problems, and sufficient control power. For an upgrade program, a key factor is the cost involved in production and certification. To minimize this cost, a hingeless design, which is a downsized version of the Bell-412 hub, was chosen to minimize development risk.

The hub consists of two composite flexbeam yokes, four steel spindles with grip lugs to hold the blades, and elastomeric dampers and bearings. A pitch horn has one end connected to the steel spindle and the other end attached to a pitch link. The design reduces maintenance by providing longer life components, and elastomeric bearings to eliminate the need for mechanical hinges and heavy viscous dampers.

5.4.1 - Hub Details

As shown in Foldout 5.1, the hub primarily consists of three components: flexbeam yokes, steel spindles and elastomeric bearings and dampers.

- a) Flexbeam yoke: The flexbeam transfers centrifugal force from the blades to the hub support structure, and also allows blade flapping motion. Two yokes, made from unidirectional S-glass/epoxy composite and attached perpendicular to one another, serve as the flexbeams. The flexbeam cross-section is tailored to provide the required stiffness along the span.
- b) Steel spindles: Four steel spindles are used to achieve blade pitch motion. A pitch horn is attached to one end of the spindle while the other end anchors the blade through two retention bolts arranged chordwise.
- c) Elastomeric bearings and dampers: An elastomeric pivot bearing is used to attach the spindle to the outboard end of the yoke, so that the spindle can pitch independent of the yoke. This pivot bearing also transfers centrifugal force from the spindle to the yoke. The inboard end of the spindle has a spherical bearing and an elastomeric lead-lag damper. Rotation about the pivot bearing and damper deflection at



the inboard end of the spindle facilitates the lead-lag motion of the blade. Blade pitch change is achieved through torsional deflection of the pivot bearing and rotation of the damper bearing.

5.5 - Autorotation Characteristics

Autorotational performance of a helicopter depends on a number of factors, including the rotor disk loading and the stored kinetic energy. Since it is difficult to analyze autorotation performance of a helicopter, an autorotation index is generally used to compare the autorotation performance with that of existing helicopters that have acceptable autorotative characteristics. Table 5.3 lists the autorotation index (which is defined as the kinetic energy of the rotor divided by the product of the gross weight and disk loading) of the TerpRanger along with that of several other helicopters of similar weight. A larger value of this index indicates better autorotational characteristics. As can be seen from this table, the TerpRanger has good autorotation characteristics compared with the other helicopters.

Table 5.3 - Autorotation Characteristics Comparison

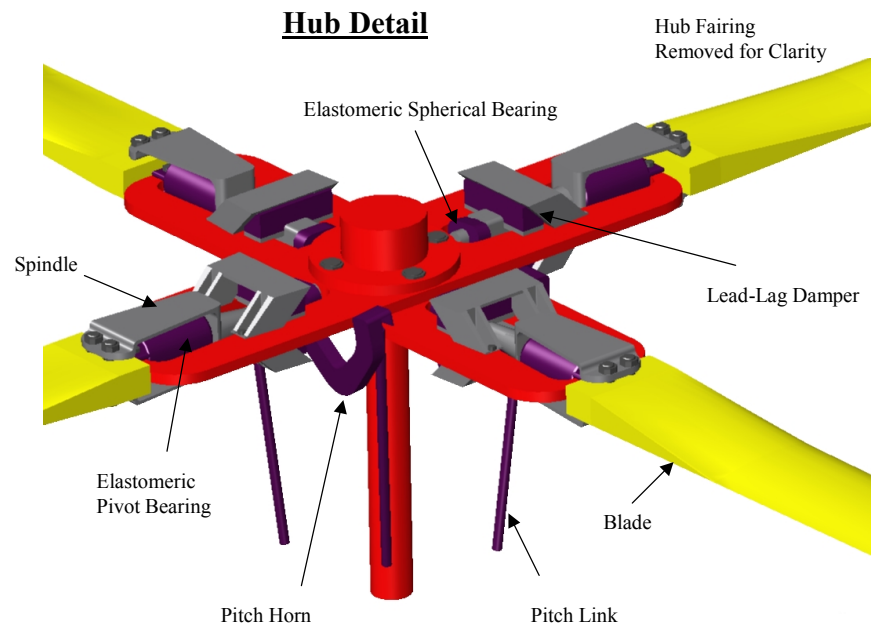
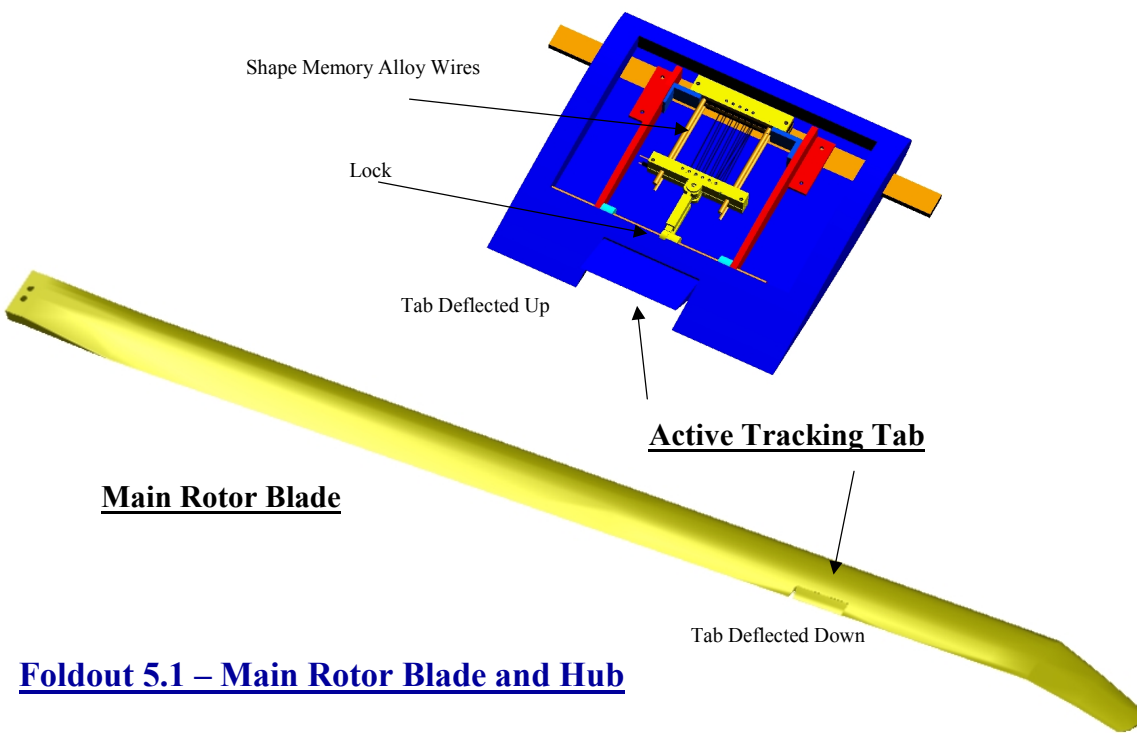
Helicopter	GTOW, (lb)	Polar Moment of Inertia, I_{Ω} (slug-ft ²)	Rotor Speed, Ω (rad/sec)	Disk Loading, (lb/ft ²)	Autorotation Index, (ft ³ /lb)
TerpRanger	3524	439.95	41.5	4.24	25.52
JetRanger	3200	510.00	41.4	3.67	37.22
MD-500E	3000	288.61	49.95	5.48	21.90
MD-900	6000	529.45	41.05	6.67	11.15

5.6 - Rotor Dynamics

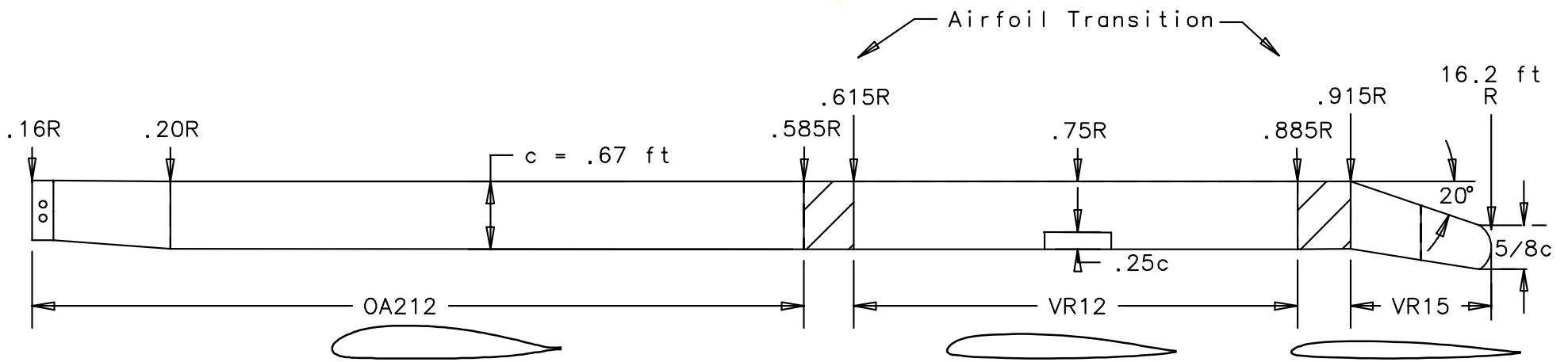
The main rotor is a soft in-plane, hingeless design, and hence its dynamic characteristics have been carefully examined to ensure proper placement of frequencies, and to maintain a sufficient safety margin from aeromechanical instabilities. Table 5.4 lists the important properties of the new main rotor.

5.6.1 - Dynamic Analysis

The University of Maryland Advanced Rotorcraft Code (UMARC) was used to obtain a rotor fan plot. The blade was modeled using 14 finite elements, 10 for the blade, and 4 for the flexbeam. Blade section inertia and stiffness properties were determined for the three airfoil cross-sections as shown in Figure 5.5. The spike in the blade mass distribution shows the location of the SMA actuator for the active tracking tab. The blade has been designed so that the rotating blade frequencies are well separated from the rotor harmonics, as shown in the fan diagram (Figure 5.6)



Foldout 5.1 – Main Rotor Blade and Hub



Blade Planform and Airfoils



Table 5.4 – Main Rotor Design Parameters

Radius	16.22 ft
No. of blades	4
Chord	0.669 ft
Tip speed	672.40 ft/s
Nominal operating rpm	396
Solidity	0.0525
Lock number	5.3
Twist	-13° (Linear)
Blade Flapping moment of inertia	109.98 slug-ft ²
First lag frequency	0.67 /rev
First flap frequency	1.064 /rev
First torsion frequency	4.32 /rev

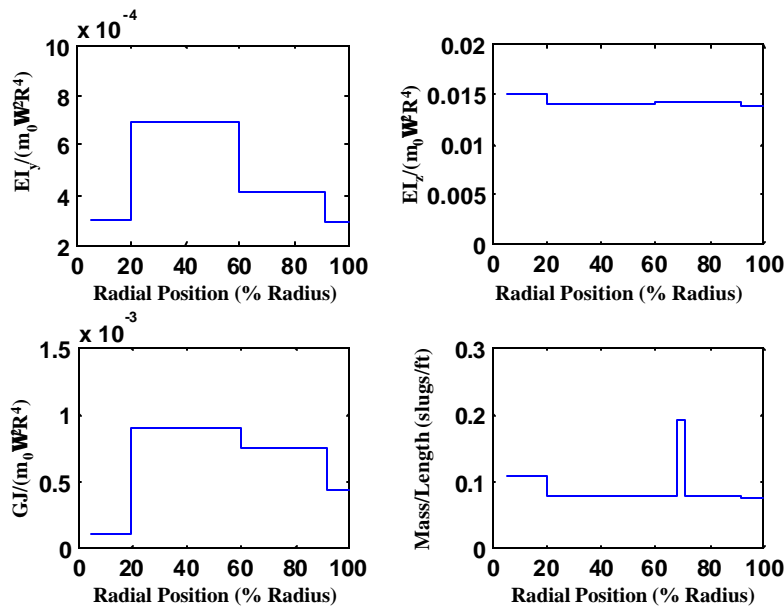


Figure 5.5 – Blade Stiffness and Mass Distribution

5.6.2 - Aeroelastic Stability Analysis

To ensure that the rotor does not encounter any aeromechanical instability in its flight regime, an aeroelastic stability analysis was carried out. A pitch-flap flutter analysis in hover shows that the critical CG offset is aft of the quarter chord position at nearly 32% of the chord from the leading edge (Figure 5.7). Tungsten tip weights were used to bring the blade CG close to the quarter chord position to maintain an adequate safety margin. A comprehensive analysis shows that the rotor modes are stable for all flight speeds over the entire flight envelope (Figure 5.8).

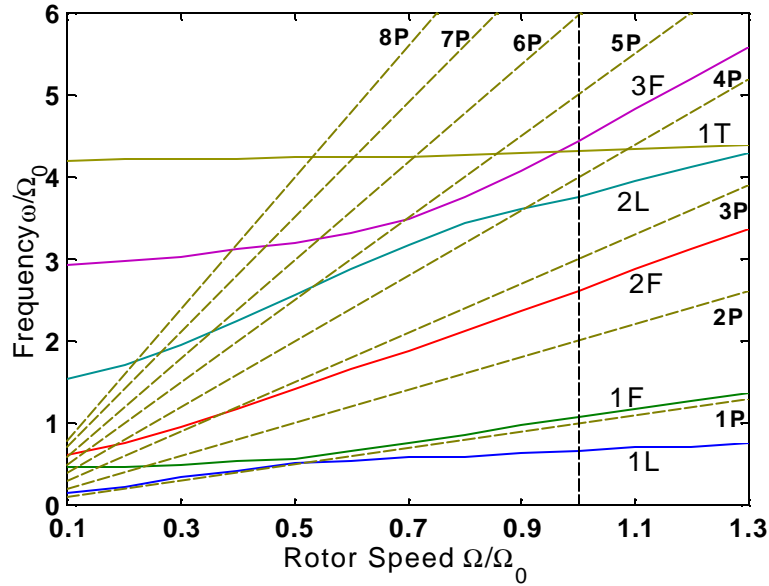


Figure 5.6 – Rotor Fan Plot

5.6.3 - Ground Resonance

The original JetRanger has a two-bladed, teetering main rotor, which is stiff in-plane, and hence free from any ground resonance instability. Since the new main rotor is soft in-plane, it may be susceptible to ground resonance, and hence adequate provisions must be made to ensure that the rotor and support modes are adequately damped at all rotor speeds.

A ground resonance analysis showed that the rotor in-plane mode (regressive) was stable, as shown in Figure 5.9. In this analysis, the body pitch and roll frequencies have been assumed to be the same as for the Bell model 654 rotor installed on the Bell-206L [Cres78]. The lead-lag damper has a damping value of 910.6 lb-ft-s.

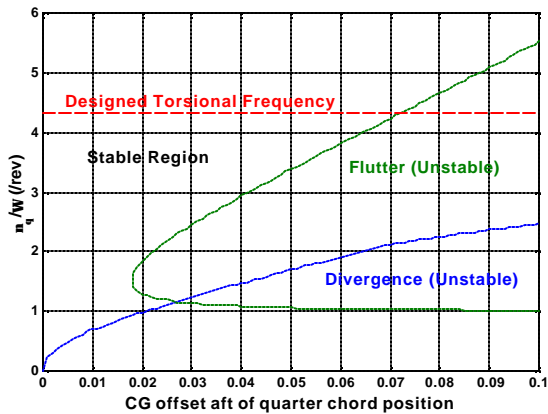


Figure 5.7 - Pitch-Flap Flutter/Divergence Stability Boundaries

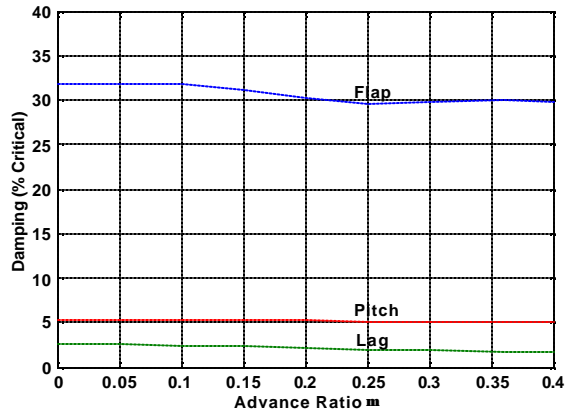


Figure 5.8 - Flap/Lag/Pitch Stability

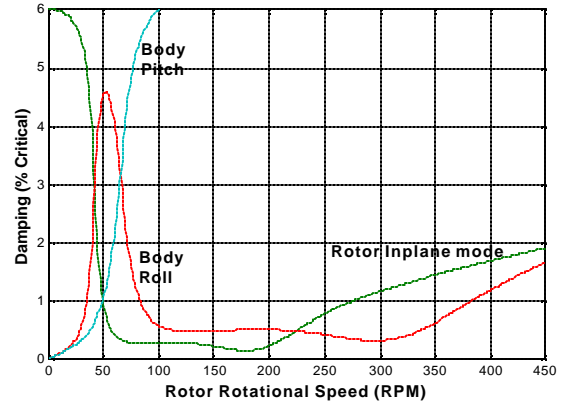
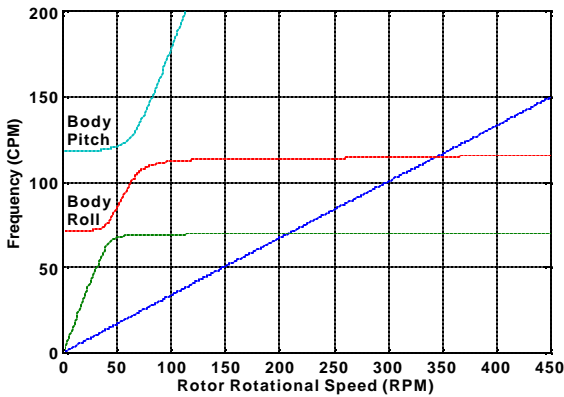


Figure 5.9 – Ground Resonance Analysis

A soft-inplane rotor is also susceptible to air resonance, which is an instability similar to ground resonance, but occurs in flight, because of the interaction of the rotor lag and flap modes with the fuselage pitch and roll modes. To ensure that the rotor is safe from air resonance, a comprehensive stability analysis was carried out assuming the fuselage to be undergoing rigid body motions. As shown in Figure 5.10, the rotor lag mode (regressing) remains stable at all advance ratios.

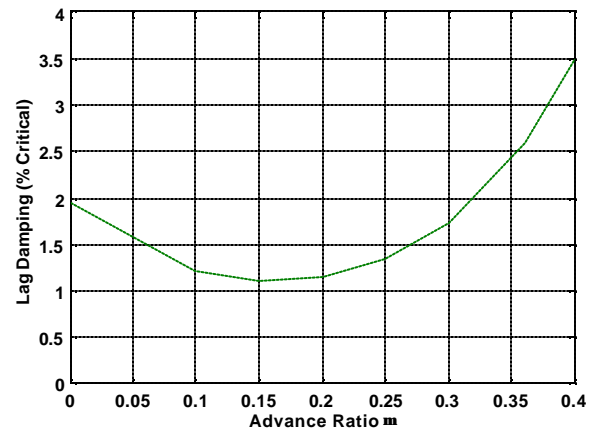


Figure 5.10 - Air Resonance Analysis

Section 6 - Anti-Torque System and Empennage Design

The primary purpose of the anti-torque system is to provide yaw control for the helicopter. The system must not only be capable of counteracting the reaction of the main rotor, but also provide the pilot with directional control. This section discusses the relevant design issues regarding the anti-torque system.

6.1 - Anti-Torque Configuration Selection

A complete redesign of the anti-torque system is not practical in an upgrade program due to high remanufacturing costs. A trade study based on weight and power efficiency was conducted to choose the most efficient configuration capable of meeting the RFP specifications. Configurations such as a conventional tail rotor, fan-in fin, and a NOTAR system were considered in this trade study.



6.1.1 - Weight Comparison of Anti-Torque Configurations

A fan-in fin configuration requires more structural weight than a conventional tail rotor. A more robust support structure is required to compensate for the high gyroscopic moments transferred across the pitch change bearings, through the hub and shaft into the load carrying members. Therefore, the weight of the fan-in-fin configuration typically, is about 14% higher than the weight of a conventional tail rotor [Moui70].

Similarly, the NOTAR configuration also requires reinforcement of the load carrying members [Robi70]. Despite the fact that the overall weight of the NOTAR configuration is approximately equal to that of a conventional tail rotor, the cost and remanufacturing effort involved with integrating such a system into an existing helicopter exceeds the scope of an upgrade program.

6.1.2 - Power Comparison

The method of Robinson [Robi70] was used to estimate and compare the induced, and profile power requirements of a conventional tail rotor, NOTAR, and fan-in-fin configurations. According to the analysis, in hover, the fan-in fin consumes 6% more of the main rotor power than a conventional tail rotor, whereas the NOTAR configuration consumes 11% more power.

The NOTAR and fan-in-fin configurations are heavier and require more power in hover than a conventional tail rotor configuration due to the higher induced power requirement. Therefore, the tail rotor configuration is unchanged in the TerpRanger upgrade.

6.2 - Rotor/Hub Assembly

The TerpRanger Upgrade will include a composite, bearingless tail rotor (CBR) system. This configuration has been flight tested on the Bell206 JetRanger with satisfactory results [Harv79]. The CBR tail rotor is advantageous because it is a corrosion free, “on-condition” rotor system. The parts count is reduced by 25%, weight by 30%, and manufacturing costs by 20% [Fena76].

A fiberglass twist-strap flexure is included to accommodate collective pitch control, and a shear reaction device counteracts the pitch link loads [Harv79]. The design is cost effective, and is already certified for the Bell 206 JetRanger.



6.3 - Design Parameters

A first-order analysis was developed and implemented for sizing the tail rotor. The JetRanger's tail rotor baseline design parameters were used to validate the analysis. The design flight condition is hover, since as forward speed increases, the vertical fin offloads the tail rotor.

6.3.1 - Tail Rotor Diameter

The tail rotor diameter is sized to provide both anti-torque thrust, and yaw control. The analysis is adopted from Prouty's sizing techniques [Prou95]. According to this method, the diameter of the tail rotor is a function of the main rotor diameter and disk loading. The tail rotor diameter is determined by the following equation:

$$D_T = \frac{D_M}{7.15 - 0.27 DL_M}$$

where D_M is the main rotor diameter, and DL_M is the disk loading of the main rotor.

For the TerpRanger upgrade, the tail rotor diameter is 5.4 ft.

6.3.2 - Tail Rotor Chord

Once the sizing of the tail rotor diameter was completed, the chord was determined. A blade chord of 0.46 ft is required to achieve a maximum turn rate of 0.75 rad/sec, and a maximum yaw acceleration of 0.4 rad/sec² [Lynn69]. The following equation is used to determine the tail rotor blade chord:

$$c = \frac{6}{c_{l_{\max}} r b (BR)^3 \Omega^2} \left(T_Q + \frac{I_{zz} \ddot{\mathbf{y}}}{l_t} + \frac{8b\Omega l_p \dot{\mathbf{y}}}{3(BR)} \right) \text{ ft}$$

where, T_Q is the required tail rotor thrust, $\ddot{\mathbf{y}}$ is the maximum yaw acceleration, $\dot{\mathbf{y}}$ is the maximum turn rate, B is the tip loss factor, R is the tail rotor radius, and Ω is the rotor rotational speed [Lynn69].

6.4 - Empennage Design

The empennage consists of a vertical fin, horizontal stabilizer and associated fuselage support structure. In conventional helicopter designs, the purpose of the stabilizers is to enhance stability about a particular axis and offload the tail rotor in forward flight.

In this preliminary design study, the vertical fin is sized to offload the fan, whereas the horizontal stabilizer is sized to provide sufficient stability about the pitch axis. The parameters of the existing stabilizers on the Bell 206 are included in the performance analysis to determine if they satisfy the current design upgrade



requirements. It was found that the current vertical fin is sufficient to offload the tail rotor in forward flight, to about 50% in cruise. Similarly, the current horizontal stabilizer dimensions provide sufficient stability about the pitch axis in forward flight. Therefore, it is not necessary to redesign the stabilizers for the upgrade; hence, no extra cost or weight is incurred for empennage re-design.

6.5 - Power Requirement

The tail rotor power requirement as a function of forward speed is shown in Figure 6.1. The results show that the power required by the tail rotor decreases sharply from hover to cruise. The tail rotor thrust required to balance the main rotor torque is significantly reduced in forward flight due to an increase of the vertical stabilizer's side for

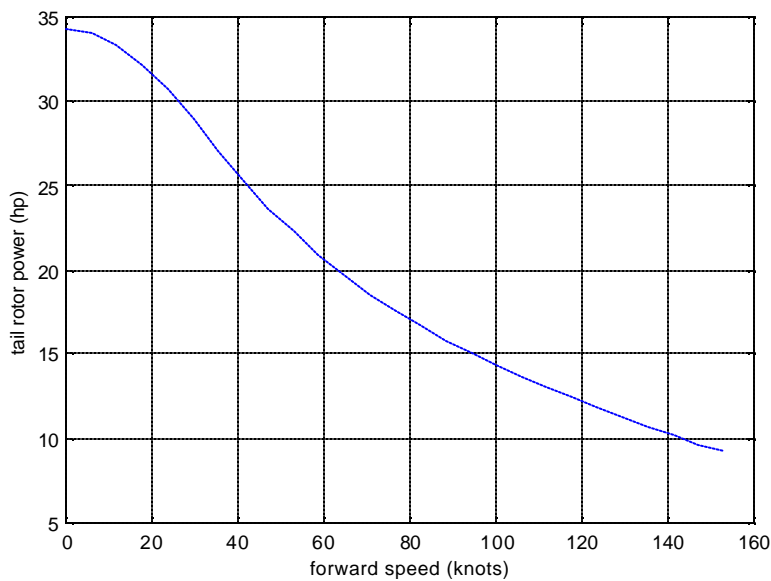


Figure 6.1 – Tail Rotor Power vs. Forward Speed

Table 6.1 - Final Design Configurations

Tail Rotor Parameter	Baseline Tail Rotor	TerpRanger Tail Rotor
Diameter	5.42 ft	5.4 ft
Chord	0.5 ft	0.46 ft
Solidity	0.12	0.1073
Number of blades	2	2
Rotor speed	2550 rpm	2378 rpm
Tip speed	723.6 ft/s	672.4 ft/s
Airfoil	NACA 0012	NACA 0012
Material	Metal	Fiberglass



Section 7 - Powerplant and Propulsion System Design

The powerplant and transmission are important elements in realizing optimum vehicle performance. By carefully selecting and designing these components, an aging helicopter such as the JetRanger can be upgraded to become a more versatile rotorcraft. This section presents the details of the engine and transmission design.

7.1 - Engine Selection

During the design process, a parallel engine development was undertaken. The size and weight, as well as the specific fuel consumption (SFC) of this future engine, were obtained using the formulae provided in the RFP. A comparison between existing engines and the hypothetical RFP engine is presented in Table 7.1.

Table 7.1 - Comparison of Engine Characteristics [Ahds01]

Manufacturer	Model	Takeoff rating (shp)	SFC (lb/hp.hr)	Dry weight (lb)	Envelope length (in)	Envelope Diameter (in)	Power/Weight ratio
Rolls-Royce	250-C20J	420	0.650	161	38.8	23.2	2.61
RFP		525	0.538	147	24.98	15.57	3.57
Turbomeca	Arrius 2F	504	0.543	227	37.2	27.4	2.22
Honeywell	LTS 101-100A-3	615	0.58	253	31.0	22.4	2.43

The powerplant specified in the RFP is consistent with the efforts made by the Integrated High Performance Turbine Technology program (IHPTET). This joint program between government and industry has the objective of developing a new generation of engines that are capable of more than doubling the current engine power-to-weight ratio, and reducing the specific fuel consumption by 40% [Hirs01].

7.2 - Engine Performance

Table 7.1, shows that the weight and size offered by the RFP powerplant is superior to that of existing systems. Compared to the less powerful Rolls-Royce 250-C20J engine installed in the 206B-III, the RFP engine offers an 8.7% weight savings and an SFC 83% that of the Rolls-Royce 250-C20J. The SFC of the RFP engine is similar to that of the Turbomeca Arrius 2F. However, the RFP engine is lighter by 80 lb and has an engine envelope volume that is 78% that of the Turbomeca Arrius 2F.



To determine the maximum power required by the engine, a detailed analysis was developed for the vertical and forward flight performance (Section 13). The results establish that for a cruise speed of 145 knots at 1000 ft ISA the engine must generate at least 390 hp. The engine power available is directly proportional to the density ratio, so at sea level, the engine can deliver a maximum continuous power of 400 hp. In the RFP, maximum continuous power is defined as 80% of the takeoff power,

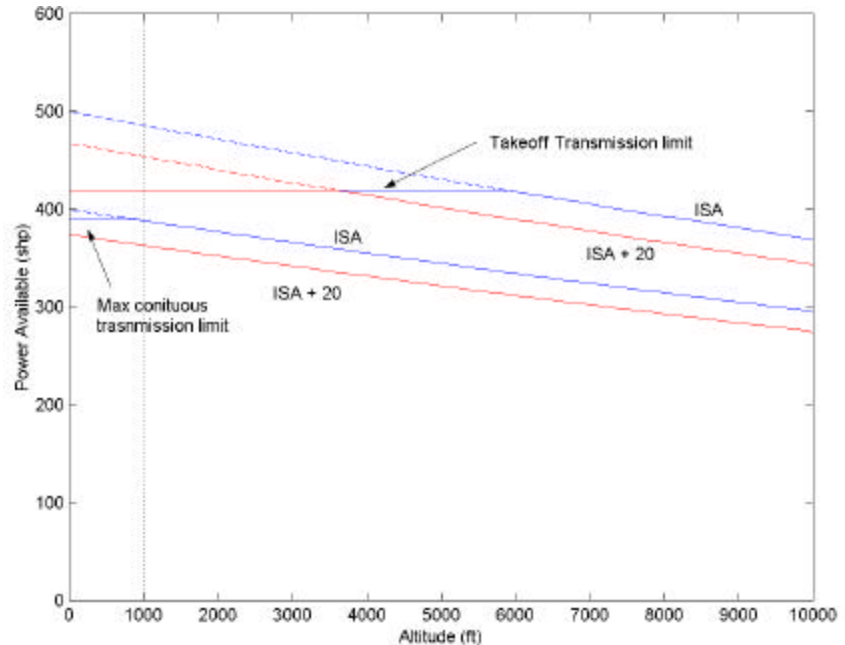


Figure 7.1 - Engine Power Available vs. Altitude

therefore an engine with 500 shp of takeoff power installed at sea level is required. The effect of altitude and temperature on the power available for the RFP engine is shown in Figure 7.1.

Following the standards in engine design, the specified powerplant was assumed to have an integrated intermediate gearbox with a reduction ratio of 1:3.48, providing an output rotational speed of 6035 rpm. In this way, the engine and the helicopter main gearbox can be directly coupled via the free-wheeling unit and the main drive shaft (refer to Section 7.5.7).

7.3 - Engine Losses

The TerpRanger requires an installed takeoff power of 500 shp. This power is obtained after the installation losses are subtracted from the maximum uninstalled power given by the engine manufacturer's tests. Losses associated with engine installation can be divided into 3 main categories: inlet losses, exhaust losses and losses due to bleed air extraction. The losses produced in the auxiliary gearbox are also included. Based on the data presented in [Prou95], installation losses of 5% were assumed.

7.4 - Structural Integration

The engine is located behind the main gearbox on the roof of the intermediate section of the fuselage between two firewalls, and is supported by two A-frames and a torque line that include "clam shell" dampers to reduce the noise transmitted through the struts. The new engine is lighter and smaller than the one originally installed in



the 206B-III, however since the power transferred is larger, the loads on the supports are increased. The reduction in length of the new engine increases the available inner space in the cowling. Since the new engine is assumed to have a single exhaust port in its aft section, the exhaust pipe is reconfigured. Changing the location of the exhausts to the port side of the cowling, reduces the parasitic drag of the fuselage, enhancing the forward flight performance of the helicopter (refer to Foldout 7.1).

7.5 - Transmission Design

The power required to attain the cruise speed of the upgraded helicopter (390 shp) exceeds the original Bell 206 JetRanger transmission and gearbox ratings by approximately 120 shp. As a result, a new transmission capable of handling the larger continuous and transient loads is necessary.

7.5.1 - Design Strategy

The original Bell 206 JetRanger airframe has undergone a large growth in takeoff weight over the years. Table 7.2 shows the sequence of rating increases for the main transmissions and tail rotor gearbox in the model 206 helicopter family. The general configuration of the transmission did not change in the different models, and no major modifications were performed in increasing the takeoff power rating from 317 to 650 shp.

Table 7.2 - Transmission ratings in hp [Harr86]

	TO Power	Max Continuous	Tail Rotor Continuous	Tail Rotor Transient
OH-58A	317	298	63	94
206L	420	370	80	100
206L-1	435	370	80	130
406(Kiowa)	650	464	110	220

Two different design options were considered in the present transmission design process. The first alternative consists of using a previously upgraded main gearbox that has a rating that meets the TerpRanger's power requirements. In this case, only changes and adaptations in the mounting configuration were required. This is a simple and inexpensive solution that avoids involvement into the expensive certification process that would be required for a new transmission. The only drawback of this strategy is that even the upgraded transmission models use relatively old technology (late 1960's to early 1970's) and are likely to be heavier than modern transmissions with similar power ratings.

The second alternative is the improvement and redesign of an existing transmission, keeping the same configuration but improving its overall characteristics with new materials and higher Hertz stress levels. The



introduction of new technology not only saves weight, it also provides an extension in life of the components, which in turn results in reduced operating costs.

This design strategy best suits the project characteristics, and is explained in detail in the following sections.

7.5.2 - Transmission Configuration

The transmission configuration used in the Model 206 series and its derivatives has a simple and robust design that has proven to be very reliable. For this reason, this general transmission arrangement will be kept in the newly designed transmission of the TerpRanger.

The design maximum torque and speed for the first generation OH-58A main rotor transmission is 3291 in-lb (372 N-m) input torque and 6060 rpm input speed. This corresponds to 298 shp (236 kW) for takeoff and 270 shp (201 kW) for continuous ratings. The transmission is a two-stage reduction gearbox (Figure 7.2). The first stage is a spiral bevel gear set. Triplex ball bearing and one roller bearing support the bevel gear shaft in an overhung configuration. A planetary mesh provides the second reduction stage. The same shaft holds the bevel gear and the sun gear. The sun gear drives three planets. The planet gears mesh with a fixed ring gear attached to the transmission housing. The planet gears are supported by double-row spherical roller bearings attached to the planet carrier. Power is taken out through the planet carrier splined to the output mast shaft. The output shaft is supported on top by a split-inner-race ball bearing and on the bottom by a roller bearing; the overall reduction ratio of the main power train is 15.23:1. The bevel gear also drives an accessory gear that runs an oil pump, which supplies lubrication through jets and channels located in the transmission housing. This drive system has undergone considerable growth in rating since its original development in 1962. The most significant improvements that have contributed to the main transmission increase in power rating are:

- A change from three to four pinion planetary gear assembly,
- Improved gear mounting,
- Increased gear life achieved through material and processing improvements and change to larger bearings,
- Shot-peened gear teeth, and
- Increased face width of input bevel gears.

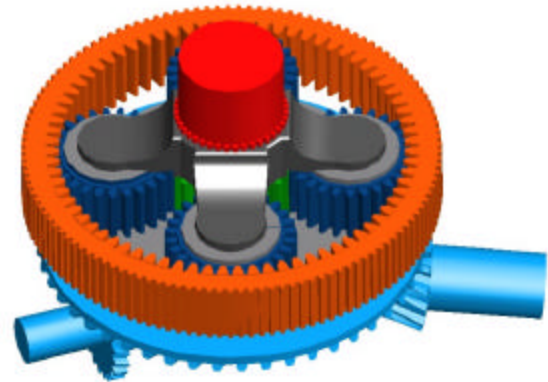


Figure 7.2 – Transmission Configuration



The transmissions listed in Table 7.2 keep a similar internal arrangement, however the housings are modified from model to model depending on the mounting configuration.

It was assumed that the input rotational speed of the TerpRanger transmission is 6035 rpm (refer to Section 7.2), and the transmission reduction ratio was kept at 15.23:1 to obtain the required rotor rotational speed of 396 rpm and tip speed of 205 m/s.

7.5.3 -Transmission Optimization Process

Based on the 390 shp maximum continuous power required at cruise, the drive system installed in the Bell LongRanger 206L was selected as the baseline system to carry out the analysis. Its power rating is 370 shp maximum continuous and 420 shp at takeoff, similar to those of the TerpRanger. The characteristics of the 206L transmission are obtained after developing a model based on the Bell JetRanger drive system whose main design parameters are known [Bell99].

7.5.4 - Weight Estimation

One of the most relevant parameters required in the analysis is the weight of the LongRanger 206L transmission since it will serve as reference point for an optimized design. The weight of a transmission depends on its configuration, gear design, design power, and the technology used. A detailed model of the two stages of the transmission was developed using Dudley's method [Dud184], [Dud154], [Dud192]. Gear size, bending and compressive stresses were calculated. The model was tuned to match closely the overall dimensions, and stresses of the OH-58A helicopter obtained from Ref [Lewi92] as well as the weight and dimensions of the JetRanger III. Weight estimation is performed using the stress values calculated with the detailed model of the drive system. A nondimensional Hertz stress index factor Sa , function of Hertz stress (Sc), Pressure angle (θ), and helix angle (Φ) is used to compare the effect of Hertz stress on weight [Dyes91]. The Hertz stress index factor Sa is given by

$$Sa = \left(\frac{Sc}{158793} \right) \cdot \left(\frac{\sin 2q}{\cos^2 \Phi} \right) + \left(\frac{\frac{Sc}{1000}}{14\Phi^2 - 9.5\Phi + 315} \right)^{0.494}$$

The equation for estimating each gearbox section weight is given by:

$$W = 150 \cdot \left(\frac{Q \cdot P \cdot U \cdot A \cdot B}{Sa \cdot N} \right)^{0.8}$$



Where Q is a nondimensional weight factor defined for every gear configuration (spur, bevel, planetary), P is the design horsepower of the gear assembly, N gear rotational speed, Sa is a hertz stress index, and A, B and U are factors used to include structural characteristics and special features of the transmission in the weight estimation. Weights of the shafts, bearings and lubrication system are also included using a series of empirical relationships found in [Schm76].

Table 7.3 -TerpRanger Weight Estimation Factors

Parameter	Bevel Stage	Planetary Stage
P	420	420
Q	2.8167	1.2361
A	0.7	1
B	1.1	1.05
U	1	1
N	6035	1810
Sa	0.995	0.762
Weight (lb)	33.3	71.7

Table 7.4 - TerpRanger Estimated Transmission Weight Breakdown

Component	Weight (lb)
Bevel Stage	33.3
Planetary Stage	71.7
Shafts & Bearings	24.4
Additional Case Weight	14.2
Structural Supports	10.2
Integrated Lubrication System	22.9
Accessory Drive	7.5
Total	184

These factors were fine tuned (Table 7.3) to match the calculated weight with the actual weight of the JetRanger transmission. Since the JetRanger and the LongRanger have similar technologies and configurations, the extra weight of the LongRanger’s transmission will depend primarily on the difference in the ability to transfer power or transmission rating. Following this procedure, the estimated weight of the LongRanger’s main gearbox is 207 lb. This baseline weight is the upper limit for the new transmission design due to the fact that the LongRanger transmission makes use of older technology.

7.5.5 - Parameter Optimization

The technological level in a transmission can be quantified by the magnitude of the compressive stresses encountered. Increasing the Hertz compressive stress primarily affects the gear weights, which in turn effectively reduces both the face width and diameter if the gear proportions are kept constant. However, after a certain point, an increase in the Hertz stress induces scoring of the gears and excessive bending of the gear’s teeth.

Scoring occurs when for a given rotational speed, the gear diameter is decreased in size so that the line velocity increases. This prevents the creation of the oil film that usually protects the mating surfaces, so direct contact of the two gear teeth occurs. The metal-to-metal contact can produce temperatures high enough to weld the two surfaces. As rotation of the gears continues, the welded surface breaks apart, damaging the teeth. One way to increase the scoring resistance of the gears is to use a VASCO x2m steel instead of a 9313 steel [Dyes91].



If the torque transferred is kept constant, increasing the Hertz stresses reduces the face width of the gears, and so the cross-sectional area of the tooth also decreases. This, in turn, increases the amount of tooth bending at the root. At a certain point, tooth bending becomes the main limiting factor, making contact stress a secondary issue.

With these two limiting factors in mind, and following the trend of Hertz compressive stress versus year of design (Figure 7.3), a new transmission designed in the early 21st century can have an increase of around 11% in the Hertz stress levels with respect to a baseline system that uses mid 1970's technology. This increase will take care of the technological advances achieved in materials, lubricants and manufacturing processes over the last 25 years.

The weight of the transmission will largely depend on the *K* factor used for design. The *K* factor is an index of the intensity of tooth load from the standpoint of surface durability. The higher this value is, the larger Hertz compressive stresses the teeth can support [Dudl84]. The weight calculations of the JetRanger were matched using typical *K* factors for 1960's technology (refer to Tables 7.4 and 7.5). An increase in *K* values (20% for the bevel gears and 40% for the planetary assembly)' followed by a better choice of the pressure and helix angles, gives the

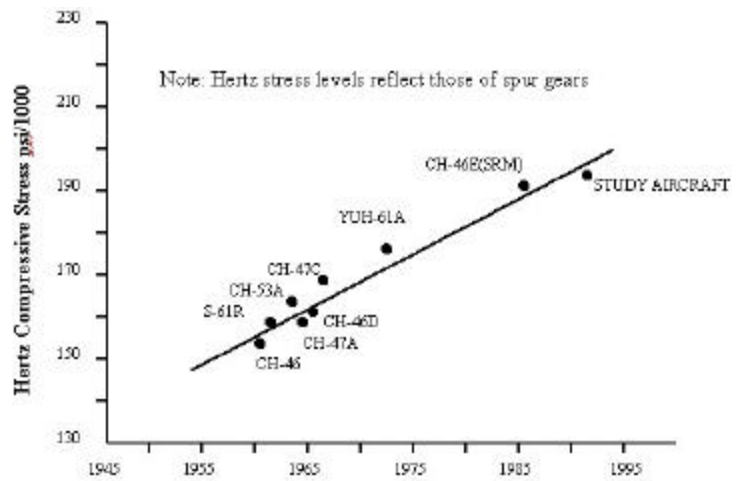


Figure 7.3 - Hertz Stress Level vs. Year of Design

recommended increase in the Hertz stress index factor. The optimization process gave a transmission weight of 184 lbs, 11% lighter than the calculated baseline value. A summary of the drive system features of the TerpRanger drive systems is given in Table 7.5. It is important to point out that the transmission redesigned for the TerpRanger can be considered an improved LongRanger transmission, hence certification costs can be minimized. This considerably reduces the overall cost of the upgrade.

7.5.6 - Oil System

The sizing of the oil cooler is a function of the amount of heat that needs to be dissipated. Based on the transmission configuration, an efficiency of 97% is estimated. The heat generated is



Table 7.5 - TerpRanger Transmission, 420 shp TO Power, 390 shp Max. Continuous Power

Drive system Parameter	Input Bevel Stage	Planetary Stage Sun-Planet
K Factor, Index of Tooth Loading	1190	720
Torque Paths	1	4
Number of Teeth	50/15	Sun 21 planets 27 ring 75
Reduction Ratio	3.333	1.2857
Diametral Pitch	5.19	6
Pressure Angle (deg)	25	25
Helix Angle (deg)	28	0
Face Width (in)	1.15	2.06
Pinion Speed (rpm)	6035	Sun 1810
Gear Diameter(in)	9.62	3.6
Pinion Diameter (in)	2.9	2.8
Compressive Stress (ksi)	179	201
Bending Stress (ksi)	27.2	52
Total Weight of Transmission	184	

calculated from the 100% input power design condition. This corresponds to 8 hp (340 BTU/min) that is dissipated in heat. The cooler is sized to keep an average sump temperature of 200°F. The required oil flow is determined by using the assumption that only 90% of the heat generated is transferred to the oil (10 % is lost in convection through the housing) and assuming a temperature rise of 40° F in the oil. The mass flow rate is given by

$$\dot{m} = \frac{q}{c_p \cdot (T_{in} - T_{out})}$$

where q is the power dissipated, c_p is the oil specific heat (0.455 BTU/lb° F), and T_{in} and T_{out} are the oil inlet and outlet temperatures respectively. From the previous equation the oil flow rate required is 2.2 gpm (8.36 L/min). Usually the sump contains around 0.4 times the flow in gallons per minute [Amc74], this would normally be adjusted during the no load lubrication survey which is the first test to be run on a new transmission. The total oil volume in the transmission lubrication system is set to be 1.5 gallons (5.7 L). Both the filter and the cooler are mounted on the transmission.

The optimized TerpRanger Transmission features standard electric chip detectors, two of which are located near the oil sump, and a third one is located near the mast bearing. When a sufficient number of particles accumulate to complete the electrical circuit of the chip detector, a warning light will turn on the caution panel. An additional magnetic particulate trap (MPT) is installed to detect and consume small metallic particles with a high



voltage spark. The transmission oil pump is a constant volume submersed type, that forces oil out of the sump to a filter and on to an oil cooler on the aft side.

In past decades, the same lubricants have been used for helicopter engines and transmissions. These lubricants provide satisfactory lubrication for turbines, but only marginal lubrication for transmissions. Corrosion and premature surface wear in gears and bearings are the consequences of this practice. Using a more viscous oil can significantly increase transmission life. The higher transmission ratings of the TerpRanger are consistent with the developments in lubricants that the Naval Air Propulsion Center is researching [Lewi92]. These lubricants are expected to have improved load-carrying capacity (about twice that of MIL-L-23699) and improved corrosion inhibiting properties.

7.5.7 - Auxiliary Gearbox

The engine output shaft rotates at 21,000 rpm, which is reduced to 6035 rpm by the use of an auxiliary gearbox integrated within the engine. The 1:3.48 reduction ratio is achieved in two stages using helical gears. As shown in Figure 7.4, the main axis of the turbine is coaxial with the pinion of the first stage, and the gear of the first stage is coaxial with the pinion of the second stage. All the gears are aligned vertically with respect to the engine output shaft, allowing the main rotor transmission input, the powerplant output, and the tail rotor drive shaft to be aligned. Table 7.6 shows the main characteristics of the intermediate gearbox.



Figure 7.4 - Auxiliary Gearbox Configuration

7.5.8 - Tail Rotor Gear Box

The tail rotor drive shaft is driven by the engine output shaft and has a rotational speed of 2175 rpm, hence a reduction ratio of 2.77:1 in the tail rotor gearbox is required. The tail rotor gearbox has a maximum continuous rating of 80 shp and contains a spiral bevel gear assembly that changes the direction of drive by 90°. It has its own self-contained lubrication system and has a magnetic chip detector. Table 7.7 shows the design parameters of the tail rotor gearbox. There is a weight reduction of 23% when current technology is used to size the gearbox. An oil level sight gauge is included in the gearbox housing that uses a self-contained lubrication system.

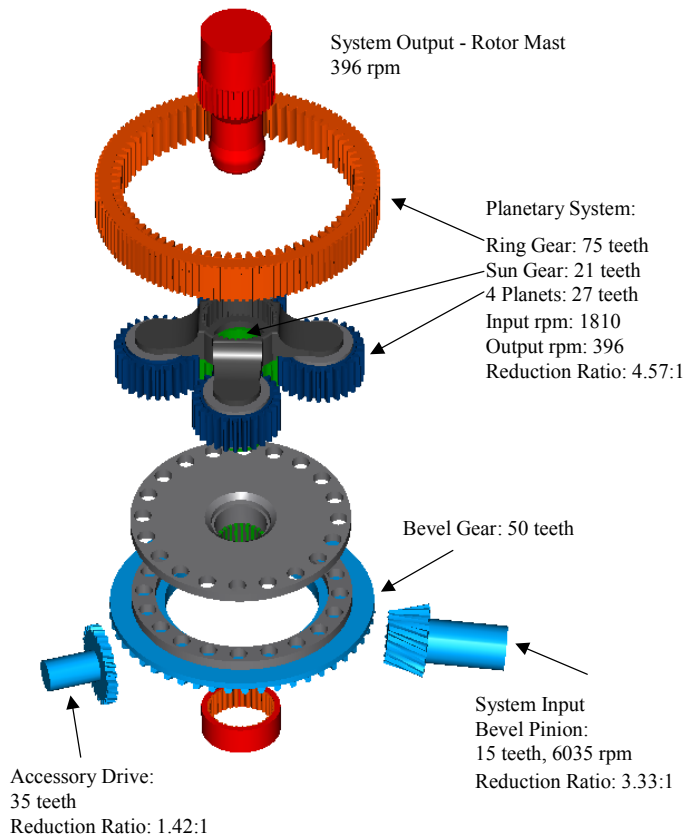


Table 7.6 – Auxiliary Gearbox Design Features

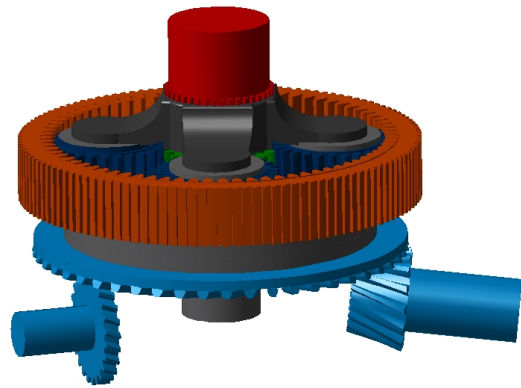
Auxiliary Gearbox Parameter	First Stage	Second Stage
Number of Teeth	69/25	34/27
Reduction Ratio	2.76	1.26
Diametral Pitch	8	8
Pressure Angle (deg)	25	25
Helix Angle (deg)	30	30
Face Width (in)	0.65	1.96
Pinion Speed (rpm)	21,000	7608
Gear Diameter (in)	8.97	3.93
Pinion Diameter (in)	3.25	3.125
Compressive Stress (ksi)	124	134
Bending Stress (ksi)	22.2	18.9
Weight (lb)	17	29

Table 7.7 – Tail Rotor Gearbox Design Features

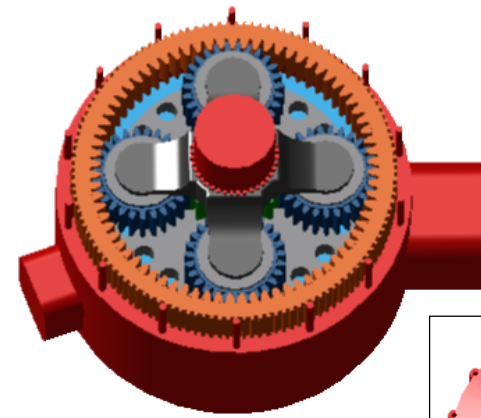
Tail Gearbox Parameter	1970's Technology	2002 Technology
K Factor, Index of Tooth Loading	850	1190
Number of Teeth	50/18	50/18
Reduction Ratio	2.77	2.77
Diametral Pitch	7.96	8.9
Pressure Angle (deg)	20	25
Helix Angle (deg)	25	28
Face Width (in)	0.75	0.67
Pinion Speed (rpm)	6035	6035
Gear Diameter(in)	8.53	6.37
Pinion Diameter (in)	3.38	5.23
Compressive Stress (ksi)	151	179
Bending Stress (ksi)	16.7	22.8
Weight (lb)	16.5	12.6



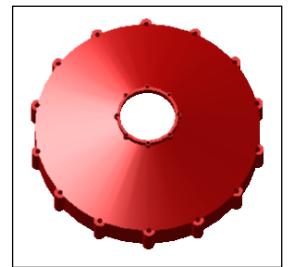
Main Gearbox Components



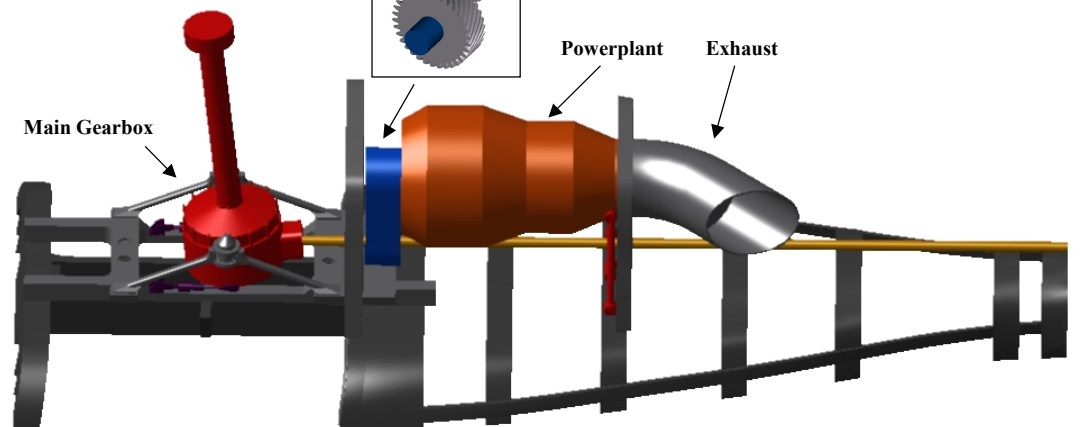
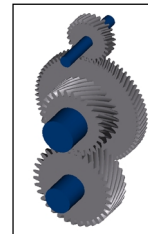
Main Gearbox Configuration



Transmission Housing



Auxiliary Gearbox



Transmission and Powerplant Installation

Foldout 7.1 - Transmission Details



Section 8 - Airframe Design and Cabin Layout

This section describes the changes that are made to the airframe and cabin of the helicopter as part of the TerpRanger upgrade program. There are two principal changes made, apart from those associated with the installation of the new engine, transmission and rotors, the auxiliary fuel tank in the luggage compartment and the new instruments and console displays for the avionics suites. These are the strengthening of the primary load-bearing structures of the airframe, to compensate for the increase in the helicopter's maximum GTOW, and the installation of an airbag system in the forward seats. The option of replacing the metal doors, body panels, vertical fin and horizontal stabilizer of the JetRanger with parts made out of composite materials was considered. The option was not included in the upgrade for the following reasons:

- These parts already have near-infinite service lives;
- Manufacturing and installing replacements for them would increase the cost of the upgrade;
- The TerpRanger is able to fulfill – and exceed – the requirements of the RFP without requiring the reduction in weight that these replacements would provide.

8.1 - Structural Strengthening

Replacing the primary load-bearing structures of the airframe, such as the principal bulkheads, would substantially/significantly increase the re-manufacturing cost of the TerpRanger program. The airframe of the JetRanger was designed assuming a 3000-pound structural design weight. The same airframe has been used for the JetRangers II and III, and for the U.S. Army's OH-58A/C Kiowa helicopters, which have gross weights on the order of 3300 pounds [Harr79]. Static tests performed by Bell Helicopter Textron have indicated that with minor strengthening, it could also be used for the OH-58D Kiowa Warrior [Jaco80]. The Kiowa Warrior has a design gross weight of 4300 lbs, 34% greater than that of the JetRanger. On the other hand, the TerpRanger has a maximum GTOW of 3524 lb, which is only 10% greater. Therefore, it was decided that, apart from overhaul requirements depending on the conditions of the individual aircraft, only minor structural strengthening would be required for the TerpRanger upgrade. The airframe members needing strengthening are the primary cabin bulkheads, the transmission deck and the engine deck. These structures are constructed of aluminum alloy frames, webs and forgings. The additional strength and stiffening required is achieved by riveting aluminum doublers onto these members in the most critical regions.

8.2 - Airbag System

A U.S. Army study conducted between 1979 and 1985 [Shan89] found that 15% of all fatalities in helicopter accidents are caused by preventable head strikes and neck injuries. Non-lethal head trauma can be equally dangerous for crashes into water, causing unconscious or disoriented occupants to drown. Therefore, in order to enhance the safety of its occupants, the TerpRanger is equipped with an airbag system for the forward two seats.



Similar to automobile airbags, this protects the pilot from head and upper torso injuries in the even of a crash. The system has both forward and side airbags because helicopters typically roll over after a crash.

The system is based on the Cockpit Air Bag System (CABS) that has been developed by Simula Safety Systems for retrofit into the U.S. Army's OH-58D Kiowa Warrior helicopters [Simu02]. The system consists of an Electronic Crash Sensor Unit (ECSU) which activates the airbags and eight airbag modules: two forward airbags mounted on the instrument console glareshield, two airbags mounted on the sides of the vertical control tunnel, and 2 lateral airbags, one on each of the front doors. The ECSU is riveted to a small aluminum tray in the forward passenger's seat well. It is a solid-state, microprocessor controlled, fully programmable sensor with multiple accelerometers for each axis. It can discriminate a true crash from other non-emergency events, such as a hard landing, by comparing acceleration data with an internal database of pre-set parameters. It can also record 60 seconds of acceleration data for post-crash analysis. The ECSU uses a standard RS-232 serial port for programming, diagnostics and data recovery, and has a Microsoft Windows 95/98™ operator interface.

Unlike automobile airbags, which deflate almost immediately, the TerpRanger's airbags stay inflated for 3 seconds to provide protection throughout an extended crash sequence. After deployment, the airbags can be folded and stowed out of the way. The cockpit airbags do not interfere with the controls, either when stowed or during and following a deployment. The airbags do not injure the occupants during deployment, and present no obstacle to aircraft egress on land or in water. The Simula CABS system was tested for accidental deployment in AH-64 Apache flight simulators and in actual in-flight tests for the Kiowa Warrior, even though the chance of such an event is predicted to be once in 20+ million flight hours. In none of the tests did the pilots lose control, even under the most demanding conditions such as nap-of-the-earth flying and transition from forward flight to hover.



Figure 8.1 - Cockpit Air Bag System for the OH-58D Kiowa Warrior

The Simula OH-58D CABS system, which consists of 4 airbag modules and an ECSU, weighs 27 lb, has a predicted maintenance requirement of 0.0004 MMH/FH, and costs approximately \$30,000 (installed). The reason for the high cost is that this system has been developed in compliance with military standards of



operational reliability and performance. A system developed for a civilian application, as for the TerpRanger, would cost an order of magnitude less. According to Simula, the technology is easily transferred to civil aircraft, with the main obstacle being the costs of test and certification of such a system. The cost of an airbag system would initially be high, but will decrease as acceptance and demand for such a system increases. This can be seen in the case of automobile airbag systems – manufacturers were initially hesitant to incorporate airbags in the 1980's because of the cost, but now they all do so, and save about 4000 lives every year. An airbag system designed specifically for helicopters is projected to reduce fatalities in accidents involving light helicopters like the TerpRanger by 30% [Shan94].

Section 9 - Vibration and Noise Suppression

A key concern for any helicopter is the issue of vibration reduction. High vibratory loads shorten the fatigue life of critical components and as a consequence, induce higher maintenance costs, and result in a poor ride quality. The proposed TerpRanger upgrade program for the Bell 206 increases cruise speed from 115 to 145 knots. This large increase in forward flight speed requires that the issue of vibration suppression be addressed, as existing vibration reduction methods on the model 206B-3 may not be adequate for such high speeds. The proposed upgrade program presents an innovative and multifaceted vibration suppression package that provides the customer with flexible options. The package is highly customizable, and offers a combination of active and passive systems that provide a cost effective solution for a wide range of operating conditions.

9.1 - Sources of Vibration

The primary source of vibration for any helicopter is the main rotor, which is exposed to an unsteady aerodynamic environment, especially in a high-speed flight condition. During forward flight, nonuniform airflow through the rotor causes periodically varying air loads on the rotor blades, that in turn lead to periodic excitation forces and moments on the rotor hub. These loads are transmitted through the hub to the fuselage and hence, to the crew and passenger seats [Brau80], [Roge01]. The dominant helicopter excitation frequency is the $N \Omega$ harmonic, where N is the number of rotor blades and Ω is the rotational speed of the rotor. For an identically tracked rotor, only harmonics at integer multiples of this frequency are transmitted through the hub. The main rotor of the upgraded 206B-3 increases the number of blades from two to four. Therefore, the dominant frequencies of vibration are 4/rev and multiples thereof.

The main rotor transmission is also responsible for vibration generation, although these are of high frequencies, which result in large internal noise levels that can be uncomfortable to the passengers and crew. Attenuation of these vibrations will improve the ride quality of the vehicle. The frequencies responsible for these noise levels are the fundamental meshing frequencies of the spiral bevel, and planetary gears. According to the analysis



method by Lewicki, [Lewi87], the fundamental frequency for the spiral bevel of the gear TerpRanger 406 is 492 Hz. The planetary gear fundamental frequency is 1500 Hz. Typically, the fundamental frequencies and the first few harmonics are responsible for most of the transmission induced noise.

9.2 - Vibration Suppression Strategies

Vibration suppression is usually achieved through passive methods that dynamically isolate the rotor and transmission system from the fuselage of the vehicle. Combinations of structural optimization, vibration absorbers, elastomeric dampers, and nodal beams have all been employed to attenuate the vibrations generated by the main rotor. Although passive methods are useful in isolating the forcing frequency, they are associated with large weight penalties, and have reduced effectiveness when the vehicle is operated away from the tuned flight condition [Roge01]. The proposed vibration suppression strategies offer a combination of active and passive methods for comprehensive vibration reduction. The level of vibration suppression is dependent on the customer’s budgetary constraints. The following table summarizes the different options, their capabilities, weight penalty and cost.

Table 9.1 - TerpRanger 406 Main Rotor Vibration Suppression Options Summary

	Capabilities	Weight (lb)	Cost (\$)
Option 1			
LIVE Pylon Isolation System	Up to 64% isolation of 4/rev frequency	33	13.9 K
Option 2			
Antiresonance Force Generators	Up to 70% isolation of 4/rev frequency	59	23.4 K
Option 3			
Active Vibration Reduction System (AVRS)	Active system , More than 50% reduction of multiple frequencies	68	64.3 K

9.3 - Previous Vibration Suppression Methods

Existing models of the 206 JetRanger achieve vibration suppression through passive means. Vibration suppression is typically achieved by introducing elastomeric isolators between the transmission and fuselage. This method of vibration reduction may not be adequate for the TerpRanger 406 upgrade, due to the broad expansion in flight performance.

9.4 - Main Rotor Vibration Suppression

The following three sections describe possible systems designed to suppress the forcing frequency of the main rotor. The first option is intended to be the most basic and cost effective solution. The second and third options provide higher performance, but are more expensive to implement because they are technologically more advanced.



9.4.1 - LIVE Isolator

The Liquid Inertia Vibration Eliminator (LIVE) force isolator system has enjoyed wide acceptance as an effective passive suppression system. Dynamically, the isolator is equivalent to the nodal beam used on the 206L [Haw180]. The LIVE isolator is composed of outer and inner cylinders joined by a coaxial rubber bushing that also functions as a spring. The inner cylinder is attached to the transmission, while the outer cylinder is connected to the fuselage. Cavities connected by a tuning port within the cylinders serve as reservoirs for hydraulic fluid. The hydraulic fluid is heavy, like mercury, and acts as the tuning mass of the isolator. By varying the diameter of the tuning port, the device may be calibrated to isolate the desired frequency. The advantages of the LIVE isolator include: a reduced mechanical complexity, bearingless, linear response at high g's, and a low weight compared to other passive systems. With the advent of new fluids by firms such as the Lord Corporation, LIVE isolators continue to improve in terms of performance and weight. These state-of-the-art isolators weigh approximately 19 lbs each, and when used in conjunction with a pylon system similar to that used on the Bell 427, a minimum of 64% of the vertical 4/rev vibratory forces are isolated. [Smit99] This system also provides vertical pitch and roll vibration attenuation. The success with this system on the Model 427, requires that it should be considered for use on TerpRanger 406. The transmission mounting for the upgraded, model 206B-3 is standard and, therefore, easily adapted to incorporate the LIVE isolator system.

9.4.2 - Antiresonance Force Isolators

In this option, a hydraulic antiresonance force isolator replaces the LIVE system mentioned above. This type of force isolator operates on the same principle as a LIVE isolator in that it contains a passive hydraulic force generator. For a certain excitation frequency (the antiresonance frequency) the dynamic component of the spring force and the dynamic force produced in the passive force generator, are opposite and equal at the node between the isolator and fuselage. The relative motion between the fuselage and rotor transmission generates the hydraulic force. As a consequence, the net vibratory force (N/rev) acting on the fuselage is minimized, thereby minimizing the vibratory response of the airframe. The difference between this design and the LIVE actuator is the performance. While LIVE actuators are capable of isolating 64% of the vibratory vertical forces, the isolation efficiency of the antiresonance force isolators is 70% because of the low self-damping of the design [Brau80]. The system is mechanically simple, has a well-defined separation of the load paths and a universal applicability that makes this design readily and easily integrated into the Model 206B upgrade.

9.4.3 - Active Vibration Reduction System (AVRS)

This option utilizes an active system currently being developed for the Sikorsky S-92 and the Boeing V-22. The system will be used in conjunction with the transmission mounted, elastomeric dampers already installed on the



original Model 206B-3. Active control systems are of interest because they offer more operational flexibility, and are able to perform over a wide range of operational conditions, unlike passive systems that are tuned to only one condition. The Active Vibration Reduction System (AVRS) utilizes a series of distributed actuators and sensors that are mounted at various locations throughout the fuselage to counteract the vibratory loads transmitted from the main rotor. A key characteristic of the AVRS system is that it adaptively suppresses vibrations at all frequencies. An AVRS actuator is comprised of two single point MOOG™ actuators, each consisting of a pair of imbalanced, counter-rotating eccentric masses. For the S-92, the dynamic force output provided by the actuators is 500 lb. The force is determined by measuring the reaction forces of the passive vibration reduction methods. For the TerpRanger 406 upgrade, the actuators are scaled down proportional to the product of gross weight and the square of the cruise speed, to provide a 61 lb dynamic force output. Vibration reduction is achieved by controlling the phasing between actuator pairs. By determining the optimum location for these actuators, significant reductions in vibration can be obtained. Currently, the system designed for the S-92 has seen a reduction of over 50% in the levels of vibration, and the optimum actuator location has yet to be determined. The weight penalty for the AVRS system is 20% less than a passive system installed to perform the same function. Figure 9.1 displays the components of the AVRS system [Bern02].

Figure 9.1 - AVRS Components



9.4.4 - AVRS Implementation

Although the principle of operation is relatively straight forward, there is much work that must be performed to practically implement the system. Determining the optimum actuator locations requires detailed analysis and modeling of the vehicle structure. Initially, the natural modes must be determined by NASTRAN or a similar finite element analysis. Once completed, the model must be validated by ground shake tests and the structural transfer matrix must be identified. The ground shake tests narrow the field to a few candidate actuator locations. Finally, once several possible actuator locations are determined, flight tests must be scheduled to validate the modeling and confirm the optimum actuator locations. These tasks are involved, and require significant resources in order to accomplish them. For a new vehicle, such as the S-92, the development costs for the



AVRS are high, in part, because of limited information on vehicle performance. The development costs for an AVRS system to be utilized on the TerpRanger upgrade should be considerably lower because of the long service life of the vehicle. Over the years, much work has been accomplished in modeling the fuselage structure and to predict its forced response [Ship72]. Also, many ground shake and flight tests have been performed on the vehicle over its service life. The existence of this information should help reduce the development costs of an AVRS system [Bern02]. Based on the NASTRAN model of the AH-1G helicopter, we require two actuators and four sensors placed on the floor of the cabin near the pilot and passenger seats. Incorporation of AVRS will help to achieve a “jet smooth ride” in the TerpRanger.

9.5 - Active Tracking Tabs

Helicopters often encounter vibratory loads that arise from rotor dissimilarities. These dissimilarities cause a tremendous increase in the 1/rev vibration level and hence larger vibratory loads are encountered. These forces have a negative effect on the fatigue life of the dynamic components, and cause undue discomfort on passengers and crew. To alleviate these dissimilarities, blades are periodically tracked by manipulating trailing edge tabs, adjusting pitch-link lengths, or by adding masses near the blade root. These operations are performed manually in an iterative procedure, and are an integral part of ground maintenance. This process is both costly and time consuming, resulting in increased operating costs and downtime. An active, in-flight tracking system would allow a rotor system to be tracked in a matter of minutes instead of hours or days, resulting in a long term benefit of reduced operating costs, relaxed blade manufacturing tolerances, and increased fatigue life of structural components and instruments [Epps00], [Sing02]. The system thus, adds precision and speed to the tracking process.

9.5.1 - SMA Actuated Tracking Tab

Shape memory alloy (SMA) actuated flap devices have shown impressive results in several different applications [Redi99], [Garn99], [Epps00]. Shape memory wire actuated tracking tabs in helicopters are an innovative solution for in-flight tracking.

Shape memory alloys have the ability to recover large strains when activated by heat. This process is reversible and strains as large as 8% can be recovered in this fashion. The actuator consists of two sets of pre-strained Nickel-Titanium (NiTi) shape memory wires attached respectively to the top and bottom surface of the tracking tab. When the upper wires are resistively heated, they contract and rotate the tab upward, and simultaneously develop strain in the lower wires. Likewise, when the lower wires are heated, the tab is deflected downward and a strain is developed in the upper wires. Figure 9.2 depicts a schematic of the tracking tab.

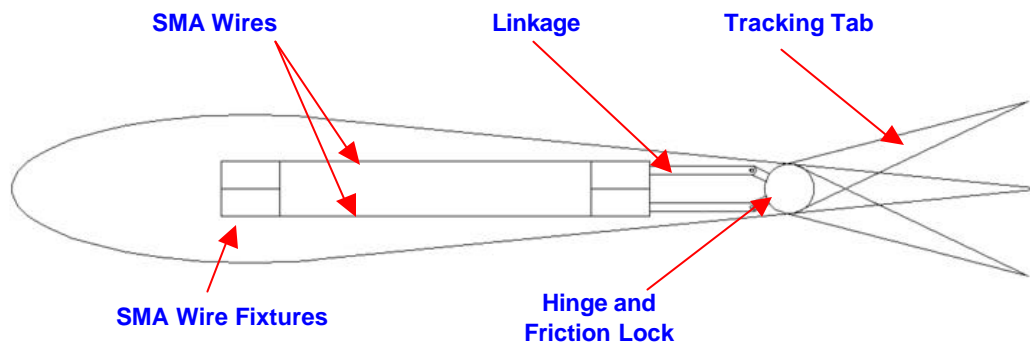


Figure 9.2 - Schematic of Active Tracking Tab

One of the advantages of the plain flap design is its compactness, which allows the tab to be integrated within the trailing edge of the airfoil. The actuator is small enough to fit inside the blade spar. Recently, this actuator design has shown promising results [Epps00], [Singh02]. Care must be taken, however to ensure that the wires are thermally insulated so that the SMA does not activate as a result of ambient conditions. A detailed illustration of the tracking tab appears in the Foldout 5.1. Once the desired position of the tabs is achieved, the tab needs to be locked in place to switch off activation.

9.5.3 - Locking Mechanism

A passive, friction-based, locking mechanism was shown to hold successfully, the tracking tab in place under different load conditions [Sing02]. The lock is set to always exert a known frictional hinge moment (adjusted manually) up to the maximum aerodynamic moment on the tab. The mechanism is simple and requires no additional power to operate. Recent tests have demonstrated the effectiveness of this lock [Sing02].

9.5.4 - Control Strategy

A simple proportional-integral-derivative (PID) controller controls the deflections of the tracking tab. When selected, it has been shown that the gains for the controller are less sensitive to flight conditions [Singh02]. The entire system draws power from the same DC supply as the de-icing system, and is transferred to the tab through the main electrical slip ring.

9.5.5 - Tracking Tab Characteristics

The 7.8-inch spanwise tracking tab is centered at 75%R, and extends 25% over the blade chord. An empirically modified, blade element momentum theory model of the rotor was used to calculate the hinge moment required by the tab. The hinge moment is a function of blade and tab geometry, location along the blade span, and deflection. As illustrated in Figure 9.2, the hinge offset is 0.33 inches. For a maximum flap deflection of 5



degrees, the aerodynamic hinge moment on the tab was determined to be 7.1 in-lb. To overcome the passive locking mechanism, the actuator moment is set to generate two times the maximum aerodynamic moment on the tab. Consequently, the actuator force provided by the SMA wires to deflect the tab 5 degrees was found to be 42.3 lb. This will be achieved by two NiTi wires of 0.01 inch diameter, on the respective top and bottom surfaces, with a prestrain of 2.5%

9.6 - Noise Reduction

While vibration suppression is critical for the operation of the vehicle, internal and external noise reduction must also be addressed. The main sources of noise levels are the main rotor, the tail rotor, and the main rotor gearbox and engine. Main and tail rotor noise on the TerpRanger has been reduced as a result of a lower tip speed [Lows92]. The transmission noise is also reduced. Tonal noise components of the meshing of the teeth in the gearbox are typically 10 to 20 dB above the broadband noise spectrum. [Gemb99] This level of internal noise degrades the quality of the ride, and excessive external noise may prevent the vehicle from being operated in urban areas because of noise pollution regulations. Isolation of the frequencies responsible for noise is clearly necessary to suppress them. One innovative method that has been successfully tested on the EC135 and the BK117 to suppress internal noise involves active struts that dynamically isolate the transmission from the fuselage. This active system consists of Lead Zirconium Titanate (PZT) layers bonded directly onto the strut. Each strut has 9 PZT segments bonded to the surface that are divided both axially and circumferentially. Independent actuation of the PZT layers has been shown to reduce noise levels by as much as 13 dB for a weight penalty of only 22 lbs. Figure 9.4 shows a schematic of the active struts and their location on the transmission support structure.

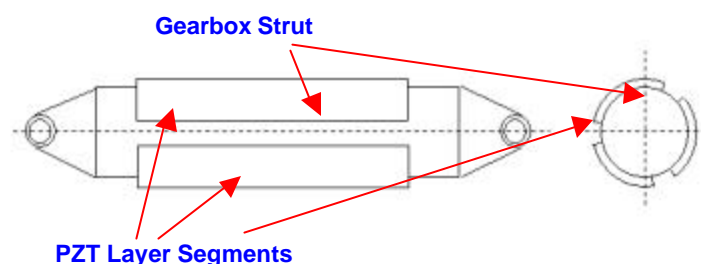


Figure 9.3 - Active Strut Concept [Gemb99]

The advantages of this system are: simplicity of design, applicability to existing struts, low weight penalty, and low maintenance. This system is relatively simple to implement onto existing helicopters because the PZT patches are bonded directly to an existing strut.



9.7 - Pricing

Prices were determined for each vibration suppression system from the cost formulas listed in the RFP. After the weight of each system was determined, the price was determined by assigning the system to an appropriate RFP pricing formula. Although we realize the costs of these systems are not dependent on weight alone, this analysis is useful for providing a first order estimate of the costs. The table below lists the components and the associated pricing equation.

Table 9.2 - Pricing Summary

	System	Weight (lb)	RFP Price Analogy	Cost (\$)
Option 1				
	LIVE Pylon Isolation System	33	Drive System	13800
Option 2				
	Hydraulic Force Generators	59	Drive Dystem	23400
Option 3				
	AVRS & Elastomeric Dampers	68	Airframe Struct.	64350
Standard				
	Active Tracking Tabs	9	Main Rotor	12700
	Smart struts	22	Drive System	960

9.8 - TerpRanger 406 Standard Vibration Suppression Package

The standard vibration suppression package for the TerpRanger 406 is as follows: The LIVE isolators are implemented to reduce main rotor vibrations, while active tracking tabs are incorporated into each blade. The active strut concept is implemented to reduce gearbox vibration. All combinations of vibration suppression and avionics upgrade options along with their influence on the acquisition price of the vehicle are presented in Section 16.1.2.

9.9 - Alternate Vibration Suppression Strategy

Other vibration control methods were studied, but deemed infeasible for implementation on a helicopter upgrade. These methods represent hi-tech solutions and are still in early stages of development. These systems could be integrated into existing helicopters once the technology matures.

Trailing Edge Flaps (TEF). The TEF concept offers an attractive solution to vibration suppression and has been shown to work on a scaled rotor model. [Kora00]. By placing independently controlled flaps at various stations along the blade length, main rotor excitation frequencies may be attenuated at the source, thereby eliminating the need for heavy, passive vibration absorbers. Implementing TEF concepts for vibration reduction may be feasible because only small flap deflections of approximately 2 degrees, are required. A TEF system is capable of attenuating up to 85% of all vibratory hub loads [Shen02], [Roge01]. Typically, a wide range of smart



materials including PZT sheets, piezostacks, and magnetic shape memory alloys may actuate these flaps. Most of these materials provide limited success, especially in a full-scale system, due in part to their low energy densities. Usually, a displacement amplification mechanism to provide the necessary flap deflections is required. Amplification devices are often mechanically complex and come with an undesirable weight penalty. One material that may be capable of superceding these shortcomings is magnetic shape memory alloy (MSMA). The most common of MSMA materials is NiMnGa. These new materials would be ideal for TEF actuator concepts because of their large stroke and high frequency range [Ulla00], [OHan98], [Couc02]. However, the MSM actuators are still relatively new and require significant resources to incorporate them onto existing rotors. Characterization of MSMA has yet to be completed, commercial MSMA actuators are not widely available, and suitable control methods for TEFs still requires more development. The technology required to make TEFs for vibration control a reality has not fully matured and, therefore, the concept is not feasible for an upgrade program at this time. If a similar upgrade program were scheduled for implementation in the next five to ten years, then the concept of TEFs would provide an innovative solution to vibration control.

Section 10 - Subsystems

Descriptions of the fuel, oil, hydraulics, electrical, avionics and other systems are presented in the following section.

10.1 - The Fuel System [Bell99], [Bell95]

The fuel system arrangement of the TerpRanger has been retained from the JetRanger design. Also, to minimize the upgrade cost, it was instructive to as much as possible, use the same fuel storage system as the JetRanger. In addition, after obtaining the performance analysis, it was found that to reach the new range, the fuel tank must have a capacity of 101 gallons (380 liters) to carry out that mission (400 nautical miles).

The JetRanger fuel system consists of a single, bladder-type, fuel cell located in the aft passenger seat bench with a fuel capacity of 91 gallons (344 liters). The fuel capacity is 10 gallons (37.6 liters) lower than the required quantity. To compensate for this fuel shortfall, an auxiliary fuel tank is added to increase the fuel tank volume. This type of auxiliary fuel tank has already been implemented on, and certified for the Bell 407. The auxiliary fuel tank can be placed in the baggage compartment. It consists of two kits, the provisions, and the tank. When the kit is installed, the total fuel capacity of the TerpRanger increases to the required 101 gallons (380 liters). There is then no requirement for additional fuel management by the pilot. Filling of the tank is through regular fuel fill port, and likewise the fuel automatically flows to the aircraft fuel system. The fuel quantity indicating system is then modified to correctly show the new fuel quantity.



The auxiliary fuel tank used in the Bell 407 has a capacity of 20 gallons (75.28 liters), However, in this mission, only 10 more gallons are needed. Therefore, to save space in the baggage compartment, the auxiliary fuel tank used in the TerpRanger is smaller, and has a capacity of only 10 gallons.

The fuel and booster pumps are the same as those on the baseline JetRanger. The fuel pump is engine-driven and a fuel filter is mounted on the engine. There are two electric submerged boost pumps in the fuel cell, connected in parallel to the engine fuel supply line. The pumps can be removed for repair or replacement from the bottom of the fuselage. If the boost pumps are malfunctioning, a fuel pump caution light will alert the pilot. The fuel system also contains two fuel-level transmitters connected to an indicator on the instrument panel as well as an airframe-mounted fuel filter with a replaceable element.

On the right side of the helicopter, just aft the passenger door there is a single filter cap and a grounding plug. Just below the filter cap, an electric fuel-sump drain valve is placed. The valve is operated by a push-button. A shut-off valve controlled from the instrument panel controls the fuel. Finally, the system has a transducer to activate the fuel pressure gauge.

The honeycomb box structure which forms the passenger seat bench provides the fuel cell with a rugged, damage resistant cavity. The smooth fiberglass inner surface further reduces risk of cell rupture, thus sharply reducing the fire hazard. The cell is reinforced to withstand a 50-foot drop test.

10.2 - The Engine Oil System [Bell99], [Bell95]

The Engine oil system remains largely unchanged from the baseline JetRanger. It is a circulating dry sump type with an external reservoir and oil cooler. Pressure and scavenge pumps are mounted within the engine and are driven by the accessory gearbox. All engine oil system lines and connections are internal with the exception of the pressure and scavenge lines to the front and rear bearings. A blower driven by the tail rotor drive shaft provides cooling air to the oil cooler. An oil temperature bulb installed in the supply tank is connected to an indicator on the instrument panel. A magnetic chip detector activates a light on the caution panel when metal particles are detected in the system.

10.3 - Hydraulic System [Bell99], [Bell95]

Bell 206B-3 is equipped with a single hydraulic system that powers three single stage servo actuators assisting the main rotor cyclic, collective and yaw flight control. Normal hydraulic pressure at 100- percent Nr is 600 ± 25 psi. Basic configuration of the hydraulic system will not change in the TerpRanger. However, the TerpRanger will replace the system with the system found on the Bell 206 L to compensate for the increase of the gross



weight and new rotor system. The normal hydraulic pressure of this system is 1000 ± 25 psi and the fluid reservoir has a capacity of 40 in^3 .

10.4 - Electrical System [Bell99], [Bell95]

The Bell 206B-3 is equipped with 28-Volt, DC system containing a battery, a starter-generator, a voltage regulator, relays, circuit breakers, and a reverse current relay. Power is obtained from a nickel-cadmium (or sealed lead acid), vented, 24-volt, 17-ampere/hour battery, and a combination main starter/generator rated at 30 volts, 150 Ampere (derated to 105 Amperes). Power is distributed through a single bus system. The various switches and circuit breakers are mounted on the overhead panel. External power may be applied through a receptacle located on the forward section of the fuselage. The reverse current relay prevents the generator from being connected to the line until reaching operating voltage. The DC common bus powers flight and main generator. In the event of a main generator failure, the battery will power the bus. The current system is adequate for all avionics options offered (with the highest requirement at ~690 Watts) and is retained for the TerpRanger upgrade [Bell02].

10.5 - Flight Control System

The TerpRanger will retain all of the lower flight control system of the baseline Model 206B including all the components from the control stick and pedals up to the non-rotating swashplate. The components of the upper control system, including the rotating swashplate, pitch links, and pitch horns, are modified for the 4bladed main rotor.

10.6 - Cockpit and Avionics Upgrade Options

A choice of multiple avionics packages are provided for the TerpRanger upgrade to meet a wide variety of customer requirements. Emphasis is placed on equipment modernization and operational safety.

The options are grouped as follows and arranged in the order of increasing capabilities, cost, and weight:

1. Full Authority Digital Engine Control (FADEC) control and displays in addition to existing avionics and instruments (Baseline Upgrade).
2. Modern digital avionics and improved flight instrument displays including an advanced GPS system with a single MFD (Multifunction Display) panel for future growth.
3. Option 2 plus Meggitt MAGIC MFDs with EGPWS™ passive CFIT and SkyWatch™ mid-air collision avoidance systems.
4. Option 2 plus Meggitt MAGIC MFDs All-weather capable active OASys™ collision avoidance system.



10.6.1 - Option 1: FADEC Control and Display Only

In Option 1, the TerpRanger is equipped with a FADEC Engine display in addition to the existing avionics systems. This display requires a minimum of 2 warning lights, 3 cautionary lights, 2 test switches, and FADEC mode switch. This option is included in the baseline TerpRanger upgrade. Figure 10.1 illustrates the FADEC instrument panel display.

10.6.2 - Option 2: Modern digital avionics and flight instrument displays including an advanced GPS system

Option 2 is designed with a goal of providing avionics and cockpit displays for safe navigation. This option utilizes the Bendix/King Silver Crown Plus™ panel mounted digital avionics—KMH 24H Audio Control, KX 155A Comm/NAV, KT 76C Panel Mounted Transponder, and KR 87 Digital ADF [Bend02]. Additionally the system is complemented with a KMD 150 Color MFD/GPS that provides a moving navigational map. Other user defined functions can be added to the MFD through a serial port. FADEC displays are incorporated on the cockpit panel.

The cockpit panel is replaced with the panel currently in production at Bell Canada for the JetRanger. Figure 10.2 displays the panel configuration of Option 2. Included is a new set of caution (shown in yellow) and warning (shown in red) displays.

10.6.3 - Option 3: Modernized Avionics including Meggitt MAGIC MFDs and Passive Collision Avoidance Systems

Option 3 offers increased operational safety by including a combination of passive collision avoidance systems namely, the BF Goodrich SkyWatch [Bfga02] and Honeywell EGPWS (Enhanced Ground Proximity Warning System) [Egpw02]. The SkyWatch provides protection from mid-air collisions especially near congested metropolitan areas. During normal operations, EGPWS protects the aircraft and crew from CFIT (Control Flight Into Terrain) and collisions with vertical objects. Basic avionics and cockpit panel displays remain unchanged from Option 2. However, engine instruments are replaced with clear and bright Meggitt MAGIC multifunction displays which are also used as navigation and warning displays [Megg02]. A Data Acquisition Unit is included to digitize analog engine information.

10.6.4 - Option 4: Modernized Avionics including Meggitt MAGIC MFDs and Active Collision Avoidance Systems

Option 4 offers maximum collision protection of all the avionics packages. Passive collision avoidance systems are useful only if other aircraft are equipped with functioning transponders. An active system is required that can



detect objects and terrains in all weather conditions. The 35 GHz radar technology based Amphitech OASys Radar System [Amph02] offers these capabilities and is included into this option. As in Option 3, the information and warnings gathered by the radar is displayed to the flight crew on Meggit MAGIC MFDs. For GPS solution, Bendix/King KLN 94 Color IFR GPS Receiver is also integrated to the system.

10.6.5 - Summary

Each of the four avionics packages is designed both to improve flight safety and to satisfy varying customer expectations while remaining affordable. Table 10.1 displays the cost, weight, drag penalty, and power requirements for each option. Antenna locations for each option are displayed in Figure 10.7.

Table 10.1 – Technical Summary of Avionics Upgrades

	Wegiht (lb)*	Drag Area (ft ²)	Power (watt)	Cost (\$)
Option 1	N/A	N/A	N/A	N/A
Option 2	33.1	0.16	287	23606
Option 3	35.8	0.16	433	77365
Option 4	83.3	0.39	690	198364

* Uninstalled

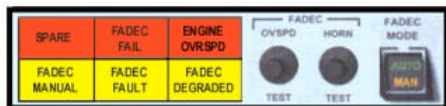


Figure 10.1 - Avionics Upgrade Option 1: FADEC control/display



- 1-KMD 150 Color MFD/GPS
- 2-KMA 24 H Audio Control
- 3-KX 155A Comm/NAV
- 4-KT 76C Panel Mounted Transponder
- 5-KR 87 Digital ADF



Figure 10.2 - Avionics Upgrade Option 2

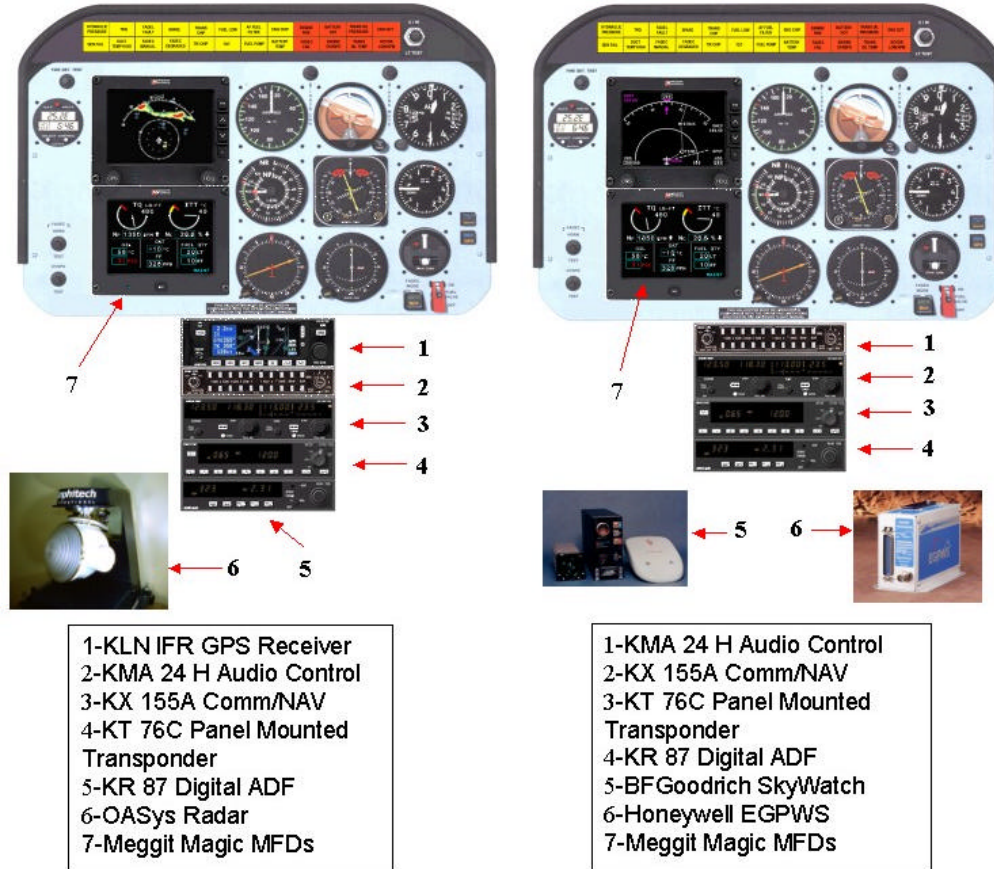


Figure 10.3 - Avionics Upgrade Option 3

Figure 10.4 – Avionics Upgrade Option 4

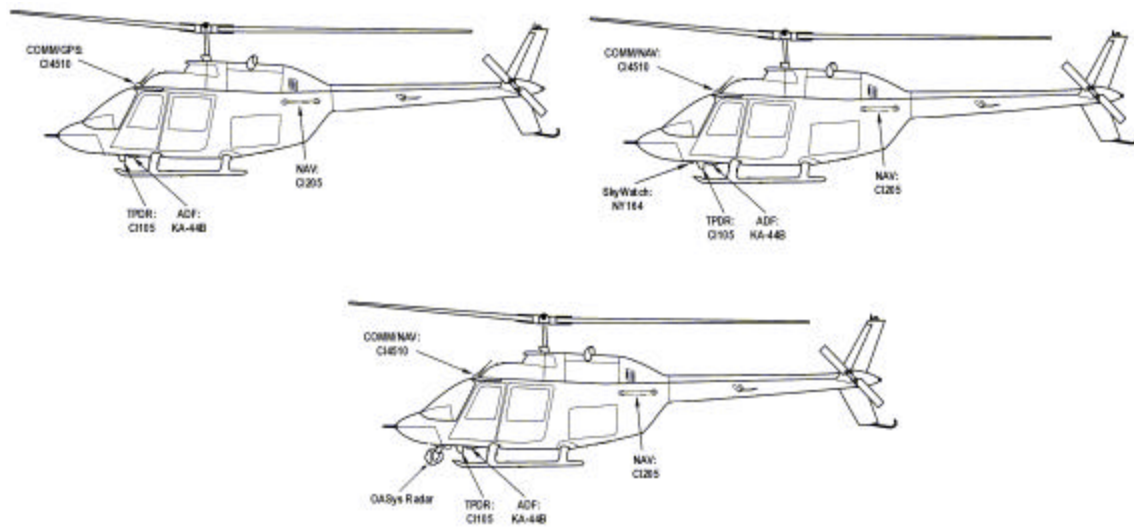


Figure 10.5 - Antenna locations for Option 2 (Top, Left), Option 3 (Top, Right), and Option 4 (Bottom)



10.7 - Health and Usage Monitoring Systems (HUMS)

Reliability and maintainability of the rotor, engine and transmission are greatly enhanced by the installed HUMS (Health and Usage Monitoring System). With advances in HUMS technology, the installation time and cost-benefit ratios have improved, leading to a 50% reduction in the payback period required to recover the cost of the system [Weit00]. The system consists of a fully integrated, cockpit mounted data acquisition unit and pilot display, which acquires data from accelerometers and tachometers installed on critical engine and transmission components. On-board data processing and analysis is carried out by the processor, which is integrated into the display and data acquisition unit. Data processing is organized into different analyses carried out sequentially during specific time intervals. Each analysis involves the selection of signals from sensors that are critical depending on the flight regime. Results of the analyses are stored on non-volatile memory and subsequently transferred to ground support equipment for generating operations, maintenance and engineering reports. The HUMS system provides health and usage status of the engine and drivetrain, vibration monitoring and load exceedance monitoring. Additionally, aircraft vibration data is stored at predefined flight regimes to monitor the performance of the active tracking tab.

The HUMS system provides significant savings in operating cost due to reduced scheduled and unscheduled engine, rotor and gearbox removals. Reduced number of spares used for unscheduled maintenance and increased time between overhaul further reduces the direct operating cost (DOC). Also, costly test flights to check rotor track and balance can be avoided. Because of the additional safety improvements provided by the HUMS system insurance costs are also reduced.

Section 11 - Stability and Control Analysis

While the development of a comprehensive dynamic model of the TerpRanger is beyond the scope of this proposal, a simplified, linearized model based on the techniques presented by Padfield [Padf96] was developed to perform the stability and control analysis. This model is represented by an aerodynamic matrix, the elements of which are functions of the stability derivatives of the helicopter. Some of the stability derivatives were calculated directly from the aircraft design characteristics, such as rotor diameter, flapping frequency, Lock number and stabilizer size. However, the values of other derivatives can only be obtained from flight test data and advanced stability analysis computations. Therefore, the values for these derivatives were obtained from helicopters with similar design characteristics, such as the U.S. Army's OH-58D (Bell Model 406) [Ham95], the Westland Lynx and the MBB BO-105 [Padf96]. The stability characteristics of the longitudinal and lateral modes were then obtained from the eigenvalues of this aerodynamic matrix.



11.1 – Stability and Control Derivatives

The stability and control derivatives are displayed in Table 11.1. The force and moment derivatives are normalized with the design gross weight and the moments of inertia, respectively. In order to simplify the stability analysis and determine the contribution of each design parameter, the estimated stability derivatives were grouped into seven categories: longitudinal, lateral, lateral into longitudinal, longitudinal into lateral, main rotor longitudinal control, main rotor lateral control, and tail rotor control.

The pitch damping, M_q , and the roll damping, L_p , are the most important derivatives in terms of the helicopter's handling qualities, because of their close association with short-term and moderate amplitude responses. The larger the magnitude of M_q and L_p the more stable the helicopter. Changing from a teetering rotor in the Bell206 model to a hingeless rotor in the TerpRanger causes an increase in the stiffness number (ratio of hub stiffness to aerodynamic moment), which results in an increase in the magnitude of these stability derivatives.

11.1.1 - Longitudinal Modes

Figure 11.1 shows the estimated longitudinal poles of the TerpRanger in hover and at a cruise speed of 140 knots. The Phugoid mode of the TerpRanger suggests that the helicopter is unstable in hover and cruise, which is normal for most helicopters. The pitch damping and heave modes are stable in all flight regimes.

11.1.2 - Lateral Modes

Figure 11.2 shows the lateral modes of the TerpRanger. It can be seen that Dutch roll oscillation is neutral in hover and stable in cruise. Dutch roll is highly dependent on the coupling of roll and yaw, where the dihedral effect (L_v) and yaw due-to roll rate (N_p) are the main contributors. Both of these derivatives are found to be large and negative in cruise. A negative value of N_p tends to destabilize the Dutch roll oscillation; however, the strong dihedral derivative stabilizes this mode.



Table 11.1 - Stability and Control Derivatives

Longitudinal				Lateral			
Derivative	Unit	Hover	140 knots	Derivative	Unit	Hover	140 knots
X_u	1/s	-0.01	-0.04	Y_v	1/s	-0.05	-0.2
X_w	1/s	0.01	0	Y_p	ft/s.rad	-0.29	-29.5
X_q	ft/s.rad	3.608	14.7	Y_r	ft/s.rad	0	-229.6
Z_u	1/s	0	-0.025	L_v	rad/s.ft	-0.01	-0.10
Z_w	1/s	-0.03	-0.9	L_p	1/s	-7.5	-7
Z_q	ft/s.rad	0	32.8	L_r	1/s	0.1	0.4
M_u	Rad/s.ft	0.01	0.01	N_v	rad/s.ft	-0.008	0.015
M_w	Rad/s.ft	-0.005	0.012	N_p	1/s	-1.5	-2
M_q	1/s	-3.75	-1.5	N_r	1/s	-0.25	-1.5
Lateral Into Longitudinal				Longitudinal Into Lateral			
Derivative	unit	Hover	140 knots	Derivative	unit	Hover	140 knots
X_v	1/s	-0.02	0	Y_u	1/s	0.02	0.005
X_p	ft/s.rad	0	0	Y_w	1/s	0	0
X_r	ft/s.rad	0	0	Y_q	ft/s.rad	0	0.2624
Z_v	1/s	0	-0.02	L_u	rad/s.ft	0.106707	-0.01524
Z_p	ft/s.rad	0	-2.296	L_w	rad/s.ft	0	0.030488
Z_r	ft/s.rad	0	0	L_q	1/s	0.5	0.5
M_v	Rad/s.ft	0.027	0	N_u	rad/s.ft	0	-0.01
M_p	1/s	-0.1	-0.2	N_w	rad/s.ft	0.003	0.006
M_r	1/s	0	0	N_q	1/s	0	0.25

Control Derivatives

Main Rotor Longitudinal				Main Rotor Lateral			
Derivative	Unit	Hover	140 knots	Derivative	Unit	Hover	140 knots
X_{θ_0}	ft/s ² rad	9.8	-16.4	Y_{θ_0}	ft/s ² rad	-1.64	-6.56
$X_{\theta_{1s}}$	ft/s ² rad	-31.1	-31.16	$Y_{\theta_{1s}}$	ft/s ² rad	-4.92	-11.48
$X_{\theta_{1c}}$	ft/s ² rad	3.6	4.6	$Y_{\theta_{1c}}$	ft/s ² rad	-32.8	-32.8
Z_{θ_0}	ft/s ² rad	-295.2	-426.4	L_{θ_0}	1/s ²	9	0
$Z_{\theta_{1c}}$	ft/s ² rad	-1.64	0	$L_{\theta_{1s}}$	1/s ²	0	-10
$Z_{\theta_{1s}}$	ft/s ² rad	0	-196.8	$L_{\theta_{1c}}$	1/s ²	25	25
M_{θ_0}	1/s ²	0	15	N_{θ_0}	1/s ²	17	10
$M_{\theta_{1s}}$	1/s ²	11	14	$N_{\theta_{1s}}$	1/s ²	-1.5	-0.5
$M_{\theta_{1c}}$	1/s ²	-3	-3.5	$N_{\theta_{1c}}$	1/s ²	-10	-10
Tail rotor							
Derivative	Unit	Hover	140 knots				
X_{θ_T}	ft/s ² rad	0	0				
Y_{θ_T}	ft/s ² rad	13.12	16.4				
Z_{θ_T}	ft/s ² rad	0	0				
L_{θ_T}	1/s ²	5	7				
M_{θ_T}	1/s ²	0	0				
N_{θ_T}	1/s ²	-8	-11				

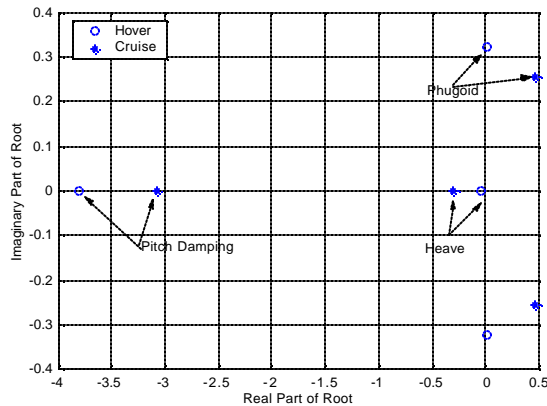


Figure.11.1 - TerpRanger Longitudinal Poles

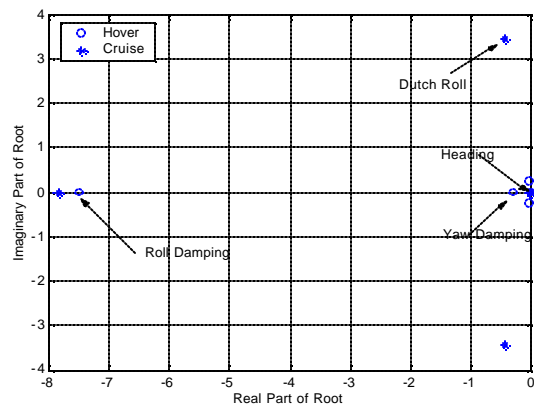


Figure.11.2 - TerpRanger Lateral Poles

11.2-Handling Qualities

The requirements for response to small-amplitude inputs are specified in ADS-33c in terms of bandwidth and phase delay. The bandwidth is the frequency at which there is at least a 6-dB gain margin and a 45-degree phase margin from the neutral-stability frequency for the aircraft angular response due to pilot control input. An aircraft with high bandwidth would nearly mirror the input, and would be described as quick, crisp, or agile. A low-bandwidth aircraft would be more sluggish, with a smoother response. According to the linear model used in this analysis, the aircraft bandwidth for pitch and roll responses are the amplitudes of pitch and roll damping (M_q , and L_p) respectively. Higher values of pitch and roll damping, thanks to the TerpRanger’s hingeless rotor, improve the handling qualities when compared to the baseline Model 206.

Section 12 - Weights and Balance

This section describes the methods used to estimate the component system weights and the empty weight of the TerpRanger, and the location of its Center of Gravity (CG).

12.1 - Weight Estimation

The weights of the various components of the helicopter were calculated using the method developed by Tishchenko [Tish02]. This method requires weight coefficients to be established for each component, by using regression analysis techniques to develop a relationship between the component weights and the design parameters that most influence these weights. For example, the weight of the main rotor blades is a function of the rotor radius and its solidity; the weight of the gearbox is proportional to the torque that it transmits; and the



weight of the rotor hub is proportional to the maximum centrifugal force that it has to withstand. The weight of the engine was calculated using the formulae specified in the RFP.

Table 12.1 - JetRanger Component Weight Breakdown

Component Categories	Calculated Weights (lb)	Actual Weights (lb)	Components Included
MR Blades	187.67	189.6	Blade Assembly
MR Hub	104.83	100.7	Hub & Hinge
TR Blades	4.79	4.80	Tail Rotor - Blades
TR Hub	6.06	6.70	Tail Rotor -Hub & Hinge
Transmission Shafts and Gearboxes	172.33	173.30	Gear Box, Lub Sys & Rot Brk; Rotor Shafts, Transmission Drive
Engine Installation	188.61	181.10	Engine Installation & Starting System
Airframe Engine Preparation	14.10	16.30	Exhaust System, Engine Control & Air Induction
Fuel System	53.35	49.60	Tanks & Plumbing
Fuselage & Cowlings	415.53	413.50	Basic & Secondary Structure; Engine Section or Nacelle Group; Aircraft & Loading Handling Groups; Armament Groups
Empennage	29.74	29.60	Stabilizer & Fin
Landing Gear	64.60	65	Main Gear & Tail Skid
Control Linkages & Swashplate	105.58	103.40	Cockpit & System Controls
Hydraulics	17.83	16.10	Hydraulic & Pneumatic Group
General Purpose Equipment	250.24	247.40	Instruments Group; Electrical Group; Anti-Icing Group; Accommodations for Personnel; Furnishings & Miscellaneous Equipment; Air-Conditioning Group; Ballast
Unusable fuel	12.58	11.1	Unusable Fuel & Undrainable Oil
Oil & Cooling System	28.17	26.70	Lubricating System
Empty Weight Growth	13.25	12.9	Manufacturing Variation
Total Empty Weight	1669.27	1647.80	Total Empty Weight

The MIL-STD-1374 weight statements for the Model 206B-3 JetRanger III (obtained from Bell Helicopter Textron) and for the OH-58D AHIP Kiowa Warrior [Harr86] were used to validate the weight coefficients used for the TerpRanger design. In some cases, the weight coefficients of the Tishchenko method were adjusted to obtain correspondence between the predicted and actual weights. This procedure ensures that the calculated weights of the TerpRanger accurately reflect the influence of the design and manufacturing practices at Bell Helicopter on the component weights. Table 12.1 shows the component weight breakdown used, with the actual and calculated category weights of the baseline JetRanger.



The MIL-STD weight breakdown for the TerpRanger was then estimated from the results of the Tishchenko weight estimation method, using the percentage contributions of the different components to their respective categories. A summary of the component weights is given below in Table 12.2. The detailed MIL-STD-1374 weight statement for the TerpRanger is attached at the end of this report.

Table 12.2 - TerpRanger Component Weight Breakdown (lb)

Tishchenko Categories	TerpRanger	JetRanger
Mass of MR Blades	152.77	189.6
Mass of MR Hub	63.91	100.7
TR Blades	8.74	4.80
TR Hub	12.29	6.70
Gearboxes and Driveshafts	239.65	173.30
Engine Installation	151.54	181.10
Engine Preparation	11.33	16.30
Fuel System	62.75	49.60
Fuselage	462.28	413.50
Empennage	26.11	29.60
Under carriage	71.28	65
Control linkages and Swashplate	99.24	103.40
Hydraulic System	12.71	16.10
General Purpose Equipment	250.24	247.40
Unusable fuel	14.80	11.1
Oil & Cooling System	42.26	26.70
Empty Weight Growth	22.84	12.9
Total Empty Weight	1704.74	1647.80

12.2 - Center of Gravity Estimation

The longitudinal location of the aircraft's CG was determined by using the fuselage station and water line coordinates of each of the items detailed in the MIL-STD-1374 weight statement. In this analysis, longitudinal Fuselage Stations are measured aft from the nose of the helicopter, while vertical Water Lines are measured upwards from the floor of the fuselage. The values of these stations were estimated from published drawings of the JetRanger. Good agreement was obtained with the C.G. limits given in the FAA Type Certificate Data Sheet [FAA01] for the Model 206 and in the maintenance manual for the Model 206A/B [Bell98], as shown in Table 12.3. Table 12.4 shows the CG locations of the TerpRanger. Note that the main rotor mast is located at Fuselage Station (+106) in., the total fuselage length is (374.4) in., and the main rotor hub height is (+97.59) in.



Table 12.3 - JetRanger Longitudinal C.G. Location

	Published	Calculated
Max. GTOW (3200 lbs)	(+106) to (+111.6) in [FAA01]	(+110.6) in
Empty Weight (1650 lbs)	(+116) to (+117) in [Bell98]	(+117.7) in

Table 12.4 - TerpRanger C.G. Locations

	Empty Weight (1690 lb)	Take-off Gross Weight (3524 lb)
Longitudinal	116.69 in	111.79 in
Vertical	46.25 in	33.08 in

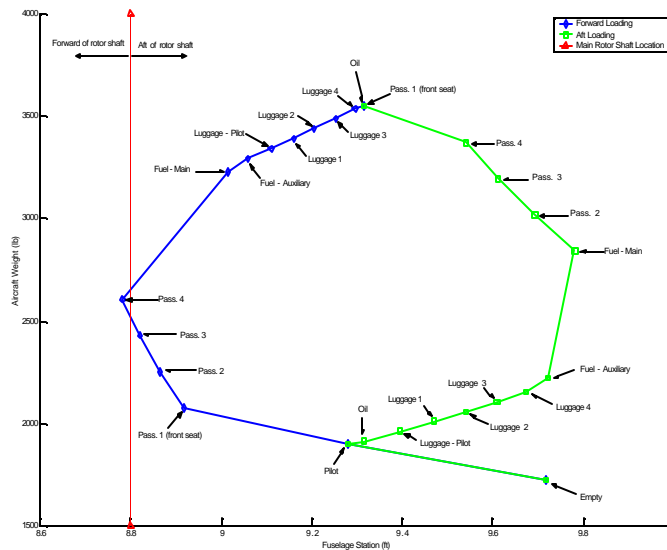


Figure 12.1 - TerpRanger Longitudinal CG Travel

Figure 12.1 shows the longitudinal CG travel for forward and aft loading of the helicopter.

Section 13 – Performance Analysis

Table 13.1 presents a summary of the performance of the baseline JetRanger and TerpRanger at sea level and 1000 ft for ISA and ISA+20°C conditions. Power requirements for hover, climb and forward flight are calculated for different weights and atmospheric conditions. The results are calculated in an iterative process that leads to the sizing of the engine and transmission, and the determination of the flight envelope of the vehicle. Details of the drag calculations and results for vertical and forward flight performance are presented in the following sections.



Table 13.1 - Performance Summary

	JetRanger (SL, 3200 lb)		TerpRanger (SL, 3524 lb)		TerpRanger (1000 ft, 3524 lb)	
	ISA	ISA + 20	ISA	ISA + 20	ISA	ISA + 20
Cruise Speed (kts)	116	N/A	144	146	145	144
Speed for best range (kts)	113	117	148	152	148	154
Speed for best endurance (kts)	48	N/A	62	64	62	64
Range (full fuel & payload), maximum (n. mi.)	368	368	424	450	433	452
Endurance (full payload), maximum (hrs)	4.6	N/A	4.05	4.21	4.11	4.27
Climb Rate, maximum (ft/min), MCP	1,280	N/A	1,715	1,590	1,700	1,500
Vertical Climb Rate, (ft/min), TOP	N/A	N/A	740	705	720	680

N/A = Not Available

	JetRanger (3200 lb)		TerpRanger (3524 lb)	
	ISA	ISA + 20	ISA	ISA + 20
Hover Ceiling, IGE (ft)	13,000	10,200	13,900	11,850
Hover Ceiling, OGE (ft)	5,300	3,000	10,000	8,250
Service Ceiling (ft)	13,500	12,800	19,860	18,020

13.1-Drag Estimation

Parasite drag limits maximum forward flight speed while vertical drag or download affects vertical flight performance. The accuracy of the TerpRanger performance calculations is dependent on the precision of the drag estimates.

13.1.1-Parasite Drag

The power-required curves in forward flight published in Bell’s Product Data Book for the JetRanger-III [Bell99] are used to estimate the parasite drag for the baseline helicopter. By varying the equivalent flat-plate area of the airframe in the trim analysis, it is found that the JetRanger has an equivalent flat plate drag area of 6.6 ft².

The empirical methods presented by Prouty [Prou95] and Stepniewski [Step84] are used to estimate the component drag build-up for the JetRanger. The drag coefficients for the different components are then adjusted so as to match the value of 6.5 ft² for the entire helicopter. The analysis for the TerpRanger includes the effects of several measures undertaken to reduce the helicopter’s parasite drag, as described below in further



detail. Table 13.2 shows the resulting distribution of parasite drag contributions in terms of equivalent flat-plate area, for both the TerpRanger and the baseline JetRanger.

Table 13.2 - Drag Build-Up

	JetRanger	% Of Total	TerpRanger	% Of Total
Fuselage (incl. cowlings)	1.541 ft ²	23.91	1.422 ft ²	25.71
Main Rotor	1.164 ft ²	18.05	1.876 ft ²	33.91
Tail Rotor	0.323 ft ²	5.02	0.282 ft ²	5.10
Landing Gear	2.222 ft ²	34.47	0.880 ft ²	15.91
Horizontal Stabilizer	0.126 ft ²	1.96	0.118 ft ²	2.14
Vertical Fin	0.093 ft ²	1.44	0.087 ft ²	1.57
Rotor-Fuselage Interference*	0.427 ft ²	6.62	0.427 ft ²	7.71
Miscellaneous**	0.550 ft ²	8.53	0.440 ft ²	7.95
Total	6.446 ft²		5.532 ft²	

* Interference drag cause by the rotor downwash on the aft fuselage, which can induce areas of local separation.

** Drag caused by antennas, door handles, hinges and latches, pitot static tubes, temperature probes, external jacking points, lights, skin gaps, steps and mismatches.

13.1.2 - Drag-Reduction Measures

The JetRanger has a cruise speed of 115 knots. In order to achieve the required cruising speed of 140 knots, a substantial reduction in parasite drag is required. Using the analysis methods outlined in Hoerner ([Hoer75]), a reduction of 1 ft² in the equivalent flat-plate area (5.5 ft² total) is achieved, by the following measures:

Aerodynamic fairings for the skid gear: Changing the effective cross-section of the landing gear cross-tubes can provide a substantial reduction in the drag of the gear. A cylindrical structure has the same drag as an airfoil section with a thickness 25 times the cylinder’s diameter [Prou95]. Detachable skid fairings are available for the JetRanger, and these are included in the TerpRanger design. With these fairings, the equivalent drag area of the landing gear cross tubes is reduced from 1.2 ft² to 0.1 ft².

The fuselage attachment brackets of the landing gear are also covered with detachable airfoil-shaped fairings. Hoerner predicts a reduction in drag coefficient of between 0.33 and 1.11, which translates to an equivalent flat-plate drag area reduction between 0.248 ft² and 0.833 ft² respectively [Hoer75]. For the TerpRanger design, the lower value was adopted, so as not to over-predict the reduction in drag.



Together, these two measures yield a total drag-area reduction of 1.348 ft^2 . This agrees well with the predictions of [Prou95], which estimate a reduction in total drag coefficient from 1.01 to 0.4 when fairings are used for this type of landing gear.

Main Rotor Hub Fairing: The 2-bladed hub for the JetRanger is a simple teetering design, and therefore does not produce substantial drag. However, the hub for a 4-bladed rotor is larger and contains several more components. Therefore, the hub is provided with a fairing to shield it from the airflow.

Increasing Main Rotor Shaft Tilt: This reduces the fuselage angle of attack in high-speed forward flight, thereby lowering the fuselage bluff-body drag. The JetRanger has a forward shaft tilt of 5° . This was initially increased to 7° in early analyses. However, in order to keep the fuselage floor level in cruise for passenger comfort, the tilt angle has been reduced to its final value of 6° .

Decreasing Main Rotor Shaft Height: The vertical height of the main rotor shaft has been reduced from the 2 ft to 1.3 ft, thus reducing the drag that it produces. The disadvantage of this is that it increases the interference effects between the rotor hub and the pylon. The option of changing the shape of the pylon cowling was considered, to make it more streamlined. However, it was recognized that the hat-like rim of the cowling around the main rotor shaft area could itself be an effective measure for reducing drag, by acting like a low aspect-ratio wing and producing “tip” vortices that energize the boundary layer on the aft portion of the pylon and thus delay separation [Prou95]. An accurate prediction requires the use of sophisticated numerical methods that were not available for this preliminary design phase. Therefore, the decision was made not to change the shape of cowlings as part of the upgrade.

Closing off Main Rotor Shaft Opening: A flat circular plate is rigidly attached to the main rotor shaft, flush with the opening in the cowling through which it passes, so as to close off the gap formed by the opening and reduce the drag that it causes. The disc rotates along with the rotor shaft. Small holes are provided in the disc itself for the control pitch links to pass through. The cover is divided in four sections designed to be easily removed for maintenance. The true reduction in drag due to this measure can only be found from wind-tunnel tests. For this analysis, the benefit was included by reducing the amount of hub-ylon interference effects by 10%.

Engine exhaust ducts: Changing the location of the engine exhaust duct from the top of the cowling to the side, and changing the shape of the outlet so that it is flush with the contour of the cowling, reduces the blunt-body drag produced. This effect is estimated by a reduction in the fuselage drag coefficient.



13.1.3 - Vertical Drag

The total thrust required by the main rotor in hover is equal to the gross weight plus the vertical drag or download on the fuselage that is produced by the rotor wake. Vertical drag is calculated by combining estimated vertical drag coefficients with an empirical downwash velocity distribution. The methods presented in [Prou95] and [Step84] are used to estimate the vertical download of the TerpRanger, an additional 2.3% of the gross weight was the result of these calculations.

13.2 - Hover Performance

The hover performance calculations determine the hover ceiling and the maximum rate of climb of the helicopter for a given gross weight and ambient condition. The calculations consist of comparing the power required to hover and the available engine installed power. When these two quantities are equal, the hovering ceiling is reached, otherwise the excess power can be used to climb. An original hover performance code was developed using a blade element momentum theory model that uses table lookup for the lift and drag coefficients for the different airfoils along the blade obtained from wind tunnel tests data. The model includes empirical corrections for tip losses, wake swirl and the effect of ground on induced velocities.

The effect of the advanced blade tip geometry is introduced by reducing the power required by the rotor by 3%. This is a conservative value considering that wind tunnel tests [Deso88] show reductions of up to 7% at high thrust coefficients with respect to rectangular blades (refer to Section 5.2.3).

The hovering ceiling OGE at ISA and ISA+20°C for the TerpRanger is larger than the unmodified 206B-3 at the same atmospheric conditions and respective maximum takeoff weights. The additional power and the aerodynamically more efficient rotor system allow for hovering ceilings higher than those of the JetRanger and LongRanger. Table 13.3 compares the hovering ceilings of these three helicopters in and out of ground effect. Weight vs. hovering ceiling (IGE and OGE) and maximum climb rate vs. altitude plots are shown in Figures 13.1 and 13.2 respectively. The good climb rate and enhanced hovering ceiling broaden the helicopter’s multi-mission capabilities, making the TerpRanger a highly versatile vehicle.

Table 13.3 - Hovering Ceiling for Different Atmospheric Conditions

	JetRanger 206 III 3200 lb	LongRanger 206L-4 4450 lb	TerpRanger 3524 lb
ISA OGE	5,300 ft	6,500 ft	10,000 ft
ISA+20 OGE	3,000 ft	4,200 ft	8,250 ft
ISA IGE	13,000 ft	10,000 ft	13,900 ft
ISA+20 IGE	10,200 ft	7,700 ft	11,850 ft

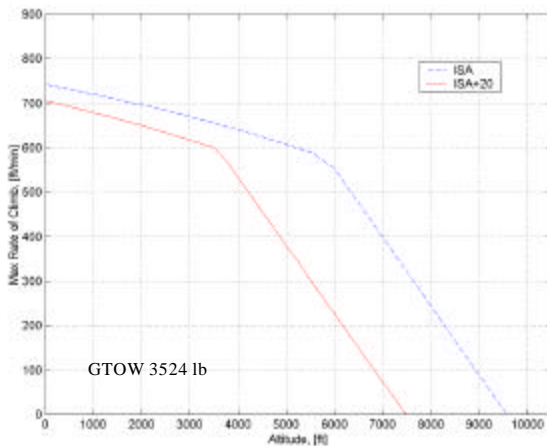


Figure 13.1 - Maximum Rate of Climb vs. Altitude

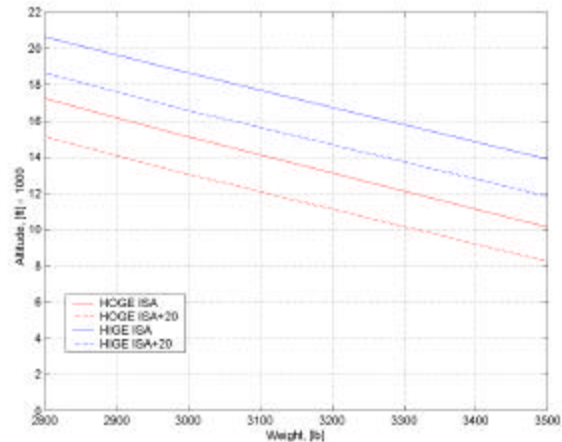


Figure 13.2 - Weight vs. Hover Ceiling

13.3 – Forward Flight Performance

Longitudinal trim analysis was carried out to determine the power required by the helicopter as a function of forward speed. The analysis assumed a constant induced velocity over the disk (Glauert’s Theory) and rigid blade flapping. A table lookup procedure was used for the airfoil properties, and the analysis is capable of handling different airfoils along the blade span, arbitrary taper and arbitrary twist. To give a more accurate prediction of the TerpRanger’s performance, the code also varies the fuselage parasite drag as a function of angle of attack, as shown in Figure 13.3 [Harr79]. In the figure, the curve shown for the OH-58A was approximated by the equation

$$C_{DF} = C_{D_0} + K (\alpha - \alpha_0)^2$$

where α_0 is the fuselage angle of attack for minimum drag. This equation was used in the trim analysis of the TerpRanger. The minimum fuselage drag was estimated by the methods described above in Section 13.1.2.

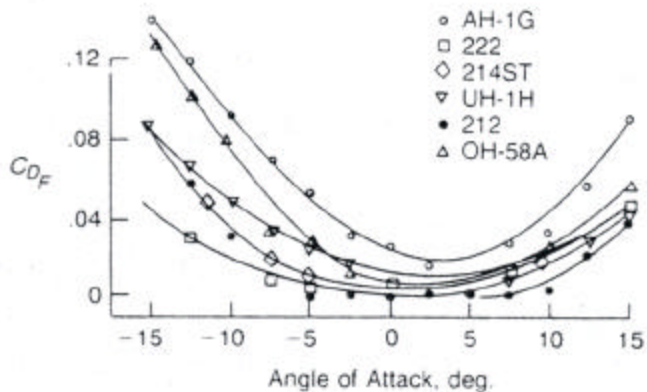


Figure 13.3: Fuselage Drag Variation with Angle of Attack [Harr79]

The RFP calls for a minimum cruise speed of 140 knots. The TerpRanger is designed to be able to cruise at approximately 145 knots at all altitudes between sea level and 1000 ft, in both ISA and ISA+20 conditions. For the purpose of this design, the cruise speed was defined to be the speed at which the power required is equal

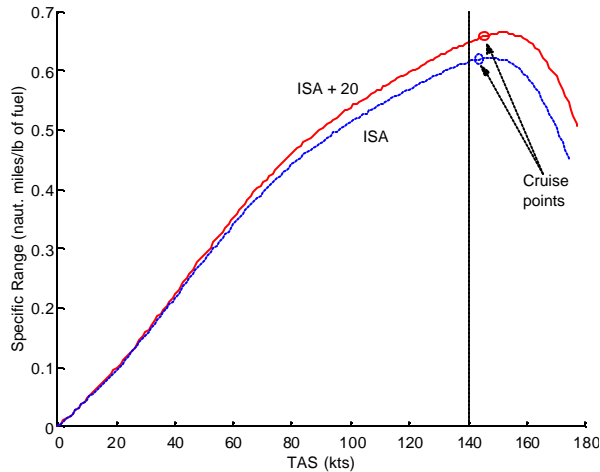


Figure 13.4 - Specific Range Variation with Forward Speed

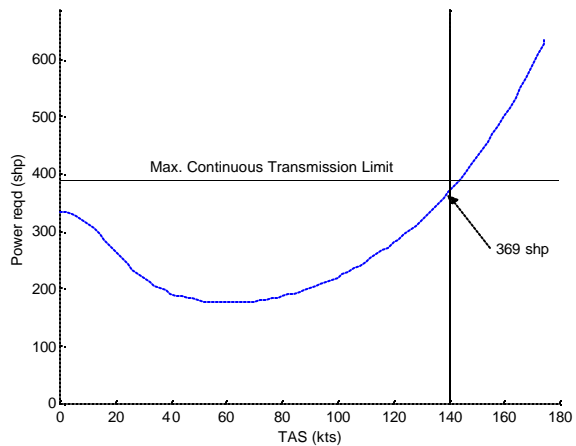


Figure 13.5 - Power Required, Sea Level, ISA. Design Gross Weight

to the maximum continuous power that can be obtained from the engine. Although not exactly equal to the speed for maximum range, it was found that the cruising and maximum-range speeds were close enough to each other that almost the same range was achieved with either, as indicated by the specific range trends shown in Figure 13.4.

For most helicopters, the power required to hover is greater than the power required in cruise. However, because of the relatively high 140-knot cruise speed for the TerpRanger, the maximum continuous power required at cruise conditions is greater than the power required for hovering, as shown in Figure 13.5. Therefore, the transmission – and consequently the engine – was sized by a maximum continuous power requirement rather than by a transient (take-off) rating requirement. The sizing of the engine and transmission is explained in Sections 7.1 and 7.2 of this report.

The cruise power required is maximum at sea level, ISA conditions. With increase in altitude or in air temperature, air density is reduced, leading to a reduction in parasite drag and in the power required to fly at a given speed. However, since the power deliverable by the engine decreases with density, the maximum continuous power available to the helicopter also decreases. Note that the available power at any density altitude also depends on how much the engine is de-rated from its maximum uninstalled rating.

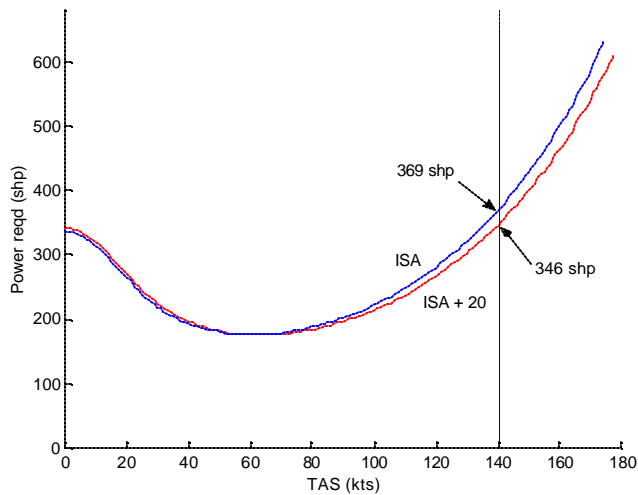


Figure 13.6 - Power Required Variation with Forward Speed

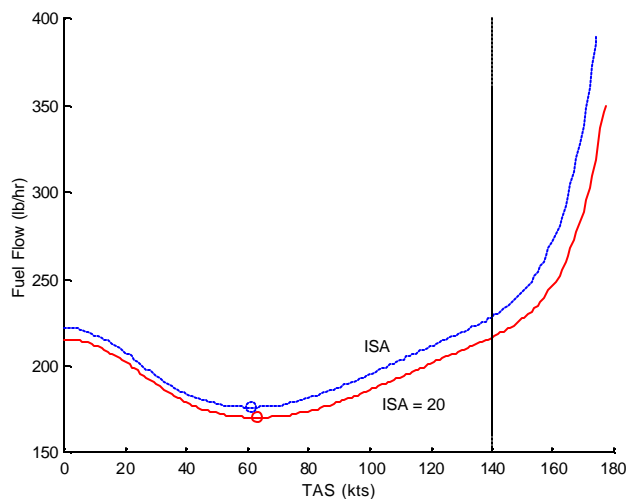


Figure 13.7 - Fuel Flow Variation with Forward Speed

These effects can be seen in Figures 13.6 through 13.14. The variations shown in these figures are for the design gross weight of 3524 lb. Figures 13.6, 13.7 and 13.8 show the variations in power required, fuel flow and specific fuel consumption with forward speed, for both ISA and ISA + 20 conditions. The variation of Specific Range (distance traveled per unit weight of fuel) with forward speed is shown in Figure 13.4. Figure 13.9 shows the power required to fly at 140 knots at different altitudes, as well as the maximum continuous power available at those altitudes. The power available stays constant up to a certain altitude (860 ft), because of the de-rating of the engine, but then decreases as the power available from the engine falls below the transmission limit. Figure 13.10 gives the variations of cruise speed and speed for maximum endurance (loiter speed) with altitude. The maximum cruising speed first increases with increasing altitude, but then decreases as the power available decreases. Figures 13.11 and 13.12 show the variations in specific range and minimum fuel flow with altitude. Both quantities improve with decrease in air density. Figures 13.13 and 13.14 show the trade-offs between payload and range, and payload and endurance. With decreasing air density (increasing altitude or increasing air temperature), the range and endurance achievable with a given payload increase.

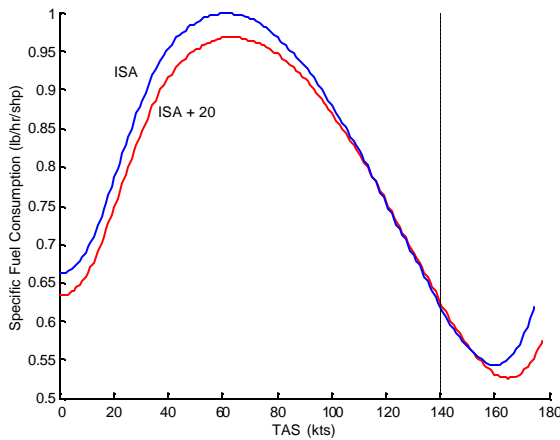


Figure 13.8 - Specific Fuel Consumption Variation With Forward Speed

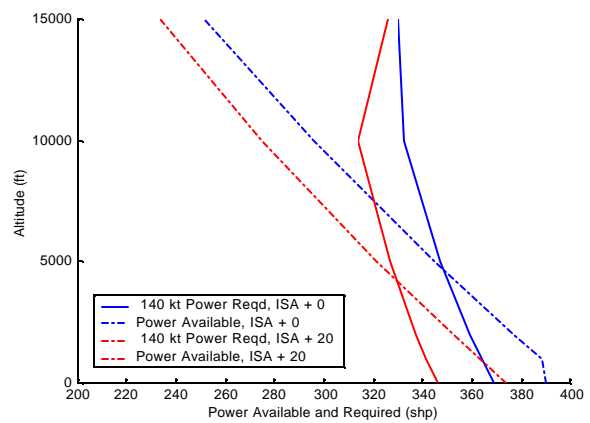


Figure 13.9 - Power Req'd. for 140 kts and Max. Continuous Power Available

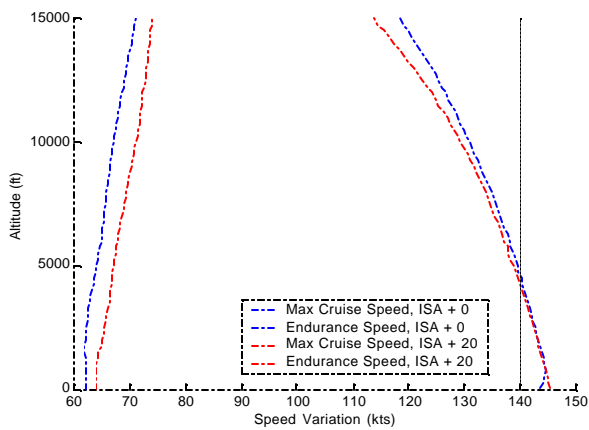


Figure 13.10 - Cruise Speed and Max. Endurance Speed Variation with Altitude

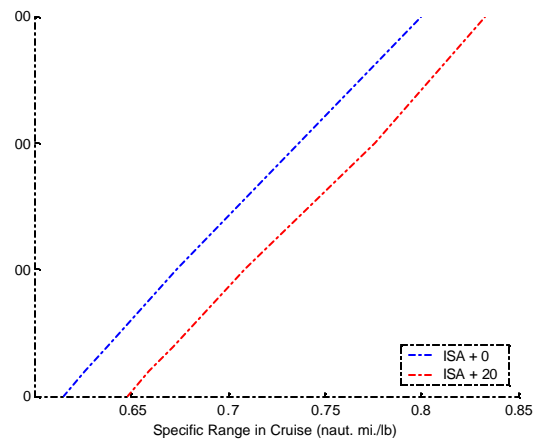


Figure 13.11 - Specific Range Variation with Altitude

The methods described in [Step84] were used to estimate the range and endurance performance of the TerpRanger. From the power required at different speeds, the specific fuel consumption of the engine was calculated using the formulae given in the RFP. The values of fuel flow and specific range at the cruising speed were then calculated at different flight weights and used to plot the payload-range and payload-endurance diagrams (Figures 13.13 and 13.14).

The analysis predicts a range of 424 nautical miles for a full-payload configuration, no fuel reserves, at 1000 SL/ISA conditions. The corresponding maximum endurance (at loiter speed) at the same condition was calculated to be 4.1 hours.

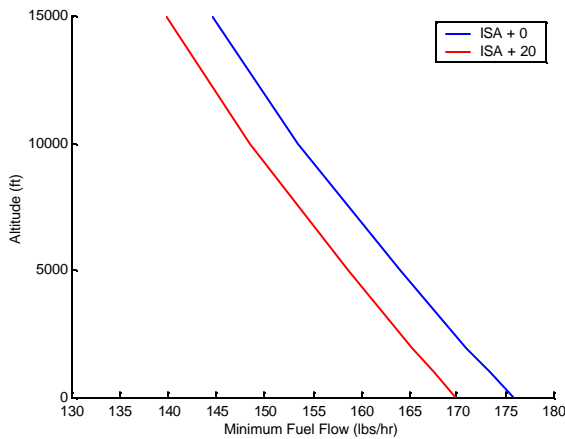


Figure 13.12 - Minimum Fuel Flow Variation with Altitude

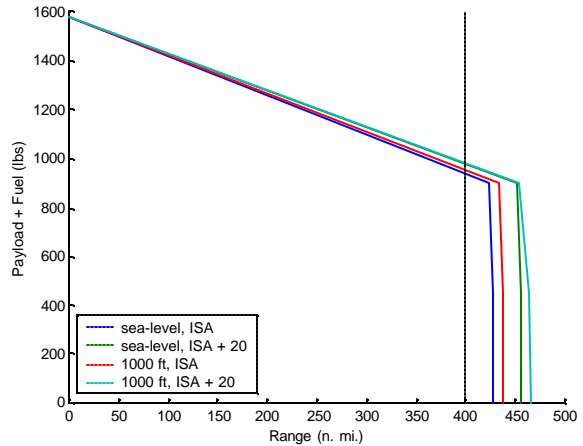


Figure 13.13 - Payload-Range Diagram

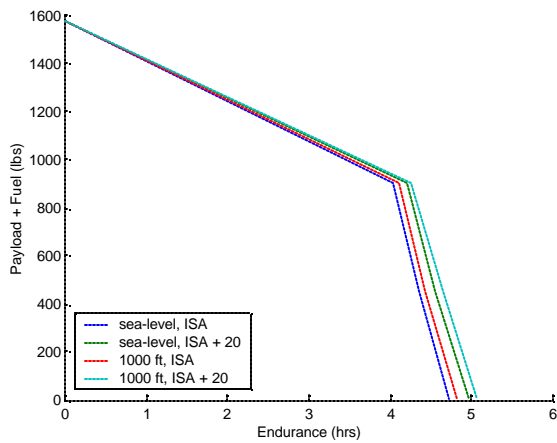


Figure 13.14 - Payload-Endurance Diagram

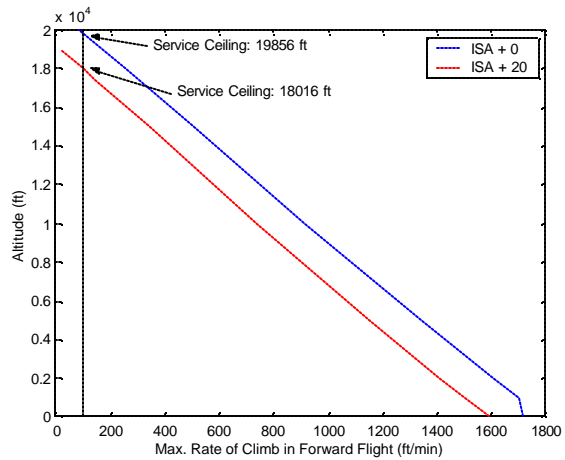


Figure 13.15 - Maximum Rate of Climb Variation with Altitude and Service Ceiling

The service ceiling is defined as the altitude at which the helicopter can no longer sustain a climb rate of 100 ft/min. The TerpRanger has a service ceiling of 19,860 ft, ISA, and 18,020 ft, ISA+20 conditions. Figure 13.15 shows the variation of maximum rate of climb in forward flight with altitude and the service ceilings.

Section 14 - Manufacturing

The purpose of the present helicopter upgrade program is to provide a high-performance helicopter at a fraction of the cost of acquiring a newly manufactured commercial helicopter. The acquisition price depends on three principal factors: research and development costs, manufacturing, overhead, certification, and value added costs. Keeping the manufacturing costs low has a direct impact on the purchase price of the aircraft. The TerpRanger



upgrade proposes the use of Product Lifecycle Management (PLM) tools throughout the implementation of the upgrade process, from conceptual and detailed design through to full-scale production. This includes the use of CAD/CAM/CAE software, electronic document tracking and sharing and Total Product Engineering. This enables the product to be designed for ease of manufacture right from the outset, promotes collaboration between the design and the manufacturing teams, and facilitates consistency and rapid dissemination of information.

The re-manufacture of the helicopters will consist of four main processes:

- a) Removal of the components to be replaced:

Cowlings, main rotor, tail rotor, engine, transmission / gearboxes and transmission mounts, fuselage body panels, cockpit instrument panel, crew and passenger seat benches, fuel cell, vertical fin, hydraulic system

- b) Repair / Overhaul of the components to be retained

Fuselage bulkheads, roof beams, cabin roof and floor panels, other structural members, tailboom and horizontal stabilizer, electrical system and wiring

- c) Manufacture of the new components
- d) Installation of the new components

This section focuses on the third process, which can be conducted in parallel with the first and second.

14.1 - Lean Manufacturing

The TerpRanger re-manufacturing program will employ “*lean manufacturing*” processes to minimize costs. Lean manufacturing is a systematic approach to perform the minimum work necessary to production. The major benefits of this manufacturing philosophy are continual quality improvement, small production runs and the ability to reconfigure the production line for different products. Lean manufacturing is composed of many elements, including: (i) elimination of waste, (ii) continuous flow and (iii) quality control. The TerpRanger upgrade program has a relatively low production run, as envisioned in the RFP. In addition, the production of the upgraded helicopters will not proceed at a regular pace, for two principal reasons:

- a) The availability of helicopter airframes to be upgraded at any given time will depend on the number of operators who wish to offer their aircraft for upgrade at that time.
- b) The airframes acquired for re-manufacture will be received in varying conditions or states of disrepair. Some operators will have faithfully maintained their aircraft and complied with all the Airworthiness Directives and Service Bulletins, while others may have not. The aircraft acquired will be of varying age (in terms of years and of flight hours), so some will need more extensive repair and overhaul than others.



For these reasons, continuous flow is of primary importance to an upgrade production line. Continuous flow manifests itself as the ability to easily convert the production line from one product to another at the conclusion of a production run or between production runs so that manufacturing down-time is minimized. Additionally, facility overhead costs are spread over more products. Optimizing the manufacturing process for low rate production will keep the production costs low [Feld00]

14.2 - Manufacturing Details

The following section discusses the manufacturing details of key components of the TerpRanger.

14.2.1 - Main Rotor

Rotor blade fabrication consists of three major cure cycles. The three molds used are machined from aluminum billets, finished to a mirror surface and lined by nickel to increase their service lives. The spar assembly is laid up by hand over an expandable mandrel. Pre-impregnated (“pre-preg”) tape is used for the inner, uniaxial layers while pre-preg woven fabric is used for the outer +45/-45 layers. The spar is then placed in a mold and cured in an autoclave, with internal pressure being provided by the expanding mandrel. The trailing-edge wedge is made from chopped glass fiber and epoxy matrix using a V-channel mold machined out of aluminum. The mold is coated with a release agent, filled with the chopped fibres and the resin, and cured at room temperature. The upper and lower skins are fabricated as precured details from bias-ply material. The Nomex honeycomb core is machined into the shape of the blade afterbody. The spar, afterbody core, trailing-edge wedge, leading-edge weights and skins are assembled in a closed-cavity mold and then cured in a hot-press or an autoclave. After removal from the mold, the leading edge cap is bonded onto the blade. The cap consists of three parts: the erosion strip, electrical insulation and the heating element. Due to its complex geometry, the tip of the titanium erosion cap is fabricated by electrodeposition of the metal. The insulation and heating elements are then bonded to the inside of the erosion shield.

14.2.2 - Main Rotor Hub

The hub yoke assembly consists of two identical S-glass/epoxy flexbeam yokes stacked perpendicular to each other and bolted together at the top of the rotor mast. The center section of the yoke contains a chamfered mast hole, surrounded by a close-tolerance eight-hole pattern for the drive bushings that transfer torque from the mast to the yokes.

Each yoke is cured in a bond tool that is machined out of aluminum. A conventional polar filament winding configuration is used to fabricate unidirectional roving belts, which are then laid up in the bond tool with bias tape plies. The tool is closed and cured in a hot-press. After removal from the tool, the center hole pattern is



machined with a conventional jig bore. The elastomeric bearings and dampers and the steel spindles are then attached onto the two yokes.

14.2.3-Tail Rotor

The blades and flexures are manufactured as a one-piece structural component with unidirectional S-glass running from blade root to blade tip. The root block is molded onto the flexure/spar component. The blade cores are made by expanding machined honeycomb. The blade/flexure assembly, which includes procured fiberglass blade skins, stainless steel abrasion strips, and phenolic tip blocks, is bonded and cured in a closed-die mold.

14.2.4 -Transmission

The manufacturing process for the main and tail rotor gearboxes will not be affected by the optimized design. Even though some of the tooth geometrical characteristics are changed, regular manufacturing processes such as gear hobbing and shaping can still be used. No special machinery or tools need to be developed for manufacturing the TerpRanger gearboxes.

Section 15 - Cost Analysis

Life Cycle cost minimization is one of the key objectives of the TerpRanger 406 upgrade program. This section identifies the cost saving features of the upgrade and estimates the operating and acquisition costs of the improved vehicle. All costs are presented in 2001 dollars. To generate year 2001 cost estimates, an average inflation rate of approximately 2.2% was used. This rate is based on changes in the consumer price index and GDP implicit price deflator [Appl01].

15.1 - Cost Reduction Features

The following features were integrated into the JetRanger upgrade program in order to reduce operating costs and provide a more affordable helicopter.

Existing Components: In an effort to minimize development and certification costs, primary systems such as the main rotor and transmission, are based on existing designs. The main rotor hub is similar to the hub of the Bell 412. The hingeless rotor configuration reduces the complexity of the system by replacing hinges with elastomeric bearings. Although, initially, the hingeless rotor costs more to develop, these costs are offset, in the long term, because of a lower maintenance costs compared to an articulated rotor. The transmission has not been completely redesigned. An existing one, similar to the one on the LongRanger 206L, is optimized for the helicopter upgrade. Integrating improved versions of existing components will reduce certification and



development costs while at the same time providing a higher degree of reliability at a lower risk than completely new systems.

Active Tracking Tabs: Although active tracking tabs are a new technology, the time saving benefits in the maintenance associated with main rotor trim will outweigh the development costs in the long term. The current tracking process is time and resource intensive, therefore an active system that can perform the task in minutes rather than hours or days will significantly influence the long term operating costs of the vehicle.

Easy and Efficient Maintenance: A Health Usage and Monitoring System (HUMS) is incorporated into the design to enhance maintenance predictability. This feature serves to significantly reduce operating costs, by reducing the maintenance cost per flight hour to one-fourth the time required by current helicopters [Tara98], and by facilitating fewer parts, tools and ground support equipment.

Vibration Reduction Technology: Improved vibration reduction technology provides higher reliability and improves the fatigue life of critical components. Improved reliability and longer fatigue life significantly reduce operating costs.

Multiple Options: The JetRanger upgrade program offers a wide variety of options for additional capabilities. Customization of the helicopter to suit a particular need enables the customer to have more control over the acquisition cost of the vehicle. A complete listing of the customization options appears in Section 16.

15.2 - Acquisition Cost

The acquisition cost of the TerpRanger 406 was determined via the relationships presented in the RFP cost model. The primary cost drivers are total production quantity, production rate and weight. Variables embedded within the cost relationships account for technological advances and manufacturing complexities to provide a comprehensive cost estimate. Table 15.1 displays the acquisition cost breakdown for the baseline TerpRanger 406.

15.3 - Operating Costs

An aircraft's operating costs may be divided into two main groups: Direct Operating Costs (DOC) and Indirect Operating Costs (IOC). The DOCs can be divided into the following subgroups: cash DOCs (maintenance, flight crew, fuel and oil), and ownership DOCs (depreciation, hull insurance, and finance). The IOCs are divided into the subgroups of aircraft IOCs (ground property, control and communications, and ground handling), and passenger related IOCs (liability insurance, amenities, and commissions). DOCs differ from IOCs in that DOCs are typically incurred per flight hour while IOCs are independent of flying hours and are expressed as annual costs. Because IOCs are dependent upon operator policy and airport location, they vary significantly from location to location and are therefore difficult to predict. IOC estimates are difficult to calculate in a preliminary design because of their sensitivity to factors such as geographical location and the policies of local



governments. Therefore they are excluded from this report. Three methods for calculating the cash DOCs are considered in this analysis. The total DOC for the JetRanger upgrade is the average value of all three methods.

Table 15.1 - Baseline Helicopter Acquisition Cost Breakdown

Aircraft Subsystem	Cost (\$)
Main Rotor	93,236
Tail Rotor	48,283
Airframe Structure	190,766
Engine	57,540
Engine Installation	87,914
Drive System	81,552
Vibration Suppression	13,902
Landing Gear	12,179
Flight Controls	14,354
Instruments	41,889
Hydraulics	2,668
Electrical Systems	15,254
Avionics	N/A*
Furnishings and Equipment	20,883
Air Conditioning	3,643
Load and Handling	528
Final Airframe Assembly	89,026
TOTAL MANUFACTURING COST	773,616
Tooling Amortization & Profit	386,808
TOTAL ACQUISITION COST	1,160,424

* Avionics costs for the baseline helicopter are accounted for in the instrument group.

15.3.1 - Fuel Cost Driver DOC Calculation

This method employs a DOC breakdown presented at the NASA Aircraft Economic Workshop [Les196]. In this model, fuel costs contribute approximately 12% of the total DOC. A comparison of the DOCs between similar helicopters and the TerpRanger is shown in Table 15.2.

15.3.2 - Maintenance Cost Driver DOC Calculation

Similar to the method above, this model assumes that maintenance costs contribute approximately 43% of the total DOC. The results of this calculation method are also presented in Table 15.2.



15.3.3 - Tishchenko Method

This method provides a global estimate of the cash DOC in terms of purchase price, fuel price and crew salary. The Tishchenko formula [Tish02] that yields DOC/ flight hour is defined as:

$$DOC_{fh} = 3 \times \frac{P_x}{10000} + P_{fuel} \times Q + N_{crew} \times M_{crew}$$

where P_r is the acquisition, or purchase price in \$, P_{fuel} is the fuel price, Q is the fuel consumption in gallons per flight hour, N_{crew} is the number of crew members, and M_{crew} is the crew salary per flight hour. The total life of the aircraft is assumed to be 10000 flight hours. The results of this method are presented in Table 15.2 below.

15.4 - Ownership DOC

According to the NASA Aircraft Economic Workshop [Lesl96], ownership DOCs constitute approximately 74% of the total DOC. Ownership DOCs were determined in each of the aforementioned cash DOC methods once the total DOC is calculated. The final estimate of the ownership DOC is the average of the results from each method. Table 15.2 displays these results for the TerpRanger upgrade and provides a comparison to other, similar helicopters.

Table 15.2 - DOC/fh Calculations and Comparison

NASA Model by 12% Fuel				NASA Model by 43% Maintenance			
	Cash DOC	Ownership DOC	Total DOC	Cash DOC	Ownership DOC	Total DOC	Cash DOC
TerpRanger	398	1212	1610	450	1370	1820	450
Bell 206B-3	355	1010	1365	497	1416	1913	497
Bell 206L-4	498	1416	1913	596	1697	2293	596
MD500 D	363	1032	1394	302	860	1163	302
SA315	688	1957	2644	756	2151	2907	756
EC120	310	882	1192	N/A	N/A	N/A	N/A

Tishchenko Method [Tish02]				TerpRanger Total DOC	
	Cash DOC	Ownership DOC	Total DOC		
TerpRanger	439	1250	1689	Avg. Cash DOC	410
Bell 206B-3	351	999	1350	Avg. Ownership DOC	1198
Bell 206L-4	515	1466	1981	TOTAL DOC	1607
MD500 D	282	801	1083		
SA315	466	1326	1791		
EC120	370	1054	1425		



The following information is applicable to the DOC calculations

- The cost analysis is based on 400 nm range and 140 knot cruise speed. The number of flight hours per year is assumed to be 1000.
- The maintenance DOC is reduced by 25% in order to account for the maintenance cost saving benefits obtained from the HUMS system, the hingeless rotor configuration, the active tracking tabs and optimized transmission technology.
- The fuel cost of 1.5 \$US/gal assumed in this analysis is based on current fuel prices defined by Leslie [Lesl96] and Bell Textron [Bell02].

The complete operating cost estimate and breakdown is shown in Table 15.3.

Table 15.3 - Operating Cost Breakdown

OPERATING COST BREAKDOWN		
Cash DOC Breakdown		
	% [Lesl96]	Cash DOC (\$/fh)
Fuel	12	49
Crew	22	90
Engine	23	94
Scheduled Inspection	6	25
Scheduled Overhaul	5	20
Unscheduled Maintenance	6	25
Scheduled Retirement	11	45
On Condition	15	61
TOTAL CASH DOC	100	410
Ownership DOC Breakdown		
Depreciation	39	467.08
Insurance	30	359.30
Finance	31	371.27
TOTAL OWNERSHIP DOC	100	1197.65
TOTAL DOC (\$/fh)		1607.16

15.5 - Cost Comparison

To demonstrate the affordability of the TerpRanger 406 upgrade proposal, the DOC estimates are compared with existing rotorcraft of similar gross weight and performance. Table 15.4 displays the results of this comparison. The calculations for the operating cost breakdown and the performance comparison, the fuel, maintenance, and acquisition costs are obtained from Jane’s All the World’s Aircraft and the Helivalue price guide [Tayl01], [Heli01]. All cash DOCs are the average values of the three methods presented above.



Table 15.4 - Cost and Performance Comparison

Parameter	TerpRanger	Bell 206B-3	Bell 206L-4	MD500 D	SA315	EC120
Gross Weight (lb)	3524	3200	4450	3000	4300	3780
Fuel Weight (lbs)	622	614	747	432	1026	724
Range (nm)	400	369	324	261	278	393
Cruise Speed (kts)	140	115	117	130	103	122
Base Price (US \$ million)	1.16	0.836	1.28	0.56	1.04	0.88
Cash DOC (US \$/fh)	410	401	536	315	636	340

Table 15.4 clearly demonstrates the affordability of the 206 JetRanger upgrade. The DOC for the upgrade is only 2% higher than the original 206B-3, and it is much lower than the operating cost of the 206L-4. Furthermore, the TerpRanger substantially outperforms both vehicles in terms of cruise speed and range. The MD-500D has a much lower operating cost, however its performance capability is inferior to the TerpRanger upgrade. Likewise, other, more modern helicopters, such as the EC120, have lower operating costs, but have lower performance than the upgrade. Operators who already own the 206B-3 would especially find it more attractive to spend money on a high performance upgrade rather than purchase a completely new, modern helicopter with poorer performance. The performance benefits gained for the upgraded 206 make for a highly competitive helicopter at only a modest increase in operating cost relative to the original 206B-3.

15.6 - Analysis Limitations

The methods used to predict the TerpRanger's acquisition and operating costs are based upon historical trends and as a result, do not accurately capture the influence of new technologies such as the active tracking tab system. Additionally, research and development costs associated with systems such as the hingeless rotor, active tracking tabs, optimized transmission, and control software are difficult to measure and are not directly factored into the estimate. The operating cost estimates are global estimates and in the absence of a more detailed cost database and economic model, these methods provide reasonable estimates of the upgraded vehicle's acquisition and operating costs.

Section 16 - Summary of Upgrade Options and Multimission Capability

The TerpRanger 406 Upgrade program offers a wide selection of interchangeable avionics and vibration suppression technologies that enhance the capabilities of the aircraft. The expanded capabilities of the vehicle



improve its mission versatility making the TerpRanger upgrade an innovative and attractive design solution for civilian as well as military operators.

16.1 - Interchangeable Upgrade Options

In addition to the standard structural, main rotor, tail rotor, and transmission modifications, the avionics and vibration suppression systems of the original aircraft have been enhanced in order to expand the mission capabilities of the aircraft. The following section summarizes the options available to the customer. Costs for each upgrade option are provided in Table 16.1, but a detailed analysis of the TerpRanger's acquisition and operating cost is provided in Section 15.

16.1.1 - Avionics Upgrades

The following list summarizes the avionics options available to the TerpRanger 406 upgrade. Details of each system are provided in Section 10.

Option 1: This option incorporates a FADEC display on the instrument panel. This is the most inexpensive and simplest option to implement.

Option 2: Digital avionics displays, GPS system, and Multifunction Display (MFD) panel.

Option 3: Option 2 plus Meggitt MAGIC MFDs with EGPWS™ passive CFIT and SkyWatch™ mid-air collision avoidance systems.

Option 4: Option 2 plus Meggitt MAGIC MFDs All-weather capable active OASys™ collision avoidance system.

16.1.2 - Vibration Suppression

The following list summarizes the vibration suppression options available to the TerpRanger upgrade. Details of each device are located in Section 9.

Option 1: Active tracking tab, PZT smart struts, and LIVE isolators.

Option 2: Active tracking tab, PZT smart struts, and Antiresonance force isolators.

Option 3: Active tracking tabs, PZT smart struts, and elastomeric dampers enhanced with the AVRS system.

16.1.3 - Aircraft Options Cost Summary

Table 16.1 displays the available combinations vibration suppression and avionics options and their influence on the acquisition cost of the TerpRanger. Details of the calculation of the vehicle's acquisition cost are provided in Section 15. The highlighted entry indicates the baseline upgrade price.



Table 16.1 - Upgrade Options Cost Summary

		Avionics			
		Option 1	Option 2	Option 3	Option 4
Vibration Suppression	Option 1	1,167,375	1,190,981	1,244,740	1,365,739
	Option 2	1,176,871	1,200,477	1,254,236	1,375,235
	Option 3	1,217,820	1,241,426	1,295,185	1,416,184

16.2 - Multimission Capability

Throughout this proposal, the TerpRanger has demonstrated itself to be an innovative upgrade solution for an aging helicopter. The 206 JetRanger is one of the most widely used helicopters in the world and has operated in many different roles including: law enforcement, forest service, air taxi, EMS, firefighting, agricultural and military. Increased speed and range along with modern avionics and vibration suppression devices enhance the original vehicle's mission capabilities and enable it to perform missions that are beyond the 206B-3's capabilities.

16.2.1 - Passenger/VIP Transport

Like its predecessor, the TerpRanger 406 accommodates 5 people with a separate area in the aft fuselage for luggage, leaving an uncluttered interior. The TerpRanger offers a high cruise speed and range combined with reduced levels of vibration and noise that make the vehicle well suited for passenger and VIP transport. The extended range and relatively low operating cost of the TerpRanger allows the vehicle to potentially provide commuter service to VIPs in areas such as the Northeast corridor of the United States.

16.2.2 - Search and Rescue (SAR)

The high cruise speed, range and 4.2-hour endurance make the TerpRanger well suited for SAR missions. In addition, advanced rotor tip geometries improve the figure of merit of the vehicle and help make it efficient to operate in hover that is desirable in a SAR mission.

16.2.3 - Military Operations

The military version of the JetRanger enjoys widespread use in the armed forces of many nations. The inherent versatility of the aircraft allows it to fulfill many military roles including: surveillance, patrol, remote area support, and medical evacuation. The enhanced range, cruise speed and efficient hovering capability offered by the TerpRanger allow the vehicle to outperform its predecessor in these missions. Therefore, the TerpRanger 406 will open a highly lucrative upgrade market for the military version.



Section 17 - Conclusion

The 2002 Student Design Competition Request For Proposals issued by the American Helicopter Society and Bell Helicopter Textron indicated the existence of a large pool of aging light helicopters that present a commercially viable opportunity for upgrade and remanufacture. This report is the response from the University of Maryland and describes the design of the 406-UM TerpRanger, an innovative upgrade program for the Bell Model 206 JetRanger. The TerpRanger exceeds all of the requirements specified in the RFP with a minimal increase in acquisition and recurring costs of the helicopter. The most stringent requirement was an increase in cruise speed from between 110 – 130 knots to 140 knots. Consequently, the TerpRanger design is optimized for high-speed flight while still maintaining low cost of operation and extensive multi-mission capability.

The heart of the upgrade program is the new four-bladed, composite, hingeless main rotor. The rotor features three different airfoils suitably distributed over the blade span in order to postpone transonic drag increases on the advancing blade and airfoil stall on the retreating blade, and an advanced-geometry blade tip design to improve its Figure of Merit in hover. Active trailing-edge tabs are provided to enable in-flight tracking of the blades, obviating the extensive downtime usually required for this task.

The TerpRanger upgrade incorporates a state-of-the-art engine and an upgraded transmission, both of which are designed to increase their mean time before repair. An auxiliary fuel tank is included in order to extend the TerpRanger's mission radius. A variety of avionics suites are offered to reduce pilot workload and improve situational awareness. Special attention was paid to vibration reduction in the TerpRanger as this is also a limiting factor for high-speed flight. A choice of three different vibration-reduction schemes is offered to the operator to improve the ride at high cruise speeds and minimize fatigue for the airframe.

Together, these modifications enable the TerpRanger to cruise at a speed of 145 knots, carrying a payload of 1125 pounds over a distance of 424 nautical miles. This represents a 24% increase in cruise speed, a 20% increase in payload and an 15% increase in range over the baseline JetRanger, all for a modest 2% increase in direct operating costs.

The JetRanger has been the world's most popular light helicopter for the past 25 years. The TerpRanger Upgrade Program will ensure that it remains so for many more years to come.



MIL-STD-1374 PART I – TAB
 NAME: UNIVERSITY OF MARYLAND
 DATE: JULY 2, 2002

GROUP WEIGHT STATEMENT
 WEIGHT EMPTY

PAGE: 2
 MODEL: TERPRANGER
 REPORT:

1	WING GROUP					
2	BASIC STRUCTURE – CENTER SECTION					
3	- INTERMEDIATE PANEL					
4	- OUTER PANEL					
5	- GLOVE					
6	SECONDARY STRUCTURE – INCL. WING FOLD WEIGHT LBS.					
7	AILERONS – INCL. BALANCE WEIGHT LBS.					
8	FLAPS - TRAILING EDGE					
9	- LEADING EDGE					
10	SLATS					
11	SPOILERS					
12						
13						
14	ROTOR GROUP					216.68
15	BLADE ASSEMBLY					152.77
16	HUB & HINGE – INCL. BLADE FOLD WEIGHT					63.91
17						
18						
19	TAIL GROUP					47.14
20	STRUCT. - STABILIZER (INCL. LBS. SEC. STRUCT.)					10.67
21	- FIN – INCL. DORSAL (INCL. LBS. SEC. STRUCT.)					15.44
22	VENTRAL					
23	ELEVATOR – INCL. BALANCE WEIGHT					
24	RUDDERS – INCL. BALANCE WEIGHT					
25	TAIL ROTOR - BLADES					8.74
26	- HUB & HINGE					12.29
27						
28	BODY GROUP					462.28
29	BASIC STRUCTURE - FUSELAGE OR HULL					
30	- BOOMS					
31	SECONDARY STRUCTURE - FUSELAGE OR HULL					
32	- BOOMS					
33	- SPEEDBRAKERS					
34	- DOORS, RAMPS, PANELS & MISC.					
35	- FUSE					
36	- BOOM					
37	ALIGHTING GEAR GROUP – TYPE SKID					71.28
38	LOCATION					RUNNING STRUCT. CONTROLS
39	MAIN					
40	NOSE / TAIL					
41	ARRESTING GEAR					
42	CATAPULTING GEAR					
43	TAIL SKID					
44						
45	ENGINE SECTION OR NACELLE GROUP *					
46	BODY - INTERNAL					
47	- EXTERNAL					
48	WING - INBOARD					
49	- OUTBOARD					
50						
51	AIR INDUCTION GROUP					0.49
52	- DUCTS					
53	- RAMPS, PLUGS, SPIKES					
54	- DOORS, PANELS & MISC.					
55						
56						
57	TOTAL STRUCTURE					797.87

* INCL. IN BODY GROUP



MIL-STD-1374 PART I- TAB
 NAME: UNIVERSITY OF MARYLAND
 DATE: JULY 2, 2002

GROUP WEIGHT STATEMENT
 WEIGHT EMPTY

PAGE: 3
 MODEL: TERPRANGER
 REPORT:

58	PROPULSION GROUP		AUXILIARY	MAIN	507.04
58	ENGINE INSTALLATION			151.54	
60					
61					
62	ACCESSORY GEARBOXES & DRIVE				
63	EXHAUST SYSTEM			2.99	
64	ENGINE COOLING			42.26	
65	WATER INJECTION				
66	ENGINE CONTROL			7.85	
67	STARTING SYSTEM				
68	PROPELLER INSTALLATION				
69	SMOKE ABATEMENT				
70	LUBRICATING SYSTEM				
71	FUEL SYSTEM			62.75	
72	TANKS - PROTECTED				
73	- UNPROTECTED				
74	PLUMBING, ETC.				
75					
76	DRIVE SYSTEM			239.66	
77	GEAR BOXES, LUB SY & ROTOR BRK			221.75	
78	TRANSMISSION DRIVE			17.91	
79	ROTOR SHAFTS				
80					
81	FLIGHT CONTROLS GROUP				99.24
82	COCKPIT Ctls. (AUTOPILOT	LBS.)			
83	SYSTEMS CONTROLS				
84					
85	GENERAL PURPOSE EQUIPMENT				250.24
86	AUXILIARY POWER PLANT GROUP				
87	INSTRUMENTS GROUP **				
88	HYDRAULIC & PNEUMATIC GROUP				12.71
89					
90	ELECTRICAL GROUP				
91					
92	AVIONICS GROUP **				
93	EQUIPMENT				
94	INSTALLATION				
95					
96	ARMAMENT GROUP (INCL. PASSIVE PROT.	LBS.) **			
97	FURNISHINGS & EQUIPMENT GROUP **				
98	ACCOMODATIONS FOR PERSONNEL				
99	MISCELLANEOUS EQUIPMENT				
100	FURNISHINGS				
101	EMERGENCY EQUIPMENT				
102					
103	AIR CONDITIONING GROUP *				
104	ANTI-ICING GROUP **				
105					
106	PHOTOGRAPHIC GROUP				
107	LOAD & HANDLING GROUP *				
108	AIRCRAFT HANDLING				
109	LOADING HANDLING				
110	BALLAST				
111	MANUFACTURING VARIATION OR CONTINGENCY				22.84
112	TOTAL CONTRACTOR CONTROLLED				
113	TOTAL GFAE				
114	TOTAL WEIGHT EMPTY - PG 2-3				1689.94

* INCL. IN BODY GROUP
 ** INCL. IN GENERAL PURPOSE EQUIPMENT



MIL-STD-1374 PART I- TAB
 NAME: UNIVERSITY OF MARYLAND
 DATE: JULY 2, 2002

GROUP WEIGHT STATEMENT
 USEFUL LOAD AND GROSS WEIGHT

PAGE: 4
 MODEL: TERPRANGER
 REPORT:

115	LOAD CONDITION						
116							
117	CREW (1)						176.4
118	PASSENGERS (4)						705.6
119	FUEL	LOCATION	TYPE	GALS.		700.29	
120		UNUSABLE		2.18		14.80	
121		INTERNAL		101		685.49	
122							
123							
124							
125	EXTERNAL						
126							
127							
128	OIL						9
129	TRAPPED						
130	ENGINE						
131							
132	FUEL TANKS (LOCATION)						
133	WATER INJECTION FLUID (GALS.)						
134							
135	BAGGAGE						242.55
136	CARGO						
137							
138	GUN INSTALLATION						
139	GUNS LOCAT. FIX. OR FLEX. QUANTITY CALIBER						
140							
141							
142	AMMO.						
143							
144							
145	SUPP'TS						
146	WEAPONS INSTALL.						
147							
148							
149							
150							
151							
152							
153							
154							
155							
156							
157							
158							
159							
160							
161							
162	SURVIVAL KITS						
163	LIFE RAFTS						
164	OXYGEN						
165	MISC.						
166							
167							
168							
169	TOTAL USEFUL LOAD						1833.84
170	WEIGHT EMPTY						1689.94
171	GROSS WEIGHT						3523.78



REFERENCES

- [AHS01] AHS International Directory, Vol. 47, No 1, 2001.
- [Alex86] Alex, F.W. and McCoubrey, G.W., "Design and Structural Evaluation of the SH-2F Composite Main Rotor Blade", *Journal of the American Helicopter Society*, April, 1986, pp. 345-359.
- [AMC74] "Engineering Design Handbook Helicopter Engineering", *AMC Pamphlet-706-201*, August, 1974.
- [Amph02] Amphitech, <http://www.amphitech.com/>, June 20, 2002.
- [Ande76] Anderson, R.G., "Composite Main Rotor Blade For the 214 Helicopter," *Proceedings of the 32nd American Helicopter Society Forum*, Washington, D.C., May 1976.
- [App102] Applied Reasoning, *The Financial Forecast Center*, www.neatideas.com/info/inflation.html, June 3rd, 2002.
- [Bell95a] Maintenance and Overhaul Instructions Manual for Bell Model 206A/B JetRanger (BHT-206A/B-M&O-1), Revision 41, © 1995 Bell Helicopter Textron Inc.
- [Bell95b] Structural Repair Manual for Bell Model 206 Series Helicopters (BHT-206-SRM-1), Revision 1, © 1995 Bell Helicopter Textron, Inc.
- [Bell98] Maintenance Manual for Bell Model 206 Series JetRanger (BHT-206A/B-SERIES-MM-1), © 1998 Bell Helicopter Textron Inc.
- [Bell99] Bell 206B-3 Product Data Book, © 1999 Bell Helicopter Textron Inc.
- [Bell01a] Bell 206B-3 Technical Information, Bell Helicopter Textron, January 2001.
- [Bell01b] Bell 407 Product Data Book, © 2001 Bell Helicopter Textron, Textron Canada Ltd.
- [Bend02] Bendixking, <http://www.bendixking.com/>, June 6, 2002.
- [Bern02] Bernhard, A., "Sikorsky," Private Communication, 22nd May, 2002.
- [Bfga02] BFG Avionics, <http://www.bfgavionics.com/>, May 28, 2002.
- [Brau80] Braun, D., "Development of Antiresonance Force Isolators for Helicopter Vibration Reduction," *Journal of the American Helicopter Society*, Sept., 1980, pp. 37-44.
- [Couc02] Couch, R.N., "Experimental Characterization of NiMnGa Ferromagnetic Shape Memory Bars Under Variable Loading Conditions," *Proceedings of SPIE Conference on Smart Structures and Intelligent Systems*, San Diego, CA, 2002.
- [Cres78] Cresap, W.L., Myers, A.W. and Viswanathan, S.P., "Design and Development Tests of a Four-Bladed Light Helicopter Rotor System", 34th Annual Forum of the American Helicopter Society, Washington D.C., May, 1978.
- [Deso88] Dessoper A., Lafon P., Philippe J.J. and Prieur J., "Effect of an Anhedral Sweptback Tip on the Performance of a Helicopter Rotor," 44th Annual Forum of the American Helicopter Society, Washington DC, June 16-18, 1988
- [Deso88] Dessoper A., Lafon P., Philippe J.J. and Prieur J., "Effect of an Anhedral Sweptback Tip on the Performance of a Helicopter Rotor," 44th Annual Forum of the American Helicopter Society, Washington DC, June 16-18, 1988
- [Dudl54] Dudley D.W., "Practical Gear Design." 1st edition, New York, McGraw-Hill, c1954.
- [Dudl84] Dudley D.W., "Handbook of Practical Gear Design" New York, McGraw-Hill, c1984.
- [Dudl92] Dudley D.W., "Dudley's Gear Handbook" 2st edition, New York, McGraw-Hill, c1992.
- [Dyes91] Dyess S.B., "Drive System Weight Optimization", *Proceedings 50th Annual International Conference SAWE, San Diego*, California, May 1991.
- [Egpw02] EGPWS, <http://www.egpws.com/>, June 18, 2002.
- [Epps00] Epps, J.J., "Methodology for In-Flight Tracking of Helicopter Rotor Blades Using Shape Memory Alloy Actuators," *Proceedings of the 56th American Helicopter Society Forum*, May, 2000.
- [FAA01] USDOT/FAA Type Certificate Data Sheet No. H2SW for Bell 206 Series Helicopters, Revision 40, April 12, 2001.
- [Feld00] Feld, W.M., *Lean Manufacturing: Tools, Techniques, and How to Use Them – APICS Series on Resource Management*, St. Lucie Press, 2000.
- [Garn99] Garner, L.J., Wilson, L.N., D.C., Rediniotis, O.K., "Development of a Shape Memory Alloy Actuated Biometric Vehicle," *Proceedings of SPIE Conference on Smart Structures and Intelligent Systems*, March, 1999.



- [Gemb99] Gembler, W., and Schweitzer, H., "Smart Struts – The Solution for Helicopter Interior Noise Problems." *Proceedings of Associazione Italiana Di Aeronautica Ed Astronautica*, Rome, September, 1999.
- [Ham95] Ham, A. J., "Flight-Testing and Frequency-Domain Analysis for Rotorcraft Handling Qualities." *Journal of the American Helicopter Society*, Vol. 40, April 1995.
- [Harr79] Harris, F. D., et al, "Helicopter Performance Methodology at Bell Helicopter Textron," Proc. 35th Ann. Forum American Helicopter Society, Washington D.C. May, 1979
- [Harr86] Harris D. H., "AHIP: The OH-58D From Conception to Production", *Proceedings of the 42nd Annual American Helicopter Society Forum*, Washington D.C. June 1986.
- [Harr86] Harris, F.D., "AHIP: The OH-58D From Conception To Production," Proc. 42nd Ann. Forum, Amer. Heli. Soc., Washington, D.C., June 1986.
- [Harr97] Harris, F. D., and Scully, Dr. M. P., "Helicopters Cost Too Much," Proc. 53rd Amer. Heli. Soc. Ann Forum, Virginia Beach, April 1997.
- [Harv79] Harvey, Keith, and Hughes, C., "Design, Analysis and Testing of a New Generation Tail Rotor," *Proceedings of the 35th American Helicopter Society Forum*, May 1979.
- [Haw180] Hawles, D.R., "Liquid Inertia Vibration Eliminator," *Proceedings of the 36th American Helicopter Society Forum*, May, 1980.
- [Heli01] Helivalve\$, Inc., *The Official Helicopter BlueBook*, Helivalve\$ Inc., 2001.
- [Hirs01] Hirschberg, M., "On the Vertical Horizon: IHPTET–Power of the Future", <http://www.vtol.org/IHPTET.HTM>, June 20th, 2002.
- [Hoer75] Hoerner, S.F., *Fluid-Dynamic Drag, Practical Information on Aerodynamic Drag and Hydrodynamic Resistance.*, Midland Park, N. J. 1965.
- [Jaco80] Jacobs, C., "Static Test of OH-58 Airframe Assembly, Part II Test Results," BHTI Report No. 206-095-013, December 16, 1980.
- [Kora00] Koratkar, N.A., and Chopra, I., "Wind Tunnel Testing of a Mach-Scaled Rotor Model With Trailing Edge Flaps," *Proceedings of the 56th American Helicopter Society Forum*, Virginia Beach, VA, May, 2000.
- [Land00] Land, J. and Weitzman, C., "How HUMS systems have the potential of significantly reducing the direct operating cost for modern helicopters through monitoring", *Proceedings of the 51st AHS Annual Forum*, Fort Worth, Texas, May, 1995.
- [Lesl96] Leslie, P., "Short Haul Civil Tiltrotor and Bell Model 412 Cost Drivers," *NASA / Industry / Operator Rotorcraft Economics Workshop* – NASA Ames Research Center, Moffett Field, CA, May, 1996.
- [Lewi87] Lewicki, D.G., and Coy, J.J., "Vibration Characteristics of OH-58A Helicopter Main Rotor Transmission," *NASA Technical Paper 2705*, 1987.
- [Lewi92] Lewicki D.G., "Development of a Full-Scale Transmission Testing Procedure to Evaluate Advanced Lubricants", *NASA technical paper 3265*, August 1992.
- [Lows92] Lowson, M., "Helicopter Noise," *The Aeronautical Journal*, June/July, 1992, pp. 209-223.
- [Megg02] Meggitt, <http://www.meggittavi.com/>, June 19, 2002.
- [OHan98] O’Handley, R.C., "Model for Strain and Magnetization in Magnetic Shape Memory Alloys," *Journal of Applied Physics*, vol. 83, No. 6, 1998, pp. 3263-3270.
- [Padf96] Padfield, G.D., *Helicopter Flight Dynamic: The Theory and application of Flying qualities and simulation Modeling*, AIAA, Washington, D.C., 1996.
- [Pegg69] Pegg, R. J., "A Flight Investigation of a Lightweight Helicopter to Study the Feasibility of Fixed-Collective-Pitch Autorotations," *NASA Technical Note, NASA TN D-5270*, June 1969.
- [Prou95] Prouty, R.W., *Helicopter Performance, Stability, and Control.*, Krieger Publishing Company, Florida, 1995.
- [Prou95] Prouty, R. W., *Helicopter performance, stability and Control*, Krieger Publishing Company, Florida, 1995.
- [Oldr96] Oldroyd, Paul K. and Sehgal, A., "Design, Development and Fabrication of the Model 430 Bearingless Main Rotor Yoke," *Proceedings of the 52nd American Helicopter Society Forum*, Washington, D.C., June 1996.



- [Redi99] Rediniotis, O.K., Lagoudas, D.C., Garner, L.J., and Wilson, L.N., "Development of a Spined Underwater Biomimetic Vehicle with SMA Actuators," *Proceedings of SPIE*, vol.3668, March, 1999.
- [Roge01] Roget, B. and Chopra, I., "Trailing Edge Flap Control Methodology for Vibration Reduction of Helicopter With Dissimilar Blades." *Proceedings of the 42nd AIAA/ASME/AHS Adaptive Structures Forum*, Seattle, WA, April 16-18, 2001.
- [Schm76] Schmidt A.H. "A Method for Estimating the Weight of Aircraft Transmissions", *Proceedings 35th Annual International Conference SAWE*, Philadelphia, Pennsylvania, May, 1976.
- [Shan89] COL Shanahan, MD, "Injury in US Army Helicopter Crashes October 1979 – September 1985," *The Journal of Trauma*, 1989.
- [Shan94] Col. Shanahan, MD, "Projected Effectiveness of Airbag Supplemental Restraint Systems in US Army Helicopter Cockpits," *Proceedings of the 50th American Helicopter Society Forum*, 1994.
- [Shen02] Shen, J. and Chopra, I., "Actuation Requirements for a Swashplateless Helicopter Control System With Trailing-Edge Flaps." *Proceedings of the 43rd AIAA/ASME/ASCE/AHS Adaptive Structures Conference*, Denver, CO, April 22-25, 2002.
- [Ship72] Shipman, D. P., "Fuselage Nodalization," *Proceedings of the 28th American Helicopter Society Forum*, May, 1972.
- [Simu01] Simula Safety Systems, Applied Technologies Division: Cockpit Airbag Systems <<http://www.simula.com/ATD/cabs.asp>>
- [Sing02] Singh, K., "Design of an Improved Shape Memory Alloy Actuator for Helicopter Blade Tracking." *Proceedings of SPIE Conference on Smart Structures and Intelligent Systems*, San Diego, CA, 2002.
- [Sinh02] Singh, K., "Design of an Improved Shape Memory Alloy Actuator for Helicopter Blade Tracking," University of Maryland Master's Thesis, College Park, Maryland, 2002.
- [Smit99] Smith, M.R., "The Model 427 Pylon Isolation System," *Proceedings of the 55th American Helicopter Society Forum*, May, 1999.
- [Step84] Stepniewski, W.Z. and Keys, C. N., *Rotary-Wing Aerodynamics*, Dover Publications, New York, 1984
- [Tara98] Tarascio, M. J., "An Advanced Rotorcraft Design Concept for Project Air 87 – Volume Two," RMIT University Undergraduate Thesis, Melbourne, Australia, 1998.
- [Tayl01] Taylor, J.W.R., *Jane's All the World's Aircraft - 2001/2001*, Jane's Publishing Company, London, England, 2001.
- [Teal01] *World Military and Civil Aircraft Briefing*, © 2001 Teal Group Corporation.
- [Tish02] Tishchenko, M.N. and Nagaraj, V. T., *ENAE 634 Helicopter Design Lecture Notes*, University of Maryland, College Park, 2002.
- [Ulla00] Ullakko, K., et. al., "Magnetic Shape Memory (MSM)- A New Way to Generate Motion in Electromechanical Devices," *ICEM 2000*, August, 2000. pp.1195-1199.
- [Weit00] Weitzman, C., "Development of Low Cost HUMS", *Proceedings of the 55th AHS Annual Forum*, Montreal, Canada, May, 1999.
- [Wils90] Wilson, F. T., "Fuselage Aerodynamic Design Issues and Rotor/Fuselage Interactional Aerodynamics," *AGARD Report on Aerodynamics of Rotorcraft*. No.781, November 1990, pp. 4-1 to 4-37.